Professur für Biochemie und Molekularbiologie

JUSTUS-LIEBIG-
UNIVERSITÄT
GIESSEN

‘Regulation of the opioid precursor proopiomelanocortin in lymphocytes in a rat model of inflammatory pain’

By

Santhosh Chandar Maddila

A thesis submitted to the Faculty of Biology and Chemistry (FB 08) in partial fulfilment for the requirements of the Doctor of Science Degree of Justus-Liebig-University Giessen, Germany

November 2014

Primirary supervisor: Prof. Dr. med. Katja Becker

Professur für Biochemie und Molekularbiologie
Institut für Ernährungswissenschaften
Justus-Liebig-Universität Giessen
Interdisziplinäres Forschungszentrum
Heinrich-Buff-Ring 26-32
35392 Giessen
Germany

Secondary supervisor: Prof. Dr. rer. nat. Michael U. Martin

Immunology FB08 - Biology and Chemistry
Justus-Liebig-University Giessen
BFS - Schubertstr. 81
D-35392 Giessen
Germany

This study was conducted at Charité – Universitätsmedizin Berlin, Klinik für Anaesthesiologie und operative Intensivmedizin, in collaboration with Molecular Tumor Genetics and Immunogenetics, Max-Delbrück-Center for Molecular Medicine (MDC), Berlin.

Declaration

I declare that this thesis is my original work and that it has not been previously presented in this or any other university for any degree.

Berlin Santhosh Chandar Maddila

Dedication

This thesis is dedicated to my God and my family.

Acknowledgements

First of all, I am very thankful to Prof. Katja Becker for her willingness to be my official primary supervisor for my thesis and also for supporting me in every situation. I am thankful to Prof. Michael Martin, who readily accepted being my official second supervisor at the Justus Liebig Universität Giessen. I would like to thank them for their great support, suggestions, and for reviewing my thesis. I am also greatful to Prof. Christoph Stein for giving me the opportunity to carry out my PhD in his lab, providing me with a great project, constant support, patience and regular supervision. I specially thank him for all that he has done to get the project going, without him the entire project and the thesis would not have been possible. I am very grateful to my mentor Dr. Melanie Busch Dienstfertig for her excellent supervision, support and patience in all situations. It was great to learn from her during the last three and a half years. Due to her motivating, enthusiastic, friendly and sincere character I was able to successfully complete the given task. It was truly a pleasure working with her.

Furthermore, I would like to thank all the members of AG Stein, who created a warm and friendly atmosphere in the lab. Special thanks go to Dr. Stefan Rahlfs of AG Becker for his valuable suggestions. Thanks to Dr. Rainer Glauben and Thorsten Stroh of AG Siegmund for their help in establishing electroporation experiments. Thanks to AG Martin Lipp and special thanks to Jenny Grobe who helped me to establish the Paraffin fixation of the knee joints and staining procedures. Thanks to Nicole Vogel (technician) and Raissa Stayszyk (animal caretaker) for their help.

I am also grateful for the generous funding given by BMBF (‘Immunopain’, FK01WC1004C) and the MDC Clinical Research Cooperation Program (KKP N11-01) to support my PhD project.

Special thanks to my daughter Judith Santhosh Maddila and my wife Hadassa Prathima Borugadda. I am very proud of them for their constant support, understanding and encouragement. Thanks to my mother Dr. Prabhavathi Chelli and my father Dr. Sonarbabu Maddila for their constant encouragement. Thanks to my entire family and friends. Above all I am thankful to God for making all things work together for good.

List of Publications

Santhosh Chandar Maddila, Melanie Busch-Dienstfertig, Christoph Stein 'Regulation of the β-endorphin precursor proopiomelanocortin in lymphocytes in a rat model of inflammatory pain', Brain, Behavior, and Immunity, Volume 29, Supplement. 10th Meeting of the German Endocrine Brain Immune Network (GEBIN).

Uta Baddack, Melanie Busch-Dienstfertig, Sara Gonzalez-Rodgiduez, **Santhosh Chandar Maddila**, Jenny Grobe, Christoph Stein, Martin Lipp, Gerd Müller, 'Cytotoxic T cells modulate inflammation and endogenous opioid functions in mice with chronic arthritis'. (Manuscript in preparation).

Santhosh Chandar Maddila, Melanie Busch-Dienstfertig, Christoph Stein, 'Proteolytic processing of proopiomelanocortin'. (Final author list to be determined upon completion of manuscript).

Posters and Presentations

Santhosh Chandar Maddila, Melanie Busch-Dienstfertig, Christoph Stein. Regulation of the β-endorphin precursor proopiomelanocortin in lymphocytes in a rat model of inflammatory pain. Berlin Brain days **2013**, Berlin, Germany.

Santhosh Chandar Maddila, M. Busch-Dienstfertig and C. Stein. Regulation of beta-endorphin synthesis in rat lymphocytes. European opioid conference **2013**, Guildford, UK.

Santhosh Chandar Maddila, Melanie Busch-Dienstfertig, Christoph Stein. Regulation of the β-endorphin precursor proopiomelanocortin in lymphocytes in a rat model of inflammatory pain. German-Endocrine-Brain-Immune-Network (GEBIN **2013**) held in Regensburg, Germany.

Summary

Proopiomelanocortin (POMC) is a precursor protein for many peptide hormones such as adrenocorticotropic hormone (ACTH), melanocyte-stimulating hormones (MSH) and β-endorphin (β-END). The major tissue that synthesizes POMC-derived peptides is the pituitary gland, where POMC is proteolytically processed by prohormone convertases (PC) 1 and 2 and by carboxypeptidase E (CPE) to cleave POMC to biologically active ACTH and β-END. Non-pituitary tissues such as immune cells can also produce β-END. Those cells migrate into inflamed tissue where they release opioid peptides and attenuate inflammatory pain by activating opioid receptors on peripheral terminals of sensory neurons. Overall knowledge about the regulation and production of POMC in immune cells is scarce, especially with respect to cells of the adaptive immune system (lymphocytes). Under naïve/unstimulated conditions, *Pomc* mRNA expression may be repressed in immune cells. The major questions of the present study were whether and how *Pomc* is repressed in lymphocytes under naïve conditions, which cell subsets can be stimulated to express *Pomc* and whether the post-translational processing involves the same proteolytic enzymes as in the pituitary. To study the regulatory mechanisms of POMC expression and β-END formation in lymphocytes and their subsets (B and T cells), we used isolated cells from lymph node (LN) tissue of rats with/without hind paw inflammation induced by intraplantar injection of complete Freund's adjuvant (CFA).

The mechanism of *Pomc* gene repression in naïve lymphocytes was investigated on the transcriptional level using a DNA-methyltransferase (RG108) and a histone deacetylation inhibitor (trichostatin A). RG108 treatment successfully induced the expression of the control transcript *Sfrp1* but had no effect on *Pomc* mRNA expression when applied separately or in combination with trichostatin A, indicating that neither demethylation nor acetylation are sufficiently derepressive with respect to this specific gene or that other mechanisms are involved in *Pomc* repression. Thereupon, the involvement of microRNAs (miRNAs) in *Pomc* repression was studied in naïve lymphocytes by knocking down Dicer using siRNA and electroporation. Dicer knockdown diminished the expression of the control transcript (*IL-10* mRNA) but had no effect on *Pomc* mRNA, suggesting that miRNAs are not involved in the repression of *Pomc*. Taken together, the nature of

Pomc repression in naïve lymphocytes was not fully unravelled, but there is evidence that it is not limited to DNA-methylation and does not involve miRNA activity.

Pomc repression in lymphocytes was switched off upon proper stimulation *in vivo* by CFA-induced inflammation (after 2 h) and by *in vitro* stimulation with IL-4 (2 h exposure). Unexpectedly, B cells rather than T cells expressed *Pomc* mRNA in both conditions, while T cells showed *Pomc* expression only after more prolonged exposure to IL-4 (after 24 h). IL-4 thereby activated *Pomc* expression in B cells indirectly. The present findings suggest a T cell-dependent mechanism leading to the liberation of one or more factors from IL-4-stimulated T cells, which finally drive *Pomc* gene expression in B cells through JAK-STAT pathway activation. Cytokine arrays were performed to identify this/these T cell factor(s) but candidate testing in *in vitro* stimulation assays remained without success. At this point the identity of the factor stimulating B cells to produce *Pomc* mRNA in our IL-4 *in vitro* model remains an open question.

On the post-translational level POMC needs to be proteolytically processed in order to yield β-END. Based on our PCR and immunofluorescence analyses *PC1* mRNA and protein were expressed under inflammatory conditions and after treatment with IL-4 plus conA but not in unstimulated lymphocytes. *PC2* mRNA and protein expression were generally detectable in naïve/untreated as well as in *in vivo* (CFA) and *in vitro* stimulated cells (IL-4 plus conA). PC2 protein was thereby upregulated in inflammation but in contrast to PC1 showed no changes after *in vitro* stimulation with IL-4 plus conA. *PC1* mRNA expression in inflammation could be ascribed to B- and T-helper cells, while *PC2* mRNA was found in all cell subsets including cytotoxic T cells. CPE was undetectable on the mRNA and protein level. This may indicate that CPE is not involved in POMC processing in lymphocytes. Transcripts of two other potential POMC processing enzymes (cathepsin L and aminopeptidase B) were found in naïve and inflamed conditions. In accordance with the expression of *Pomc* mRNA and the presence of PC1 and PC2 in *in vivo* stimulated B cells, β-END levels increased in this cell subset in inflammation. Immunofluorescence experiments showed that β-END levels were also upregulated in LN cells treated with IL-4 plus conA, which is in agreement with the expression of *Pomc* mRNA and PC1 protein. Taken together, these findings suggest that PC1 is crucial for the formation of β-END in

lymphocytes, while PC2, cathepsin L, and aminopeptidase B may be of minor relevance.

To extend our studies to chronic inflammation, the presence of endogenous opioid peptides was investigated in a new mouse model of rheumatoid arthritis (ACIA-model). We examined Met-enkephalin and β-END in the draining LNs and at the site of primary inflammation (joint) using immunohistochemistry, radioimmunoassay (RIA), and EIA measurements. Met-enkephalin levels increased with increasing cell numbers in draining LN tissue during antigen challenges. In established chronic arthritis, however, the amount of Met-enkephalin in the draining LNs was not different from baseline values. Opioid peptide release from explanted knee cells demonstrated that Met-enkephalin and β-END are liberated to a similar extent in chronic arthritis. This release could not be clearly ascribed to immune cells, pointing towards the involvement of other cell types in chronic inflammation.

In conclusion, the present studies suggest that the expression of *Pomc* and β-END production in rat lymphocytes involve additional mechanisms to DNA-methylation, that are overcome under certain circumstances as in acute CFA-induced inflammation and IL-4 stimulation of mixed cell cultures. Although the key factor triggering *Pomc* mRNA expression in B cells remains unknown, the event seems to be cytokine- and JAK/STAT-dependent. The processing of POMC into β-END seems to be linked to PC1. These findings may help to develop strategies for pain therapy by boosting opioid peptide production in immune cells. This might be especially interesting for chronic inflammation.

Zusammenfassung

Proopiomelanocortin (POMC) ist der Vorläufer für mehrere Peptidhomone wie z.B. Adrenocorticotrophes Hormon (ACTH), Melanozyten-stimulierendes Hormon (MSH) und β-Endorphin (β-END). POMC Peptide werden hauptsächlich in der Hypophyse gebildet, wo POMC proteolytisch durch die Prohormonconvertasen (PC) 1 und 2 sowie Carboxypeptidase E (CPE) in biologisch aktives ACTH und β-END prozessiert wird. Immunzellen können ebenfalls β-END bilden. Solche Zellen wandern in entzündetes Gewebe ein. Dort können sie Opioidpeptide freisetzen und Schmerz durch Aktivierung von Opioidrezeptoren auf peripheren sensorischen Neuronen reduzieren. Bisher ist das Wissen über Regulation und Produktion von POMC in Immunzellen begrenzt, insbesondere bezüglich Zellen des adaptiven Immunsystems (Lymphozyten). Unter naiven/unstimulierten Bedingungen könnte die *Pomc* mRNA Expression unterdrückt sein. Die Hauptfragestellung dieser Arbeit ist, ob und wie eine solche Unterdrückung stattfindet, welche Zellsubpopulationen zur *Pomc* Expression stimuliert werden können und ob an der posttranslationalen Prozessierung dieselben Enzyme wie in der Hypophyse beteiligt sind.

Wir isolierten zunächst Lymphozyten und deren Subpopulationen (B- und T-Zellen) aus poplitealen Lymphknoten von Ratten mit (bzw. ohne) Complete Freund's Adjuvant (CFA)-induzierter Hinterpfotenentzündung. Um Transkriptionsmechanismen zu untersuchen, wurden Inhibitoren der DNA-Methyltransferase (RG108) und der Histondeacetylierung (Trichostatin A) verwendet. RG108 induzierte das Kontrolltranskript *Sfrp1*, hatte jedoch weder alleine noch in Kombination mit Trichostatin A eine Wirkung auf *Pomc* mRNA Expression. Dies weist darauf hin, dass weder Demethylierung noch Acetylierung eine entscheidende Rolle spielen. Wir untersuchten dann die mögliche Beteiligung von microRNAs (miRNAs) durch Knockdown von Dicer mittels siRNA und Elektroporation. Dies reduzierte die Expression des Kontrolltranskripts (*IL-10* mRNA), jedoch nicht *Pomc* mRNA. Letztendlich konnten wir die Mechanismen einer möglichen *Pomc* Repression in naïven Lymphozyten nicht endgültig aufklären, jedoch fanden wir Hinweise darauf, dass weder DNA-Methylierung noch miRNA entscheidend daran beteiligt sind. Hingegen fanden wir bereits nach 2 Stunden erhöhte *Pomc* Expression in entzündeten Lymphknoten von Ratten mit

CFA-induzierter Hinterpfotenentzündung und nach *in vitro* Stimulation mit IL-4 (2 Stunden).

Unter beiden Bedingungen exprimierten vorrangig B-Zellen *Pomc* mRNA, während T-Zellen *Pomc* nur nach prolongierter Stimulation mit IL-4 (24 Stunden) bildeten. IL-4 aktivierte indirekt die *Pomc* Expression in B-Zellen nach JAK/STAT Aktivierung, vermutlich durch Faktoren, die aus IL-4-stimulierten T-Zellen freigesetzt werden. Diese Faktoren konnten mittels Zytokin-Arrays von uns bislang nicht identifiziert werden.

Mittels unserer PCR und Immunfluoreszenz-Analysen konnten wir zeigen, dass *PC1* mRNA und Protein unter Entzündungsbedingungen und nach IL-4/conA Behandlung nicht jedoch in unstimulierten Lymphozyten exprimiert werden. *PC2* mRNA und Protein waren jedoch sowohl in naïven als auch in stimulierten Zellen (nach *in vivo* CFA oder *in vitro* IL-4/conA Behandlung) nachweisbar. PC2 Protein war infolge der Entzündung hochreguliert, blieb jedoch, im Gegensatz zu PC1, nach *in vitro* Stimulation durch IL-4/conA unverändert. *PC1* mRNA Expression in der Entzündungssituation erfolgte in B- und T-Helferzellen, während *PC2* mRNA in allen Subpopulationen einschliesslich zytotoxischen T-Zellen gefunden wurde. CPE war nicht nachweisbar und scheint daher nicht an der POMC Prozessierung in Lymphozyten beteiligt zu sein. Zwei weitere möglicherweise beteiligte Enzyme (Cathepsin L und Aminopeptidase B) konnten in naïven und Entzündungs-assoziierten Zellen nachgewiesen werden. In Übereinstimmung mit der Expression von *Pomc* mRNA, PC1 und PC2 in *in vivo*-stimulierten B-Zellen, stieg auch β-END in diesen Zellen während der Entzündung an. Immunfluoreszenz-Experimente zeigten, dass β-END auch in Lymphozyten nach IL-4/conA Behandlung anstieg, in Übereinstimmung mit der Expression von *Pomc* mRNA und PC1 Protein. Daher scheint PC1 wichtig für die Produktion von β-END in Lymphozyten zu sein, während PC2, Cathepsin L und Aminopeptidase B weniger vorrangig sind.

Schließlich untersuchten wir das Vorkommen von Opioidpeptiden auch in einem neuen Mausmodell für chronische rheumatoide Arthritis. Wir untersuchten Met-Enkephalin und β-END in Lymphknoten und in entzündeten Gelenken mittels Immunohistochemie, Radioimmunoassay und Enzymimmunoassay. Met-Enkephalin stieg mit steigenden Zellzahlen in Lymphknoten während der Antigenstimulation an. In der etablierten chronischen Arthritis war jedoch die Menge an Met-Enkephalin in den drainierenden Lymphknoten unverändert

gegenüber Ausgangswerten. Aus Zellen des Kniegelenks wurden ähnliche Mengen von Met-Enkephalin und β-END freigesetzt.

Zusammengefasst deuten unsere Ergebnisse darauf hin, dass in die Expression von *Pomc* in Lymphozyten Faktoren involviert sind, die unter bestimmten Umständen wie z.B. der akuten Entzündung *in vivo* oder der IL-4 Stimulation von Zellkulturen *in vitro* aktiv werden. Obwohl der entscheidende Stimulationsfaktor der *Pomc* mRNA Expression momentan noch unbekannt ist, scheint diese abhängig von Zytokinen und JAK/STAT zu sein. PC1 erscheint notwendig für die Prozessierung von POMC in β-END. Diese Erkenntnisse könnten in neue Strategien zur erhöhten Opioidpeptidproduktion in Immunzellen einfließen und zu neuartigen Ansätzen in der Behandlung von akutem und chronischem Entzündungsschmerz beitragen.

Table of Contents

List of Figures

List of Tables

List of Abbreviations

ACIA	Antigen-collagen-induced arthritis
ACPA	Anti-citrullinated peptide/protein antibodies
ACTH	Adrenocorticotrope hormone
Ala	Alanine
AMV	Avian myeloblastosis virus reverse transcriptase
Arg	Argenine
Asp	Aspartic acid
B cells	B lymphocytes
bp	Base pairs
BSA	Bovine serum albumin
BSP	Bisulphite specific primers
cAMP	Cyclic adenosine monophosphate
CaRE	Ca^{2+} responsive elements
CD	Cluster of differentiation
cDNA	Complementary DNA
CFA	Complete Freund's adjuvant
ConA	Concanavalin A
CPE	Carboxypeptidase B
CPM	Counts per minute
CRE	Cyclic adenosine monophosphate- responsive elements
CRH	Corticotropin releasing factor/hormone
CTLs	Cytotoxic T cells
CTNF	Ciliary neurotrophic factor
DNA	Deoxyribonucleic acid
DNMT	DNA (cytosine-5) methyltransferase
dNTP	Deoxyribonucleoside triphosphate
DTT	Dithio-1,4-threitol
ECL	Enhanced chemiluminescence
EDTA	Ethylenediaminetetraacetic acid
Egr	ETS-related gene
EIA	Enzyme immunoassay
ER	Endoplasmic reticulum

F	Fluorescence
FACS	Flow cytometry
FBS	Fetal bovine serum
FC	Flow cytometry
FITC	Fluorescein isothiocyanate conjugate
FW	Forward
Gln	Glutamine
Glu	Glutamic acid
Gly	Glycine
GPCRs	G protein-coupled receptors
H_2O	Water
HAT	Histone acetyltransferase
HDAC	Histone deacetylase
HE	Hematoxylin and eosin
HPLC	High-performance liquid chromatography
i.a.	Intraarticular
IF	Immunofluorescence
IFN-gamma	Interferon gamma
Ig	Immunoglobulin
IHC	Immunohistochemistry
IL	Interleukin
i.pl.	Intraplantar
Ir	Immunoreactive
JAK	Janus kinase
JP	Joining peptide
LIF	Leukaemia inhibitory factor
LN	Lymph node(s)
LPH	Lipotropin
LPS	Lipopolysaccharide
LUMA	Luminometric methylation assay
LYS	Lysine
kDa	Kilodaltons
M	DNA standard marker
MACS	Magnetic cell sorting

mBSA	Methylated bovine serum albumin
MC	Melanocortin
MCP1	Monocyte chemotactic protein 1
MCR	Melanocortin receptor
MDB	Membrane desalting buffer
MENK	Met-enkephalin
mGlu2	Metabotropic glutamate 2
MHC	Major histocompatibility complex
MIP-3	Macrophage inflammatory protein-3
miRNA	MicroRNA
MMP	Matrix metalloproteinase
MSH	Melanocyte-stimulating hormone
MSP	Methyl-specific primers
mRNA	Messenger ribonucleic acid
MS-HRM	Methylation-sensitive high-resolution melting analysis
NC	Negative control
NF	Nuclear factor
NLXM	Naloxone methiodide
NMDAR	N-methyl-d-aspartate receptor
PBS	Phosphate-buffered saline
PC	Prohormone convertase
PCR	Polymerase chain reaction
PI	Propidium iodide
PFA	Paraformaldehyde
PLA2R1	Secretory phospholipase A2 receptor
Phe	Phenyl alanine
POMC	Proopiomelanocortin
P	Pituitary
PL	Placenta
PTX	Pertussis toxin
qRT-PCR	Quantitative reverse transcriptase - polymerase chain reaction
RA	Rheumatoid arthritis
RG108	2-(1,3-Dioxo-1,3-dihydro-2H-isoindol-2-yl)-3-(1H-indol-3-yl) propionic acid

RIA	Radioimmunoassay
RISC	RNA-induced silencing complex
RNase	Ribonuclease
RPMI 1640	Roswell Park Memorial Institute 1640 medium
RT	Reverse transcriptase
RT-PCR	Reverse transcriptase - polymerase chain reaction
RV	Reverse
SA-HRP	Streptavidin - horseradish peroxidise
SD	Standard deviation
SDS	Sodium dodecylsulphate
SEM	Standard error of the mean
SFRP1	Secreted frizzled-related protein 1
SIG	Signal peptide
siRNA	Small interfering RNA
Sp1	Specificity protein 1
SPARC	Secreted protein, acidic, rich in cysteine
STAT	Signal transducer and activator of transcription
T	Temperature
T cells	T lymphocytes
TBE	Tris boric acid (buffer)
TGN	Trans-Golgi network
TIMP-3	Tissue inhibitor of metalloproteinases-3
Tm	Melting temperature
TNFα	Tumour necrosis factor α
TRBP	Tar RNA binding protein
Tris	Trishydroxymethylaminomethane
Triton	t-Octylphenoxy-poly-ethoxyethanol
UTR	Untranslated region
β-END	Beta-endorphin
ΔΔCP	Delta-delta CP
5-aza-dC	5-aza-2´-deoxycytidine
7B2	Neuroendocrine secretory protein

1 Introduction

1.1 POMC distribution and function

POMC is a polypeptide and precursor protein for many peptide hormones with diverse biological functions such as adrenocorticotropic hormone (ACTH), different melanocyte-stimulating hormones (MSHs), β-endorphin (β-END), etc. (Nakanishi et al., 1979). The major tissue that synthesizes POMC is the pituitary gland, POMC is produced in the corticotrophs of the *pars distalis* and in the melanotrophs of the *pars intermedia* (Seidah et al., 1993; Bennett et al., 1992). Several non-pituitary tissues also express POMC and related peptides. In the brain, POMC-expressing neurons are predominantly present in the arcuate nucleus located in the mediobasal hypothalamus (Abrams et al., 1980; Gee et al., 1983). Moreover, tissues for reproduction such as testis, ovary (Bardin et al., 1987; DeBold et al., 1988a; DeBold et al., 1988b), and placenta (Rees et al., 1975; Grigorakis et al., 2000) are shown to express POMC peptides. ACTH, β-Lipotropin (β-LPH), γ-MSH, and β-END were shown to be expressed in adrenal gland, kidney, lung, thyroid gland, liver, colon, and duodenum (DeBold et al., 1988a; DeBold et al., 1988b). POMC, β-LPH, different MSHs, and β-END are in skin cells like keratinocytes, melanocytes, and dermal microvascular endothelial cells (Schauer et al. 1994; Wintzen et al., 1996; Scholzen et al., 2000). Immune tissues/cells such as spleen (Lolait et al., 1984; Mechanick et al., 1992; Lyons and Blalock, 1995), lymph nodes (Cabot et al., 1997; Mousa et al., 2000; Sitte et al., 2007; Busch-Dienstfertig et al., 2012), and circulating blood leukocytes (Smith and Blalock 1981; Harbour et al., 1991) express POMC related peptides.

ACTH and the MSHs bind to the melanocortin (MC) receptors 1 to 5 (Mountjoy et al., 2003). The receptors for β-END are opioid receptors (Li et al., 1981; Stevens CW, 2011) and can be divided in three classes that have been termed mu (μ), delta (δ), and kappa (κ) (Childers, 1993). Each type of opioid receptor possesses distinct yet overlapping ligand-binding properties and functional characteristics (Corbett et al., 1993). The μ and δ receptors bind the opioid peptides to enkephalins and endorphins. Both are G protein-coupled receptors (GPCRs) with seven transmembrane domains (Wittert et al., 1996; Boston BA, 2000). Upon stimulation with CRH ACTH binds to melanocortin type 2

receptors and induces steroidgenesis. Glucocorticoids, androgenic steroids, and mineralocorticoids are subsequently released from the adrenal gland (Cowley et al., 1999). Appetite and energy expenditure are regulated by the release of α-MSH (Cowley et al., 1999). Knock down of melanocortin type 4 receptors leads to adiposity and linear growth due to the lack of α-MSH signaling (Butler and Cone, 2003). Eumelanin is produced in melanocytes by Plasma ACTH and β- or γ-LPH leading to a brown coloration of the skin. In the absence of these peptides or melanocortin type 1 receptors, pheomelanin is produced leading to red pigmentation (Schioth et al., 1999; Ringholm et al., 2004).

ACTH-, MSH-, and LPH-related effects such as regulation of body temperature, feeding, and emotional states are mediated via melanocortin receptors END bind to the opioid receptors and are involved in dampening of pain signals (analgesia). (Li et al., 1976).

Mice lacking END showed impaired endogenous antinociception (Rubinstein et al., 1996) and also involved in the modulation of the immune response. (van Epps et al.,1984) the activity of END is not restricted to opioid receptors; END can also act via non-opioid receptors in the nervous and immune system (Wollemann et al., 2004). The facts that POMC is expressed in such a variety of cell types and that each tissue has its own regulatory mechanisms make POMC an important model system for understanding the complex interaction of regulatory factors and intracellular mechanisms that establishes the required level of gene expression.

1.2 Regulation of POMC and β-endorphin expression in the pituitary gland

The *Pomc* gene expression in the pituitary is largely controlled at the transcriptional level, and the formation of β-END is the result of extensive proteolytic processing of the precursor molecule. The most important regulatory molecules are described in the following two sections.

1.2.1 Transcriptional regulation

There is an involvement of various transcription factors and responsive elements in regulating *Pomc* gene expression in the corticotroph cell, together with intracellular signaling pathways acting on the transcription factors. One of the most

important transcription factors is the T-box factor TBX19 (Tpit) (Seidah et al., 1993; Bennett et al., 1992), which is specifically expressed in corticotroph and melanotroph cells (Lamolet et al., 2001). *Pomc* transcription control by Tpit requires the involvement of paired-like homeodomain transcription factor 1 (Pitx1), another transcription factor. Moreover, *Pomc* transcription is sensitive to stress hormones such as the corticotropin-releasing hormone (CRH) (Jinet et al., 1994). Studies in murine, ACTH-positive AtT-20 cells (pituitary tumor cell line) showed that the *Pomc* promoter activity can also be stimulated by inflammatory cytokines such as IL-1β, IL-6, and TNFα (Katahira et al., 1998). Cyclic adenosine monophosphate (cAMP)-responsive elements (CRE) and Ca^{2+}-responsive elements (CaRE) play an important role in coordinating the degree of *Pomc* gene expression and the rate of secretion of POMC-derived peptides from corticotrophs and melanotrophs (Jenks et al., 2009). From the above studies we can say that *Pomc* is regulated by various factors.

1.2.2 Post-translational regulation

Post-translational modifications and processing increase the functional diversity of the whole proteome. Post-translational processing of POMC in mammals is well studied (Smith et al., 1989; Castro et al., 1997). Studies on POMC from rodents, ox, sheep, and humans revealed that in mammals it is composed of three major segments: *N*-POMC, ACTH, and β-LPH. These segments are divided from each other by two or more basic amino acid residues, which act as cleavage signals and contain one MSH sequence. The β-END sequence is always located at the C-terminal end of the β-LPH segment. Therefore, mammalian POMC is described as the 3MSH/1END type (Takahashi et al., 2013). Studies of POMC in non-mammalian species such as birds (Naudé et al., 2006), reptiles (Kobayashi et al., 2007) and fish including teleosts, cartilaginous fish, lobe-finned fish, and agnathans (Takahashi et al., 2006), showed that the POMC structures are not always the 3MSH/1END type. It was also shown that different POMCs are generated in the *pars distalis* (PD) and *pars intermedia* (PI) of the most primitive vertebrates, the lampreys (Takahashi et al., 1995). The adult human pituitary gland lacks the *pars intermedia* and is only composed of the anterior lobe containing the *pars distalis* and *pars tuberalis* (Asa et al., 1995). Here, POMC is predominantly processed into ACTH, and β-LPH

(Takahashi et al., 2013). Similar to the human pituitary gland, the adult avian pituitary gland is only composed of the *pars distalis* (Gorbman et al., 1983). Several POMC-derived peptides have been isolated from the ostrich (*Struthio camelus*), including ACTH (Li et al., 1978), β-LPH (Naudé et al., 1981), β-END (Naudé et al., 1981), γ-LPH (Litthauer et al., 1984), and pro-γ-MSH (Naudé et al., 1993). The generation of a substantial amount of β-END in the ostrich pituitary gland is different from what was observed in the human pituitary, in which β-LPH is the predominant form (Holm et al., 1995). Similar to other tetrapods, the *Pomc* gene from snakes and alligators also codes for α-MSH, β-MSH, γ-MSH, and β-END (Kobayashi et al., 2007). Together these studies demonstrate that POMC is highly conserved across species. However, there seem to be differences amongst the POMC-derived products generated in the same tissues from different species, which points to the differences in prohormone cleavage.

1.2.2.1 Proteolytic processing of POMC

Proteolytic cleavage is a post-translational process commonly employed to regulate the cellular proteome and the resultant cellular activity. It occurs at distinct amino acid side chains or peptide linkages and is most often mediated by enzymatic activity. Such cleavage is especially important for peptide hormones, which often are initially synthesized as inactive precursors (e.g. pro-insulin). The proteolytic processes involved can vary between different cell types. Peptide bonds of proteins are usually cleaved by a class of enzymes called proteases, which among others include the group of prohormone convertases (PC). In mammals, PCs participate in the formation of biologically active products from precursor molecules such as prohormones like pro-insulin through their endoproteolytic actions (Bergeron et al., 2000). In endocrine and neuronal cells, most peptide hormones and neuropeptides are produced through limited endoproteolysis at pairs of basic amino acids during their transport along the secretory pathway. The majority of prohormones are cleaved in a cell-specific manner by members of the family of calcium-dependent subtilisin-like endoproteases, which includes furin, PC1, PC2, PC4, PACE4, PC5/6, PC7/LPC/PC8, and SKI-1/S1P (Steiner et al., 1998; Seidah et al., 1999). PC1,

unlike furin, PC4, PACE4, PC5-B, PC7, and SKI-1, is predominantly expressed in neural and endocrine cells (Seidah et al., 1990; Day et al., 1992).

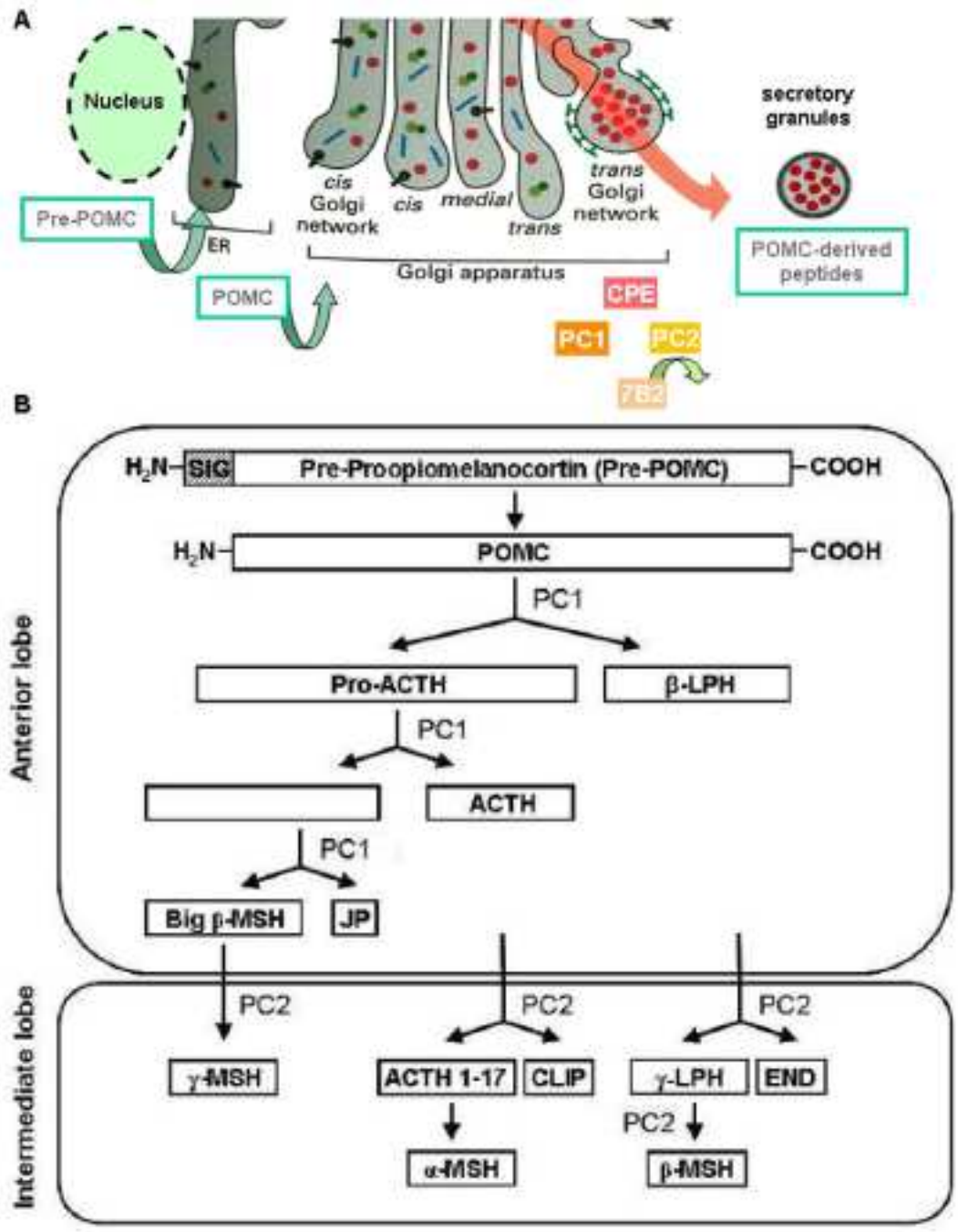

Figure 1.1 Schematic representation of POMC processing and POMC-cleavage sites of PC1 and PC2 in the pituitary A. POMC processing begins as the nascent polypeptide chain (pre-POMC) enters the endoplasmic reticulum with the help of a signal peptide (SIG). Within the ER, the signal peptide is removed from the N-terminus, giving rise to a mature POMC. After binding POMC to the membrane-bound sorting receptor carboxy peptidase E (CPE) in the trans-Golgi network, POMC cleavage occurs within the secretory granules. Adapted from Melanie Busch-Dienstfertig (2003). **B.** In the anterior pituitary gland, POMC is cleaved by PC1 to generate proACTH and β-LPH. ProACTH is further cleaved by PC1 to generate JP and ACTH. In melanotrophs of the intermediate lobe, hypothalamus, and skin PC2 cleaves ACTH to generate ACTH 1–17 and

corticotropin-like intermediate lobe peptide (CLIP). PC2 also cleaves β-LPH to generate γ-LPH and β-END. Adapted from Pritchard and White (2007).

POMC is one of the most extensively studied peptide precursors processed in pituitary cells (Mains et al., 1990; Loh et al., 1987). All proteolytic processing of human POMC occurs between either the two amino acids lysine (lys) and arginine (arg) or between two args. Every lys-arg and arg-arg site within the human precursor can be cleaved *in vivo*, whereas in the mouse and rat, additional arg-lys and lys-lys sequences at the N-termini of γ1-MSH and β-MSH respectively, appear to be utilized for cleaving POMC (Bicknell et al., 2008). In the pituitary and hypothalamus, post-translational proteolysis of POMC is mediated by PC1 and PC2 (Seidah et al., 1993). PC1 and PC2 were identified in the early 1990s (Hakes et al., 1991; Nakayama et al., 1991; Seidah et al., 1990; 1991; Smeekens et al., 1990; 1991) and were shown to be involved in the cleavage of POMC and many other peptide precursors (Benjannet et al., 1991; Korner et al., 1991; Nakayama et al., 1991; Thomas et al., 1991). Both enzymes are localized in secretory vesicles along with the neuropeptide precursors (Christie et al., 1991; Bennett et al., 1992). It is known that POMC cleavage begins in the trans-Golgi network (TGN) and continues coordinately with the maturation of secretory granules (Tanaka et al., 1991; 1992; Schnabel et al., 1989; Tooze et al., 1987). In addition to its proteolytic processing, POMC and POMC-derived peptides also undergo several other post-translational modifications such as acetylation, amidation, phosphorylation, glycosylation, and disulphide linkage formation while residing in the Golgi apparatus and secretory vesicles (Christie et al., 1991).

In the mammalian pituitary it has been shown that PC1 is expressed in both the anterior and the intermediate lobe and that it cleaves POMC mainly at the paired basic sites flanking the ACTH sequence. In contrast, PC2 is mainly expressed in the intermediate lobe and cleaves POMC in concert with PC1, yielding JP, α-MSH, and β-END (Seidah et al., 1992; 1993). Tissue-specific proteolytic processes to generate functional peptides have also been described by (Takahashi et al., 2013). In corticotrophs, larger peptides such as ACTH are the final products, whereas in melanotrophs smaller peptides such as α-MSH are predominately generated. As shown in (Fig. 1.1 A), post-translational POMC processing begins as the nascent polypeptide chain (pre-POMC) enters the endoplasmic reticulum with the help of the signal peptide (SIG) (Cool et al., 1994;

Loh et al., 2002). The molecular weight of pre-POMC is approximately 32 kilodaltons (kDa). Within the ER, the SIG is removed from the N-terminus, giving rise to the mature POMC. After binding POMC to the membrane-bound sorting receptor carboxy peptidase E (CPE) in the trans-Golgi network, PC1 cleaves POMC within the secretory granules in the anterior lobe of the pituitary (Tanaka et al., 1991; 1992; Cool et al., 1997). The sites Glu-Gly-Lys-Arg, Glu-Phe-Lys-Arg, and Lys-Asp-Lys-Arg are cleaved by both, PC1 and PC2. Additionally, PC2 cleaves Ala-Gln-Arg-Arg and Gly-Lys-Lys-Arg motifs. Because of the limited proteolytic action of PC1 at POMC cleavage sites, four different major end products corticotropin, β-lipotropin, the joining peptide (JP), and big γ-MSH are generated in the anterior lobe (see Fig. 3.1 B). In the intermediate lobe of the pituitary, the end products are α-MSH, corticotropin-like intermediate product (CLIP), β-MSH, and β-END (Fig. 3.1 B). If both enzymes are present, PC1 mediates the initial cleavage of POMC into the corticotropin-biosynthetic intermediate molecule and β-LPH (Benjannet et al., 1991; Seidah et al., 1999; Tanaka et al., 2003). Thereafter, PC2 is able to cleave β-LPH to generate β-MSH and β-END (Marcinkiewicz et al., 1993). In humans, β-LPH is processed to γ-LPH and β-END, and then γ-LPH is further cleaved by PC2 to β-MSH. After cleavage of POMC by PC1 and PC2, the end products have two basic pair residues at their C-terminal that are removed by CPE (Douglass et al., 1984; Che et al., 2001). An exception is β-END that does not have any C-terminal amino acid residues, since it is C-terminally terminated by the STOP codon. In summary the formation/generation of POMC-related end products is directed by the enzymatic machinery of a cell.

1.2.2.1.1 Activation and inhibition of PC1 and PC2

In neuroendocrine and endocrine tissues, activation of mouse PC1 occurs auto-proteolytically (Fig. 1.2). When the 94 kDa pre-proPC1 mouse protein enters the endoplasmic reticulum, the SIG is cleaved, resulting in the 87 kDa intermediate form proPC1 (Lee et al., 2004). This intermediate form is then transported to the Golgi apparatus, where it undergoes different post-translational modifications such as N-glycosylation (Benjannet et al., 1993). The N-terminal pro-segment is processed within the *trans*-Golgi network and the secretory granules, generating

the enzymatically active 66 kDa form (Goodman et al.,1994; Seidah et al.,1999; Lee et al., 2004).

PC1 is specifically inhibited by proSAAS, an endogenous convertase-binding protein of 26 kDa belonging to the calcium binding and acidic protein family of granins, which in turn belongs to a protein family of regulated secretory proteins (Qian et al., 2000; Fortenberry et al., 2002). ProSAAS is predominantly expressed in neuronal and pituitary tissues and is processed in parallel to proPC1. Cleavage of the signal peptide results in the 23 kDa form SAAS (see Fig. 1.2). The inhibitory region of proSAAS comprises 8-12 amino acid residues. The inhibitory region of proSAAS is located C-terminally and is completely conserved in humans, rats, and mice (Qian et al., 2000). This motif includes a critical lys-arg sequence, which determines the inhibitory effect of proSAAS by mimicking substrate characteristics. As shown by (Qian et al., 2000), mutation of lys and arg into alanine (ala) abolished the inhibition of PC1 activity by proSAAS. Moreover, the pro-region and C-terminal region of PC1 show amino acid sequences similar to the inhibitory motif of proSAAS and seem to have autoinhibitory properties (Jutras et al., 1997; Boudreault et al., 1998).

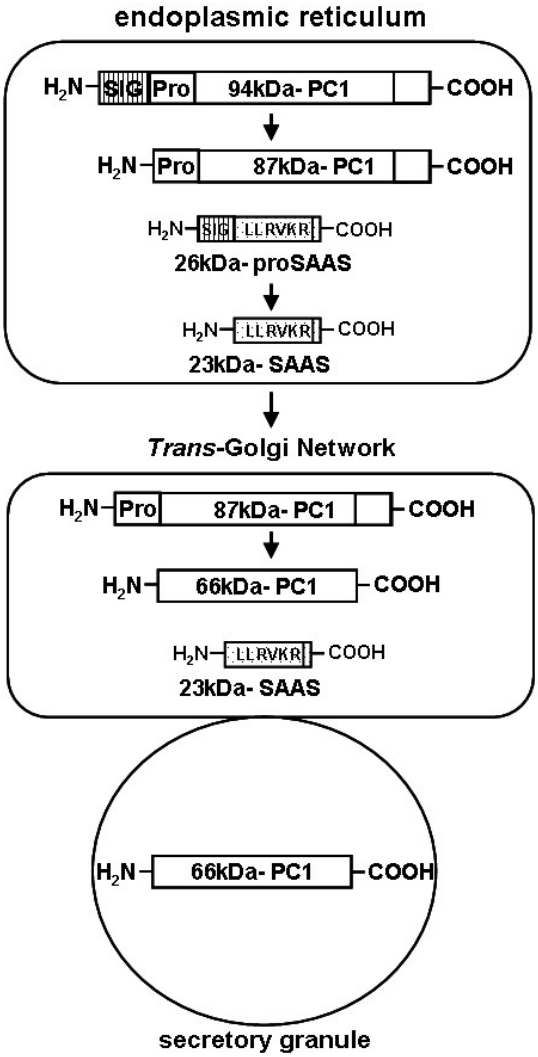

Figure 1.2 Maturation of mouse PC1 Post-translational processing of proPC1 is a multi-step procedure that starts in the endoplasmic reticulum. The enzymatically active form of 66 kDa PC1 is present in the trans-Golgi network and in secretory granules. In parallel to PC1 its endogenous inhibitor proSAAS is processed along the secretory pathway. Modified from Tanaka (2003) and Lee et al., (2004).

PC2 is also synthesized as an inactive precursor (proPC2) that undergoes autocatalytic processing (Fig. 1.3). This processing depends on the presence of the neuroendocrine granin 7B2. The 27 kDa precursor pro7B2 specifically binds to proPC2 (75 kDa) within the endoplasmic reticulum (Benjannet et al., 1995; Braks et al., 1996; Lamango et al., 1996). This complex is then transported to the *trans*-Golgi network. Here, the 27 kDa pro7B2 is cleaved into an N-terminal domain of 21 kDa and a C-terminal domain of 6 kDa by a serine endoprotease (Paquet et al., 1994). (Martens et al., 1994), demonstrated that the 27 kDa pro7B2 is a potent inhibitor of PC2 while the processed 21 kDa form has no inhibitory capacity. However, like its precursor, the C-terminal peptide of 7B2 potently inhibits PC2 (Li

et al., 2003). The N-terminal 21 kDa form of 7B2 dissociates from proPC2; the 6 kDa C-terminal domain remains bound to it. In the *trans*-Golgi network, proPC2 undergoes an autocatalytic cleavage of the N-terminal pro-domain producing the active PC2 of 66 kDa, and the C-terminal domain of 7B2 dissociates from it (Lamango et al., 1996; Zhu et al., 1996; Muller et al., 1997; 1999). (Muller et al.,1997) demonstrated that rather than promoting proPC2 folding, 7B2 acts as a helper protein involved in proPC2 transport and is required in the proPC2 activation process. Thus, the post-translational regulation of the POMC processing is not limited to the presence of PC1 and PC2 but is extended to additional regulatory factors such as proSAAS and 7B2.

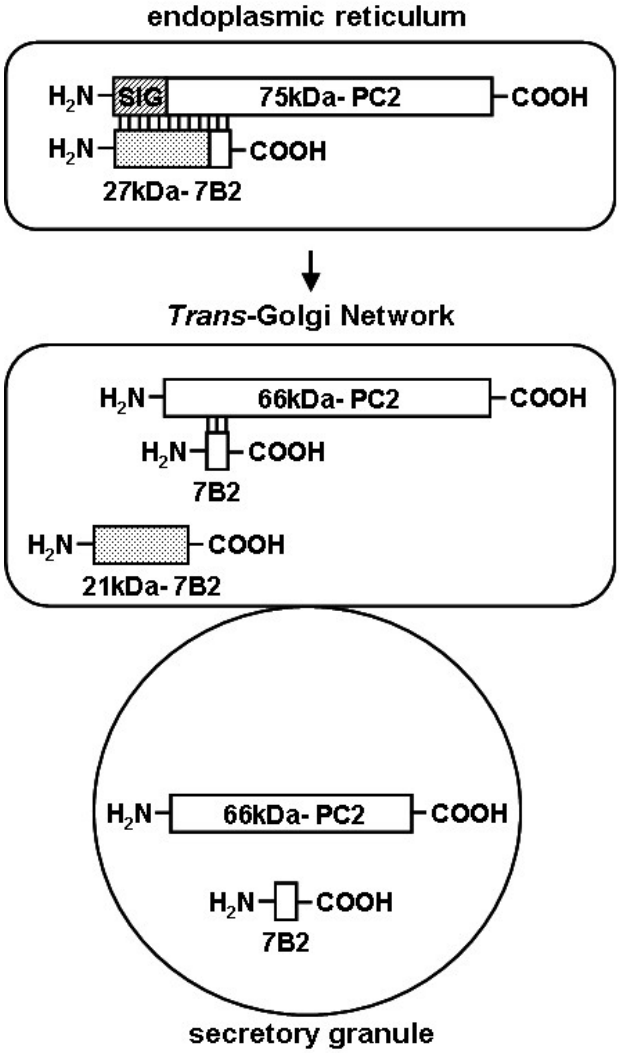

Figure 1.3 Activation mechanism of mouse PC2 Post-translational processing of proPC2 involves the formation of a proPC2/pro7B2 complex within the endoplasmic reticulum, which is transported into the trans-Golgi network where pro7B2 is cleaved. The N-terminal part of 7B2 is

released from this complex while the C-terminal part remains associated. In parallel to the autocatalytic cleavage of the N-terminal pro-domain of PC2, the C-terminal part of 7B2 also dissociates. The enzymatically active form of 66 kDa is released in secretory granules at pH 5. Modified from Lehmann (2009).

1.3 POMC and β-endorphin expression in immune cells

As mentioned above, POMC is also expressed and processed in several non-pituitary (non-neuroendocrine) tissues such as skin, hypothalamus, testis, thyroid gland, placenta, pancreas, gut, kidney, adrenal gland, and liver (Smith et al.,1989). POMC-related peptides such as ACTH and β-END were also identified in immune cells (e.g. splenic macrophages, peripheral blood lymphocytes) in the early 1980s (Smith et al., 1981; Lolait et al., 1984). Under the conditions of painful inflammation, immune cells release opioid peptides such as β-END (Busch-Dienstfertig et al., 2012; Rittner et al., 2006), which can activate opioid receptors on peripheral sensory neurons, resulting in the attenuation of pain.

1.3.1 Opioid peptide containing immune cells in a model of painful inflammation

Animal models that mimic clinical inflammatory pain use e.g. complete Freund's adjuvant (CFA), a suspension of oil and heat-inactivated mycobacteria (*M. butyricum, M. tuberculosum*), to induce an inflammation of peripheral tissue. A local subcutaneous unilateral application of CFA into the hind paw of rats induces nociceptive behaviour, such as reduced locomotor activity, avoids putting weight on the paw, lifting the affected limb from the ground, and permanent flexion of the knee joint, indicating spontaneous pain at rest (Stein et al., 1988). Nociceptive thresholds to thermal or mechanical stimuli are decreased when heat or pressure is applied (thermal and mechanical hyperalgesia), leading to the withdrawal of the paw. In parallel, peripheral mechanisms of intrinsic opioid antinociception become functionally active within such injured tissues (Stein et al., 2003). Intraplantar inoculation with CFA leads to the migration of circulating β-END-containing leukocytes to the inflamed tissue (Rittner et al., 2005). Concurrently, opioid receptors are upregulated on peripheral endings of sensory neurons (Przewlocki et al., 1992; Stein et al., 1996; Mousa et al., 2001). Upon stressful stimulation such as a cold water swim or surgery, leukocytes locally liberate β-END to elicit potent and clinically relevant opioid receptor-specific analgesia (Stein et al., 1990; 1993).

Further analysis determined that β-END is liberated from leukocytes in the presence of a variety of releasing stimuli such as CRH (Schafer et al., 1994; Cabot et al., 1997), chemokines (Rittner et al., 2006), and catecholamines (Binder et al., 2004; Mousa et al., 2004). Together these studies suggest that immune cells contribute to the endogenous pain control in inflammation by opioid peptide release.

1.3.2 Regulation of POMC expression in lymphocytes

As mentioned earlier, POMC-related peptides such as ACTH and β-END had already been identified in immune cells (e.g. splenic macrophages, peripheral blood lymphocytes) in the early 1980s (Smith et al.,1981; Lolait et al., 1984). Macrophages predominantly produced unacetylated, opioid-active β-END, while N-acetylated β-END was present in lower amounts as seen in the pituitary (Lolait et al., 1986; Westly et al., 1986). At the same time other studies revealed that the production of β-END in human peripheral leukocytes can be induced by CRH and suppressed by the glucocorticoid analogue dexamethasone (Smith et al., 1986), suggesting that the *Pomc* gene may be expressed and similarly controlled in leukocytes and pituitary cells.

The *Pomc* gene comprises three exons that are transcribed into full-length *Pomc* mRNA. Exons 2 and 3 give rise to the pre-propeptide. In neuroendocrine cells, the formation of the active peptides is accomplished by entering the regulated secretory pathway and involves extensive proteolytic cleavage as described above. However, the extensive analysis of several non-pituitary tissues demonstrated that these tissues predominantly express shorter *Pomc* mRNA transcripts than found in the pituitary (Bardin et al., 1987). These truncated *Pomc* transcripts comprising about 800 bp of exon 3 but lacking exon 2 were detected by several groups in naïve lymphocytes and other immune cell subsets (Lacaze-Masmonteil et al., 1987; DeBold et al., 1988; Oates et al., 1988; Przewlocki et al., 1992; van Woudenberg et al., 1993; Cabot et al., 1997; Lolait et al., 1986; Westly et al., 1986; Mechanick et al., 1992; Lyons et al.,1997). Therefore, the regulation of opioid gene expression and processing in immune cells has not been further studied in detail.

On the other hand, there is evidence that full-length POMC may be expressed in lymphocytes under stimulated and pathological conditions. In a case

report of a patient with ectopic ACTH syndrome, lymphocytes in thymic hyperplasia were the source of high ACTH production (Ohta et al., 2000). In another study, (Buzzetti et al., 1989) detected full-length POMC mRNA in a CD4-positive, HIV-infected T lymphoma cell line. This *Pomc* gene expression was accompanied by higher ACTH levels in the lymphoma cells than detected in normal human peripheral blood mononuclear cells not expressing the full *Pomc* mRNA transcript. Moreover, lymphocytes were shown to express full-length *Pomc* mRNA after stimulation with mitogenic substances such as concanavalin A (Lyons et al., 1997) or after infection with pathogens such as the Newcastle disease virus (Westly et al., 1986). Lymphocytes were shown to express full-length *Pomc* mRNA after stimulation with IL-4 (Busch-Dienstfertig et al., 2012). Usually, the expression of full-length *Pomc* mRNA appears to be suppressed in mature, unstimulated leukocytes, but it can be induced under pathological conditions such as lymphoma formation (Buzzetti et al., 1989 and Ohta et al., 2000) or virus infection (Westly et al., 1986). Moreover, *Pomc* transcripts containing the signal sequence necessary for correct routing into the regulated secretory pathway are upregulated in lymphocytes from rats with painful paw inflammation (Sitte et al., 2007). These findings raised the question of whether the lymphocytic expression of *Pomc* mRNA and the processing of its translation products may be different in normal versus pathological states. The ultra-structural analysis of macrophages and lymphocytes in inflamed paw tissue revealed that β-END was located within vesicular structures (Mousa et al., 2004). These findings supported the view that immune cells are indeed capable of expressing *Pomc* derivates containing the signal peptide, an essential missing link in the pathway leading to regulated β-END secretion.

The difficulties in detecting *Pomc* mRNA in naïve immune cells as described above suggest a repressive mechanism, e.g. methylation of the DNA, which is an epigenetic signaling tool to lock genes in the ‘off’ position. Consistently, methylation of the *Pomc* gene was shown to be absent in ACTH-secreting pituitary corticotroph cells but strong in non-ACTH-secreting human lymphocytes (Newell-Price et al., 2001). Whether the methylation status of the *Pomc* gene defines its expression in rat lymphocytes has not been previously analyzed. Another possibility is that *Pomc* mRNA levels in lymphocytes are repressed by rapid mRNA degradation through miRNA targeting or by controlling the translation of other factors involved in *Pomc* gene expression (e.g. transcription factors). In the

anterior pituitary of mice the conditional knock-out of *Dicer1* resulted in the loss of mature miRNAs without affecting *Pomc* mRNA levels (Righi et al., 2010). However, since miRNA expression in lymphocytes differs from that in the pituitary, a relevance of miRNA in those cells needs to be determined.

At present, the repressive mechanisms of *Pomc* expression in lymphocytes have not been investigated in any detail. The following two paragraphs are providing background information on DNA methylation, histone acetylation, and miRNA which may be of relevance for the negative regulation of *Pomc* expression.

1.3.2.1 Transcriptional repression via DNA methylation and histone deacetylation

DNA methylation at cytosine residues is an important epigenetic mechanism that determines gene expression patterns and the stability of chromatin. DNA methylation patterns are inherited and tightly correlated with the chromatin structure. This essential mechanism regulates cellular differentiation during development and maintains the cellular phenotype (Doehring et al., 2011). The maintenance of DNA methylation is ensured by DNA (cytosine-5-)-methyltransferase 1 (DNMT1), which predominantly methylates hemi-methylated DNA during replication of proliferating cells. If DNMT1 function is impaired, the wrong DNA methylation pattern can easily result in tumours and cancer. Other DNA methyltransferases (DNMT3A and DNMT3B) implement the so-called *de novo* methylation of previously unmethylated DNA regions (e.g. during cell differentiation). In general, DNA methylation is plastic and can be reversed by DNA demethylases. The consequence of DNA methylation is the inhibition of gene transcription by blocking transcription factors from binding to the gene and by attracting histone deacetylases and other chromatin-remodelling proteins that modify histones, resulting in inactive chromatin. Conclusively, active regions of the chromatin that enable gene expression are associated with hypomethylated DNA, whereas hypermethylated DNA is packaged in inactive chromatin. Histone protein modifications either impair the docking of transcription factors onto DNA via deacetylation or open the area of DNA to transcription factors through acetylation. Histone deacetylation is catalysed via histone deacetylase (HDAC) and results in the acetyl group being transferred to coenzyme A. Histone acetylation involves the addition of an acetyl group (acetyl–coenzyme A) on lys residues in the N-terminal

tail of the protein and on the surface of the nucleosome core, which is catalysed by the enzyme histone acetyltransferase (HAT). Acetylated histones and nucleosomes represent a type of epigenetic tag within chromatin and result in greater levels of gene transcription (Renthal et al., 2008). Histone acetylation is therefore a global marker of gene activity. Many transcription factors are regulated via acetylation and are specifically targeted by HDACs (Spange et al., 2009). The nuclear factor (NF) κB family of transcription factors in particular is dependent upon acetylation for full transcriptional activity, whereas deacetylation inhibits the transcription of NF-κB target genes. A key regulator of N-methyl-d-aspartate receptor (NMDAR) activity, metabotropic glutamate 2 (mGlu2) receptors, is transcriptionally regulated by the NF-κB pathway. Activation of (metabotropic glutamate receptor 2) mGlu2 receptors causes analgesia in inflammatory and neuropathic pain by decreasing NMDAR activity and thereby downregulating neurotransmitter release from primary afferent fibres in the dorsal horn of the spinal cord (Jones et al., 2005; Simmons et al., 2002; Yang et al., 2002; 2003). Selective HDAC inhibitors have been shown to upregulate the expression of mGlu2 receptors in the dorsal root ganglion and spinal cord in a mouse model of inflammatory pain, thereby causing analgesia (Chiechio et al., 2009). These studies suggest that HDACs may be epigenetic targets in the treatment of pain (Lotsch et al., 2009). The potential contributory role of epigenetic changes in the development of diverse pain phenotypes is particularly intriguing because these mechanisms have also been associated with high levels of stress (Wolkowitz et al., 2008), depression and aging (Huzen et al., 2008), major factors associated with increased pain sensitivity. For instance HDACs, which silence certain genes, were found to play a role in pain-signal transmission in the spinal cord (Bai et al., 2010). Specifically, class IIa HDACs were upregulated.

1.3.2.2 Post-transcriptional repression by miRNA

MiRNAs are a family of endogenously derived, non-coding RNAs that epigenetically regulate gene expression (He et al., 2004). Rosalind Lee et al., 1993) discovered that the expression of the LIN-14 protein is regulated by a small RNA derived from the lin-4 gene in *Caenorhabditis elegans*. Meanwhile, miRNA expression has been studied in several species and cell types, and it is becoming apparent that they are important post-transcriptional gene regulators. Mature

miRNAs are formed from their immature precursors (Kim et al., 2009). miRNA biogenesis is therefore realized by a protein machinery that involves the class III endoribonuclease Dicer, which is well conserved among eukaryotes. The biogenesis of miRNA begins with its transcription from genomic DNA containing the miRNA sequences via RNA polymerase II. The transcription product was termed pri-miRNA, which is further processed into pre-miRNA by a nuclear protein complex called the microprocessor complex. Pre-miRNAs are transported from the nucleus to the cytoplasm by exportin-5. In the cytoplasm, the pre-miRNAs are loaded onto a protein complex composed of Dicer, argonaute-2, the TAR RNA binding protein (TRBP), and other proteins known as the RNA-induced silencing complex (RISC) (Koscianska et al., 2011). RISC-loaded pre-miRNAs are cleaved to their mature form (approximately 22 nucleotides) by Dicer. The mature miRNAs are capable of binding their cognate mRNA target through miRNA-mRNA interactions, while they are still associated with the RISC. The miRNA-mRNA interactions are established through complementary base pairing between a sequence on the miRNA called the seed region and the 3' untranslated region on the target mRNA, leading to translational inhibition and/or mRNA degradation (Krol et al., 2010). However, miRNAs do not target specific mRNAs and do not have to perfectly match the sequence of their targets; Therefore, they can coordinate the expression of large sets of genes (Bartel et al., 2009). It is estimated that up to 60% of the human genome may be regulated by miRNAs (Friedman et al., 2009).

1.3.2.3 Proteolytic processing of POMC in lymphocytes

POMC alone or co-localized with PC1, PC2, and CPE was detected in circulating leukocytes, particularly under conditions of painful inflammation in animals (Smith et al., 2003; Mousa et al., 2004). To date there are only a few studies that have investigated the presence of prohormone convertases specifically in lymphocytes. (Lansac et al., 2006), observed *PC1* and *PC2* mRNA expression in the spleen of rats using *in situ* hybridization histochemistry, demonstrated that macrophages and lymphocytes contained these enzymes. Basal expression of *PC1* mRNA was seen in the macrophage-rich red pulp/marginal zone areas of the spleen. Moreover, *PC1* and *PC2* mRNA expression was inducible within germinal centres (B lymphocytes) after *in vivo* lipo-polysaccharide-treatment. These findings point towards a differential expression of

the two proteolytic enzymes in different types of immune cells. (Mousa et al., 2004), further analysed the expression of PC1, PC2, 7B2, and CPE in blood leukocytes at the protein level using western blotting and immunohistochemistry. In normal rats, the proteolytic enzymes were detectable in granulocytes and monocytes/macrophages but not in circulating lymphocytes. From previous studies, we have seen that after induction of a CFA-inflammation in the paw, the amount of PC1, PC2, POMC, and β-END increased in lysates of blood leukocytes, and proteolytic enzymes were then detectable in granulocytes, monocytes/macrophages, and in circulating lymphocytes. These findings raised the questions of whether the cells of lymph nodes draining paw tissue also express enzymatically active PC1 and PC2 and whether these enzymes are upregulated and involved in the processing of POMC under conditions of painful inflammation.

1.4 Antigen- and collagen-induced arthritis (ACIA) models

Chronic disorders accompanied by inflammation are the most common diseases of aging and represent the greatest health threat (Tabas et al., 2013). Such disorders include rheumatoid arthritis (RA); Chronic joint inflammation and pain are the two main symptoms in patients with RA and are associated with significant morbidity (Firestein et al., 2005). RA is a chronic autoimmune disease characterized by infiltration of leukocytes into the synovial and periarticular tissues (Wipke et al., 2001; Liew et al., 2005; Coelho et al., 2008), which results in the destruction of cartilage and bone (Firestein et al., 2003). Although significant progress has been made regarding anti-inflammatory therapies, chronic pain is still an unresolved clinical problem (Perrot et al., 2013). Inflammatory mediators are released into the inflamed tissue in response to inflammatory stimuli that in turn release a cascade of cytokines such as tumour necrosis factor (TNF)-α and IL-1β that further drive the inflammatory reaction (Cunha et al., 2005; Verri et al., 2006). Therefore, cytokines such as TNF-α and IL-1β are interesting therapeutic targets to treat RA patients (Scott et al., 2006). Problems associated with anti-cytokine therapies are expensive and the need to be administered via the parenteral route. Additionally, many patients fail to respond to TNF-α (Moreland et al., 1997) or IL-1β (Jiang et al., 2000) blockade. Standard analgesic treatments such as nonsteroidal anti-inflammatory drugs or steroids often exhibit detrimental side effects in the long-term use (e.g. gastrointestinal ulcers, bleeding, myocardial

infarction, stroke, infections) (Huscher et al., 2009; Trelle et al., 2011). Thus, there is an urgent need for alternative therapeutic approaches. Since opioids can interfere at different stages with the cascade of pro-inflammatory events in peripheral tissues (Stein et al., 2011; 2013), we set out to investigate endogenous opioids in an animal model of chronic arthritis. Antigen-collagen-induced arthritis (ACIA) is a new mouse model representing key features of RA such as chronicity, cartilage and bone erosion, and prominent autoimmune responses against autologous collagen II, vimentin, and ACPA (Baddack et al., 2013). Immune cells infiltrating inflamed tissue can potently reduce pain by liberating opioid peptides such as enkephalins, endorphins, and dynorphin (Stein et al., 2011; 2013; Rittner et al., 2005). Such mechanisms have been predominantly investigated in animals and humans with acute inflammatory injuries as already mentioned above, but their relevance in chronic inflammation is unknown. In acute stages of ACIA, the cellular infiltrate is mainly composed of neutrophils, macrophages, and mononuclear cells (lymphocytes), while mononuclear and fibroblast-like cells are predominant at chronic stages (Baddack et al., 2013). This raises the question of whether opioid peptides are also present under chronic inflammatory conditions, laying the basis for opioid-mediated antinociception.

1.5 Objectives

POMC processing occurs in peripheral tissues including immune cells. One of the end products is the opioid peptide β-END. Following its release, β-END can activate opioid receptors on peripheral sensory neurons in order to inhibit pain within inflamed tissue. However, our knowledge of the regulation of POMC expression and its processing in immune cells such as lymphocytes is poor to date. In order to provide insight into the regulatory mechanism of POMC expression as well as into the relevance of PC1 and PC2 for the formation of β-endorphin in lymphocytes, the present study focused on the following specific aspects:

1) Transcriptional regulation of POMC in lymphocytes.
2) Repression and expression of POMC in native lymphocytes.
3) POMC Processing enzymes in lymphocytes.
4) Endorphin production in lymphocytes.
5) Opioid peptides in mice with chronic arthritis.

Pomc gene transcription in lymphocytes can be regulated by various mechanisms such as methylation, acetylation, and miRNA. Our aim was to see the involvement of these mechanisms in the regulation of Pomc gene expression. Methylation status would be investigated using bisulfite sequencing, if this strategy does not yield a conclusive result, we would investigate using a DNA-methyltransferase inhibitor to see if it effects *Pomc* gene expression. To address the question of acetylation we would use a histone deacetylation inhibitor to study whether *Pomc* is deacetylated. To study the involvement of miRNA in *Pomc* repression, we intended to knock down Dicer using siRNA, as Dicer is very important for the maturation of miRNA. Therefore in the absence of Dicer, there would be no miRNA so that we could see how the absence of miRNA would have an effect on Pomc gene expression.

Pomc repression in lymphocytes was switched off upon proper stimulation *in vivo* by CFA-induced inflammation (after 2 h) and by *in vitro* stimulation with IL-4 (2 h exposure). The present aim of the study was to see which subsets of lymphocytes would express *Pomc*. It is known that *Pomc* in lymphocytes is expressed upon IL-4 stimulation via JAk/STAT pathway. Our aim is to study which pathway is involved in the subsets of lymphocytes. Lymphocytes would be separated into subsets using MACS separation columns, and supernatant transfer experiments would be performed to see which subsets are responsible for expression of *Pomc*. If a specific subset is responsible for *pomc* expression, we would investigate the signalling pathway involved. Then using cytokine array we would look for the factor that stimulates the expression of *Pomc*.

In the pituitary, POMC is proteolytically cleaved by PC1, PC2, and CPE into β-END. Our aim was to investigate whether the same proteolytic enzymes are involved in the cleavage of POMC in lymphocytes. To answer this question we would study the expression of PC1, PC2, and CPE in both *in vitro* (IL-4) and *in vivo* (CFA) using PCR and immunofluorescence or western blot. Then we would measure β-END levels in both the *in vitro* (IL-4) and *in vivo* (CFA) studies using radioimmunoassay (RIA) and immunofluorescence. We would then study the functionality of proteolytic enzymes via knockdown using siRNA of the specific enzymes and also measure the β-END levels to see if they are affected by knocking down a particular processing enzyme.

To extend our studies to chronic inflammation, the presence of endogenous opioid peptides would be investigated in a new mouse model of rheumatoid arthritis (ACIA-model). We would measure Met-enkephalin and β-END in the draining LNs and at the site of primary inflammation (joint) using immunohistochemistry, RIA and EIA measurements.

2 Materials and Methods

2.1 Materials

2.1.1 Enzymes

Table 2.1 List of enzymes

Name	Company
50× Advantage 2 polymerase mix	Clontech Laboratories
Avian myeloblastosis virus reverse transcriptase (AMV)	Roche
DNAse	QIAGEN
RNAse inhibitor	Roche
Fast start DNA master plus SYBR green 1	Roche
Thermus aquaticus (Taq) polymerase	Roche

2.1.2 Radioactively labelled peptides

Table 2.2 List of radioactively labelled peptides

Name	Company
(^{125}I)rat β-endorphin	Peninsula Laboratories
(^{125}I) Met-enkephalin	Peninsula Laboratories

2.1.3 Antibodies

Table 2.3 List of antibodies

Antibody	Application	Company
Anti-mouse CD8a (LY2.2)	For *in vivo* depletion	Leinco Technologies
Anti-rabbit IgG, peroxidase-conjugated	IHC	Vector Laboratories
Donkey anti-mouse IgG, FITC	IF	Vector Laboratories
Rat IgG2b	Isotype control for *in*	Leinco Technologies

	vivo depletion	
Goat anti-rabbit IgG, biotinylated	IHC	Vector Laboratories
Goat anti-rabbit, Texas red-conjugated	IF	Vector Laboratories
Mouse 3E7 (pan opioid)	FC	Gramsch Laboratories
Mouse anti-rat CD3 (G4.18) PE/FITC	FC	Pharmingen
Mouse anti-rat CD4 (Ox-35) PE/FITC	FC	Pharmingen
Mouse anti-rat CD4 microbeads	MACS	Miltenyi Biotec
Mouse anti-rat CD45 microbeads	MACS	Miltenyi Biotec
Mouse anti-rat CD45RA microbeads	MACS	Miltenyi Biotec
Mouse anti-rat CD8 microbeads	MACS	Miltenyi Biotec
Mouse anti-rat MHC class II	MACS	Miltenyi Biotec
Rabbit anti-rat beta-endorphin	RIA	Peninsula Laboratories
Rabbit anti-rat beta-endorphin IgG	IF, IHC	Peninsula Laboratories
Rabbit anti-rat met-enkephalin IgG	IF, IHC	Peninsula Laboratories
Prohormone convertase 1/3	IF	Donald Steiner, Chicago
Prohormone convertase 2	IF	Donald Steiner, Chicago
Dicer	IF	Abcam
ProSAAS	IF	Abcam

Abbreviations used: IF = immunofluorescence, IHC = immunohistochemistry, FITC = fluorescein isothiocyanate conjugate, FC = flow cytometry, MACS = magnetic cell separation, RIA = radioimmunoassay.

2.1.4 siRNA

Table 2.4 List of siRNA

siRNA name	Application	Company
Control siRNA sc-37007	Electroporation	Santa Cruz

Dicer(rat) sc-270275	Electroporation	Santa Cruz
PCSK1 (rat) sc-270276	Electroporation	Santa Cruz
PC2 (rat) sc-270277	Electroporation	Santa Cruz

2.1.5 Chemicals, kits

Table 2.5 List of chemicals and kits

Name	Company
β-mercaptoethanol	C. Roth GmbH
Agarose LE	Roche
Ampicillin	E. Merck AG
Bovine serum albumin (BSA)	Sigma-Aldrich
Bovine collagen type II	MD Bioproducts, Zurich
Bordetella pertussis toxin (PTX)	Calbiochem, La Jolla, CA
Bradford reagent	Biorad
Bromphenol blue	Sigma-Aldrich
Collagenase II	Sigma-Aldrich
Complete Freund's adjuvant (CFA)	Calbiochem
Concanavalin A (con A)	Sigma-Aldrich
Cytokine array	Ray Bio
Deoxy-nucleotide triphosphate mix (dNTP)	Roche
Dextran 500	Amersham Pharmacia Biotech
Dithiothreitol (DTT)	Sigma-Aldrich
Donkey serum	Jacksons Immuno Research Laboratories
DNA molecular weight markers (100 bp)	Roche

Ethanol (99%)	C. Roth GmbH
Ethidium bromide	Sigma-Aldrich
EZ DNA methylation kit	Zymo research
Fast Start DNA Master SYBR Green I Kit	Roche
Fetal bovine serum (FBS)	Biochrom AG
Glycerol	Sigma-Aldrich
Glycine	Sigma-Aldrich
Goat serum	Vector Laboratories
Horse serum	Biochrom
Hyaluronidase	Sigma-Aldrich
Imidazole	Sigma-Aldrich
Interleukin (IL-2 rat, recombinant)	R & D Systems
Interleukin (IL-4 rat, recombinant)	R & D Systems
Interleukin (IL-6 rat, recombinant)	R & D Systems
Interleukin (IL-6 Rα rat, recombinant)	R & D Systems
Interleukin (IL-10 rat, recombinant)	R & D Systems
Isofluran Curamed ((1-Chlor-2,2,2-trifluorethyl) difluormethylether)	Rhodia
JAK II inhibitor	Calbiochem
Leptin	Sigma-Aldrich
Leukaemia inhibitory factor (LIF)	Sigma-Aldrich
mBSA (methylated bovine serum albumin)	Sigma-Aldrich
Methanol	C. Roth GmbH
Normal rabbit IgG	Sigma-Aldrich
pan-JAK inhibitor	Calbiochem

Paraformaldehyde (PFA)	Sigma-Aldrich
Penicillin/streptomycin (10,000 U / 10,000 µg/ml)	Biochrom
Phosphate buffered saline (PBS, sterile, 0.1 M, pH 7.4)	GIBCO Invitrogen Corporation
Primer dT for cDNA synthesis (oligo dT)	Roche
Pyridon 6	Calbiochem
Qiaquick gel extraction kit	QIAGEN
rat-beta-endorphin kit	Peninsula Laboratories
RB108	Calbiochem
RNAse-free DNAse (1500 U/µl)	Macherey- Nagel
Nucleospin RNA II	Macherey- Nagel
RPMI-1640 medium (+Glutamax I)	GIBCO Invitrogen Corporation
Saponin from *Quillaja* bark	Sigma-Aldrich
Sodium dodecyl sulphate (SDS)	Sigma-Aldrich
STAT-5 inhibitor	Calbiochem
Tissue-Tek compound	OCT Miles
Trishydroxymethylaminomethane (Tris)	Sigma-Aldrich
Triton X-100 (t-Octylphenoxy-poly-ethoxyethanol)	Sigma-Aldrich
Trypan blue stain (0.4%)	GIBCO Invitrogen Corporation
Trypsin/EDTA	GIBCO Invitrogen Corporation
Xylene cyanole FF	Sigma-Aldrich

2.1.6 Oligodeoxynucleotides

Oligonucleotides purchased from TIBMOLBIOL. Primer names, sequences, base pairs, melting temperature (Tm) and primer type are given. Names indicate the target gene.

Table 2.6 List of oligodeoxynucleotide sequences

Name	Sequence (5`- to -3`)	bp	Tm (°C)	Primer type
POMC2ex2se	TGGCCCTCCTGCTTCAGAC	19	63.8	Se
3POMCex3as	CTCACTGGCCCTTCTTGTGC	20	63.2	As
rat-RPL19b-as	TGCTCCATGAGAATCCGCTTG	21	65.8	As
ratRPL19b-se	AATCGCCAATGCCAACTCTCG	21	66.7	Se
Rat GAPDH-se	ACAGTCAAGGCTGAAAATGG	20	54.5	Se
Rat GAPDH as	CATGAGCCCTTCTACAATGC	20	54.5	As
PC2 primer se	GAGAGGAGACCTGAACATCA	20	50.4	Se
PC2 primer as	GCAAGCCCTTCTGTGGTGCA	20	63.5	As
7B2 se	AATCCAGCATTCGCTTATAG	20	50.7	Se
7B2 as	TAGGAATATTGTCGCCAGTC	20	50.9	As
PC1/3 se	AATCCTGTAGGCACCTGGAC	20	55.8	Se
PC1/3 as	GGAGTTTTTGGGTACCAGGA	20	55.6	As
PC2 FW (new)	GGGCCCACAGACAACGGGA	20	66	Se
PC2 RV (new)	GCCGTCGTTGATGGCCGAGT	20	68	As
Rat Dicer FW	GTGGCGCTGAGACCGCAACT	20	65.3	Se
Rat Dicer RV	AGGGTCCCAGGACGACCAGC	20	65.0	As
Rat proSAAS FW	GGCCGGGGGCGTAGGCCTTT	20	71.1	Se
Rat proSAAS RV	CGCCAGCTCCTGCACCGCAC	20	70.9	As
Rat Ctsl1 FW (cathepsin L)	TGTGGCTAACGACACAGGGT	20	61.4	Se

Rat Ctsl1 RV (cathepsin L)	GCAGTGGTTGTTCCGGTCTT	20	60.8	As
Ap-B (RNPEP) FW (aminopeptidase B)	GGCCATTGGAGATCTGGCTT	20	60.11	Se
Ap-B (RNPEP) RV (aminopeptidase B)	TTGGCATTGGTGACCAGGTT	20	60.11	As
IL-10 F1	TGGCTCAGCACTGCTATGTT	20	59.67	Se
IL-10 R1 (rat)	GGCTTGGCAACCCAAGTAAC	20	59.68	As

2.1.7 Other materials

Table 2.7 List of instruments used

Instruments	**Company**
Cell counting chamber	Glaswarenfabrik Karl Hecht
Cell scraper	Sigma-Aldrich
Cell strainer (70 µm mesh)	BD Biosciences Discovery Labware
Cryostat (Microm HM560)	MICROM
Electrophoresis apparatus (Power Pac 300)	Bio-Rad Laboratories
Flow cytometry apparatus (FACS Calibur)	Becton-Dickinson
Fluorescence microscope	Carl Zeiss Mikroskope
Gamma-Counter, Wallac Wizard 1470	Wallac
Heraeus incubator	Kendro
Kryo tubes	Nunc
Laminar flow (Hera Safe)	Kendro
Microscope (Axiovert 25)	Carl Zeiss Mikroskope
Photometer (Gene Quant II RNA/DNA calculator)	Pharmacia Biotech
pH meter	Mettler Toledo
Separation columns (mean size)	Miltenyi Biotec

Separator (VarioMACS™)	Miltenyi Biotec
Sterile filters	Millipore
Real time PCR	Eppendorf
Thermocycler (Mastercycler personal)	Eppendorf
Tubes (15 and 50 ml)	Falcon
Twin tech real time PCR plates 96 well	Eppendorf
Ultrapure Water Systems (Direct-Q™ 5)	Millipore
UV-Light (Macro Vue UV=25)	Hoefer

2.2 Methods

2.2.1 Animals and animal housing

Experiments were carried out using male WISTAR rats (Janvier, France), (200-250)g and female Balb/c mice (Janvier, France 10–14 weeks of age). They were housed in cages lined with ground corncob bedding. Standard laboratory rodent chow and tap water were available *ad libitum*. Room temperature was maintained at 22°C and a relative humidity between 40% and 60% was maintained. A 12/12 hr (7 a.m. / 7 p.m.) light/dark cycle was used. Experiments were approved by the animal care committee of the State of Berlin and strictly followed the guidelines of the International Association for the Study of Pain (Zimmermann 1983).

2.2.2 Animal models

2.2.2.1 CFA-induced inflammation

Rats received an intraplantar (i.pl.) injection of 0.15 ml complete Freund's adjuvant (CFA) into the right hind paw under brief isoflurane anaesthesia. This inflammatory model is routinely used in our own as well as in other research groups (Stein et al., 1988; Barber et al., 1992). From 2-96 hours after CFA injection, there is a swelling of the paw tissue, hyperaemia and hyperalgesia (animals showing an increased sensitivity to pain). During the observation period

the inflammation remained confined to the right paw and no significant changes were observed in feeding behaviour, body weight, body temperature, and general activity range compared to untreated animals (Stein et al., 1988). Control animals remained untreated.

2.2.3 Rat cell and tissue preparation

Using an overdose of inhalation anaesthesia (isoflurane), rats were killed, then decapitated and then the skull and brain overlying the pituitary were dissected. Care was taken to cut the pituitary stalk, and the pituitary with the remaining stalk were then dissected free of the *sella turcica* on the base of the skull. The pituitary gland was taken and immediately stored at –80°C; cDNA was prepared as described in (2.3.10.3). Popliteal lymph nodes (LNs) draining the CFA-treated rat hind paw or in case of untreated animals, popliteal and inguinal LNs from both sides were dissected. Embedded fat tissue around the LN was thoroughly removed using scalpels. The tissue was homogenized using sterile plastic pestles and blades. Cells were dissociated from homogenates using 70 µm and 40 µm mesh cell strainers and suspended in sterile-filtered 1x phosphate buffered saline (PBS) or RPMI-1640 medium. In parallel to cell counting, the cell viability was examined via the trypan blue exclusion method using Fuchs-Rosenthal cell counting chambers. Finally, cell suspensions were used for various experimental procedures such as magnetic cell sorting (MACS), flow cytometry, immunohistochemistry, immunofluorescence, electroporation, RNA-isolation, *ex vivo* stimulation and radioimmunoassay (RIA) or the cells were pelleted for storage at –20°C for subsequent RIA or PCR analysis.

2.2.4 Magnetic cell sorting (MACS)

Freshly isolated rat and mouse cells as described in (2.3.3.) were centrifuged for 10 min at 450 × g at room temperature and then resuspended in 1 ml of RPMI medium-1640 medium (+Glutamax I). Then 20 µl/10^7 cells of (1) anti-rat CD8, (2) anti-rat CD45RA, (3) anti-rat CD4, (4) anti-mouse CD45, or (5) anti-rat MHC class II (OX6) microbeads were added to isolate cell subsets from the cell suspensions. Samples were incubated for 15 min at 6 °C sitting on a slow rotor socket. Thereafter, cells were washed twice in RPMI medium to remove unbound beads.

Labelled cell suspensions were loaded onto separation columns placed in a magnetic field according to the manufacturers' instructions. Unlabelled cells passing the magnetic field were collected as negative fractions (e.g. $CD8^-$, $CD45RA^-$ etc.). To collect the labelled cells, the columns were removed from the magnetic field and rinsed with RPMI medium under high pressure. The labelled cells were collected as positive fractions (e.g. $CD8^+$ or $CD45RA^+$). Fractions were then centrifuged for 5 min at 4 °C and 350 × g. Supernatants were removed and cell pellets were resuspended in PBS for cell counting. Separated cells were subjected to release or cell stimulation experiments or they were used for gene/protein expression analysis (PCR, RIA, immunohistochemistry).

2.2.5 Rat LN cell experiments

2.2.5.1 Stimulation of total LN cells

Unseparated LN cells (1 - 2 x 10^7 cells/well) were loaded on 6-well plates and serum-free RPMI-1640 medium supplemented with 1% penicillin/streptomycin was added to a final volume of 3 ml/well. IL-2 (20 ng/ml), IL-4 (10 ng/ml), IL-5 (25 ng/ml), IL-6 (10 ng/ml), IL6-Rα (100 ng/ml), IL-10 (50 ng/ml), Leptin (10 ng/ml), and leukaemia inhibitory factor (LIF, 10 ng/ml) and/or the mitogen concanavalin A (ConA, 1 µg/ml) were added to the culture medium. Cells were subsequently incubated for 2 - 24 h at 37°C and 5% CO_2. Control cells were incubated without stimulating agent.

2.2.5.1.1 Treatment with methyltransferase and histone deacetylase inhibitors

A DNA methyltransferase inhibitor was used to study the effect of methylation on POMC gene expression, based on (Brueckner et al., 2005). 2-(1,3-Dioxo-1,3-dihydro-2H-isoindol-2-yl)-3-(1H-indol-3-yl)propionic acid (RG108) is a small molecule that effectively blocked DNA methyltransferases *in vitro* in human cancer cell lines (B cells: NALM-6, colon: HCT116). We supplemented media with 10% fetal bovine serum and RG108 to a final concentration of 10 µM, and primary naïve LN-derived cells were harvested after 7, 10, and 15 days followed by RNA isolation, cDNA synthesis and qRT-PCR analysis for POMC gene expression. The serum-containing medium and RG108 were refreshed every 5 days.

The histone deacetylase inhibitor trichostatin A interferes with deacetylation and produces an accumulation of acetylated histones, which is expected to enhance transcription. A final concentration of 1 µM trichostatin A was applied for 24 to 120 h followed by RNA isolation, cDNA synthesis and qRT-PCR analysis for *Pomc* gene expression.

2.2.5.2 Stimulation of LN cell subsets and T cell supernatant transfer experiments

Magnetically separated T and B cells (1 - 2 x 10^7 cells/well) were loaded onto different 6-well plates and serum-free RPMI-1640 medium supplemented with 1% penicillin/streptomycin was added to a final volume of 3 ml/well. Different cytokines and/or inhibitors were added to the culture medium RPMI.

2.2.5.2.1 Cytokine stimulation and inhibitor treatment of lymphocytes

Naïve lymphocytes were incubated with microbeads (CD45RA, MHC class II from Miltenyi Biotech) and separated into T and B cells using MACS separation columns. B cells were unstimulated; T cells were pre-treated with cell-permeable small molecule inhibitors (Calbiochem, EMD Chemicals Inc., Darmstadt, Germany) prior to the addition of IL-4. Pyridon 6 (a pan-JAK inhibitor) and STAT-5 inhibitor were added at concentrations of 0.3, 0.6 and 1 µM for 30 min. 2 h after the addition of IL-4 (10 ng/ml), the supernatants from T cells were collected and transferred to untouched B cells. After B cell stimulation for 2 h at 37 °C, cells were collected on ice, centrifuged and pellets were stored at −80 °C. (Fig. 2.1) depicts a scheme of the experimental procedure.

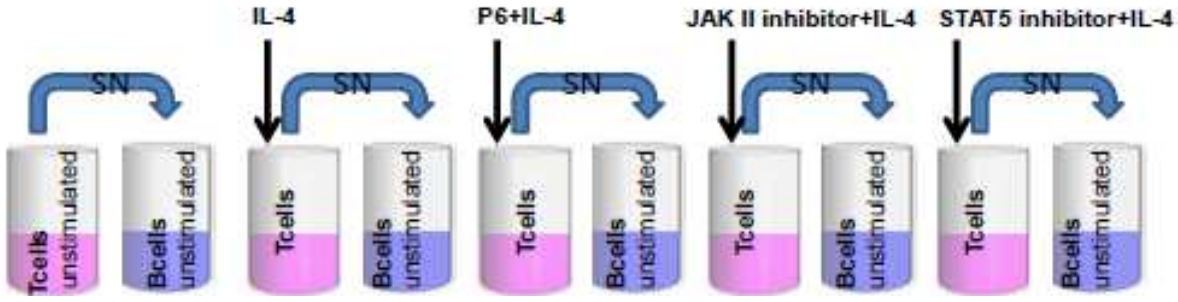

Figure 2.1 Primary naïve T and B cells were separated from dissociated LN cells using anti-CD45RA microbeads and MACS columns. T cells were pre-treated for 30 min with/without inhibitors prior to the addition of IL-4. Controls were left untreated. After 2 h of IL-4 stimulation, the

supernatant from T cells was collected and transferred to untouched B cells. B cells were exposed to the T cell supernatants for 2h.

In a second series of experiments, B cells were pre-treated with cell-permeable small molecule inhibitors (Calbiochem, EMD Chemicals Inc., Darmstadt, Germany). Pyridon 6 and STAT-5 inhibitor were added at final concentrations of 0.3, 0.6, and 1 µM each and incubated for 30 min at 37 °C. Meanwhile, T cells were stimulated with IL-4 for 2h, and then the supernatant from the T cells was collected and transferred to pre-treated B cells. After 2 h of B cell stimulation at 37 °C, cells were collected on ice, centrifuged and pellets were stored at −80°C. (Fig. 2.2) depicts a scheme of the experimental procedure.

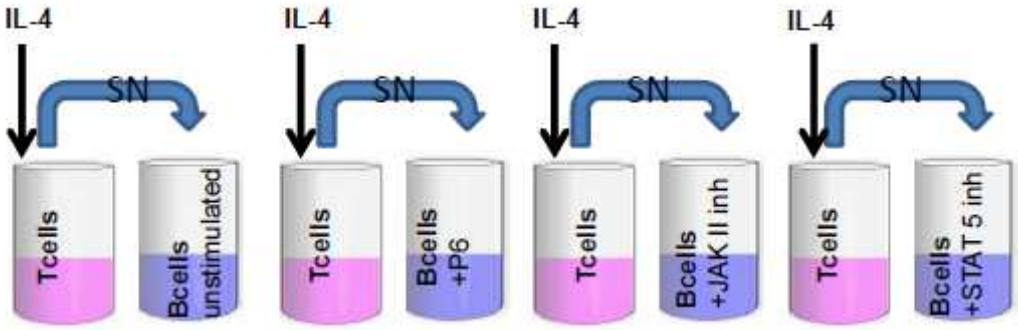

Figure 2.2 Primary naïve T and B cells were separated from dissociated LN cells using anti-CD45RA microbeads and MACS columns. B cells were pre-treated for 30 min with inhibitors, controls were left untouched. T cells were stimulated with IL-4 but not with inhibitors; After 2 h the supernatant was transferred to the pre-treated B cells. B cells were exposed to the T cell supernatant for 2 h.

2.2.5.3 Electroporation of rat LN cells for siRNA delivery

Lymphocytes were isolated from rat LNs as described in (2.3.3), and vital cells were treated with hypotonic solution. We chose to deliver siRNA using two different electrical devices: one system was developed by a research group at the Charité Campus Benjamin Franklin (Thorsten Stroh of the AG Siegmund); the other is a commercially available Multiporator system from Eppendorf. The AG Siegmund setup can produce high voltage/low duration and low voltage/long duration pulses, which can be used as single pulses or can be combined as double pulses. The application of a double pulse (1^{st} pulse: 400-500 volts for 100 microseconds, 2^{nd} pulse: 200 volts for 10 milliseconds) delivered a FITC-tagged control siRNA (BLOCKiT, Invitrogen) most efficiently after 24 to 48 h (75% uptake,

approx. 50% viability) as monitored using flow cytometry analysis with the help of Dr. Rainer Glauben (AG Siegmund, Department of Internal Medicine with Gastroenterology and Nephrology, Charité Universitätsmedizin Berlin, Campus Benjamin Franklin). The cell number was 2-3 million per sample. The pulse profile of the Eppendorf Multiporator does not offer a similar double pulse condition. This system instead runs a profile of an exponential voltage drop every 5 microseconds (soft pulse technology) in combination with a hypoosmolar electroporation buffer. A starting pulse of 600 volt and a time constant of 25 microseconds produced similar uptake and viability rates to those obtained with the AG Siegmund setup. The electroporated cells were suspended in a medium containing penicillin, streptavidin, and FBS (fetal bovine serum) and incubated for different time periods ranging from 1 to 7 days. The cells were spun down, and the pellet was used for either real-time PCR or western blot. When used for real-time PCR, the samples were prepared as described in section (2.2.10) to analyse the mRNA expression.

2.2.6 Preparation of knee joint cells from ACIA mice and release experiments

The knees that had received the intraarticular (i.a.) mBSA-injections were dissected; the knee capsule was cut into halves. The knees were digested in 3 ml RPMI-1640 medium containing 9 mg hyaluronidase and 3 mg collagenase II per ml for 45 min at room temperature. The soft tissue surrounding the bones was thoroughly removed and ground. The homogenate was transferred into new tubes via 70 micron and later through 40 micron sieves and rinsed with enzyme-free medium. After spinning for 10 min at 450 x g at room temperature, the supernatant was discarded and the cells were resuspended in 1 ml culture medium and incubated with 25 µl anti-mouse CD45 micro beads for 15 min at 4 ºC in a rotor. Samples were spun down again at 2,000 rpm for 10 min at 4 ºC to remove unbound beads. The supernatant was discarded, and the pellets were resuspended in 1 ml medium. Cells were counted and resuspended in 250 µl pure medium and kept for 2 h at 37 ºC under agitation (350 rpm). Later the tubes were spun down (2,000 rpm for 10 min) at 4 ºC and supernatants and pellets were stored at –80ºC for further analysis of opioid peptide release and cellular content, respectively, using RIA.

2.2.7 Radioimmunoassay (RIA), enzyme immunoassay (EIA) and cytokine array

Immunoreactive Met-enkephalin (ir-MENK) was determined using a RIA kit. All substances were dissolved in 1 × RIA buffer. Mouse knee cells were isolated as described in 2.2.6. Whole cell lysates were prepared from frozen cell pellets via freeze-and-thaw lysis in 200 µl RIA buffer. Freezing and thawing was repeated five times: first, samples were kept for 5 min in liquid nitrogen; they were then quickly thawed in a water bath (22 °C) and briefly vortexed. After a final incubation of 10 min on ice, the samples were centrifuged for 10 min at 27,000 × g and 4 °C to remove debris. Clear cell lysates (100 µl each) were used for measurements thereafter. Supernatants (100 µl each) from release experiments as detailed above (2.2.6), were directly used for RIA measurements without further processing steps. All samples were prepared in duplicate. Serial diluted MENK standards containing 1-1,280 pg MENK / 100 µl RIA lysis buffer were prepared in parallel using a standard peptide supplied by the company. Then, antiserum (100 µl) was added to all tubes except the total count, non-specific binding, and total binding tubes. According to the manufacturers' specifications, the rabbit anti-MENK does not cross-react with other agents such as Dynorphin, β-Endorphin, or ACTH. Tubes were incubated for 16-24 h at 4 °C. Then 100 µl ^{125}I-labeled MENK with 11,000-15,000 counts per minute (CPM) was added to each tube, and tubes were left for another 16-24 h at 4 °C. Thereafter, 100 µl each of goat anti-rabbit IgG and normal rabbit serum were added to all samples in order to precipitate antibody-protein complexes. The reaction was stopped after 90-120 min at room temperature by adding 0.5 ml RIA buffer. Finally, tubes were spun at 3,000 rpm for 20 min at 4 °C. Supernatants were aspirated of all except total count tubes, and the radioactivity in the pellets was counted as CPM in a gamma-counter. To determine specific binding, the mean CPM of non-specific binding samples was subtracted from all other samples. The CPM thereby decreases with an increasing peptide concentration of the unknown samples or standard peptide. The amount of ir-MENK was calculated in pg/well.

The β-endorphin-immunoreactivity (ir-END) was determined using an END enzyme immunoassay (EIA). The remaining supernatants (approximately 50 µl each) from release experiments as described in (2.2.6), were directly used for EIA

measurements without further processing steps. The release of END was determined in cell supernatants using a human/rat-fluorescent EIA kit according to the manufacturers' instructions (Phoenix Peptides Inc.). Wells of EIA plates were loaded with 25 µl of the supernatants per well and incubated overnight at 4 ºC. Then 25 µl of biotinylated peptide was added and incubated at room temperature for 1.5 h, and the plates were washed with the buffer three times before adding 100 µl SA-HRP (streptavidin-horseradish peroxidise) solution for 1 h. The plate was washed three times and incubated with 100 µl substrate solution at room temperature for 20 min. The reaction was terminated by stop solution. The fluorescence intensity was measured with a plate reader. The amount of ir-END was assessed in duplicate and calculated in pg/well from the standard curve.

Cytokine release was analysed using RayBio Rat Cytokine Antibody Array 2 kits (RayBiotech, Inc., Norcross, GA, USA) following the manufacturers' instructions. Array membranes carrying antibodies for the detection of 34 cytokines and anti-rat IgG (loading control) were incubated with T cell supernatants for 2 h. After washing, the membranes were incubated for 2 h with a mixture of biotin-conjugated antibodies, followed by peroxidase-conjugated streptavidin. Immunoreactive dots were subsequently visualized using an enhanced chemiluminescence (ECL) system, and membranes were exposed to autoradiograph hyperfilms for 10 to 40 seconds. Films were scanned and pictures were analysed using Image J. After inverting the pictures, the background signal was measured at the negative control spots of the blot using an area of fixed size. This background signal was subtracted from all other measurements. The signal of each antibody spot was determined and recorded as 'intensity'.

2.2.8 Cytospins

Cells were counted using Fuchs-Rosenthal cell counting chambers and cell viability was examined with the trypan blue exclusion method. 1.5 million cells were taken for cytospin in a volume of 100-200 µl of PBS. Before plating the cells, slides were cleaned to remove any greasy stains. A filter paper and a cuvette were placed on the slide. To the cuvette 300 µl of 1 x phosphate-buffered saline (PBS) were added before spinning at 300 rpm so that the filter paper was wet and did not absorb the cells. Next, 100 to 200 µl of cell suspension containing approximately 1.5 million cells were loaded into the cuvette followed by another spinning at

300rpm to gently plate the cells onto the slide. Once the cells were plated, the slides were used for immunofluorescence stainings.

2.2.9 Immunofluorescence stainings

Cells that were plated on slides were dried and then fixed with 4% PFA and 4% sucrose for 30 min at room temperature and washed three times with PBS for 10 min each. Non-specific binding was prevented by incubating the slides for 30 min at room temperature or overnight at 4 °C in blocking buffer (0.1 M PBS, 0.3% Triton X-100, 1% BSA, 4% goat or donkey serum). The slides were then incubated overnight at 4 °C or for 2 h at 37 °C with primary antibodies (anti-PC1, anti-PC2, anti-END, anti-MENK, anti-Dicer). Unbound antibody was removed by washing three times with PBS for 10 min each. Incubation with the secondary antibody was performed for 1 h at 37 °C followed by three washes with PBS. The slides were dried, and the cover slips were sealed with 10 µl of Mowiol. After the Mowiol hardened, the slides were imaged using a fluorescence microscope system and the AxioVision program (Zeiss Axioskop 2). Image analysis was performed using Image J (Version 1.47 developed by the NIH) as follows:

At first, fluorescence intensity was measured for the sample incubated with the secondary antibody only to determine the background threshold. This threshold was subtracted from the fluorescence of all other images. Then the number of particles above threshold, their area, and the mean fluorescence was determined using the option ‘analyse particles’ in Image J. The size of single cells was measured using the circle tool and values of 30 cells were used to obtain a mean area. This mean was used to calculate the cell numbers from the total area above the threshold determined with the particle analyser. The mean fluorescence and cell numbers above threshold were plotted on graphs.

2.2.10 Gene expression analysis

2.2.10.1 Total RNA preparations

Total RNA was prepared using the Total RNA Isolation NucleoSpin RNA II kit (Macherey and Nagel) following the manufacturers' protocol. Fresh or frozen cells or tissues (pituitary and LN) were homogenized in 4 M guanidine thiocyanate buffer containing 10 µl β-mercaptoethanol per ml. Homogenates were loaded onto

shredder columns to remove cell debris by spinning samples for 1 min at 11,000 rpm at room temperature. After adding 70% ethanol to the flow-through, samples were immediately mixed and then transferred to silica membranes to bind DNA and RNA. The membranes were desalted using membrane desalting buffer (MDB). To remove DNA, membranes were treated with RNase-free DNase for 15 min. Subsequently, membranes were washed with wash buffers provided by the kit. Total RNA was eluted in 30-40 µl RNase free ddH_2O and stored at –80°C. RNA was isolated from LN or pituitary tissue on separate days to avoid contamination.

2.2.10.2 RNA/DNA quantification and quality

The amount of single-stranded RNA or double-stranded DNA was measured photometrically at a wavelength of λ = 260 nm. An $A_{260\ nm}$ = 1 corresponds to a concentration of 40 µg RNA/ml or 50 µg DNA/ml. The quality of RNA and purity of DNA was verified by $A_{260\ nm}/A_{280\ nm}$ ratios. This ratio lies between 1.5 and 1.9 for intact RNA and between 1.75 and 2.0 for DNA.

2.2.10.3 First-strand synthesis and negative controls

Total RNA (1 - 2.5 µg/15.6 µl) was reverse-transcribed in 26 µl reaction mixture containing 0.2 µg/ml primer oligo dT, heated for 3 min at 63 °C and subsequently chilled on ice. Then the following reagents were added to a final volume of 30 - 40 µl: 1 $\times$ RT reaction buffer (50 mM Tris HCl, pH 8.3; 75 mM KCl, 3 mM $MgCl_2$), 10 µM dithiothreitol (DTT), 1 µM deoxynucleotide triphosphate mix (dNTP), 1 U RNAse inhibitor and 6 U AMV reverse transcriptase (RT). For negative controls, RT was replaced by RNase-free H_2O (RT^-). Mixtures were incubated for 120 min at 42 °C. cDNA was stored at –20°C thereafter.

2.2.10.4 PCR primers

Oligodeoxynucleotides were designed by applying the OLIGO Primer Analysis Software Version 5.0 for Windows (Wojciech Rychlik, National Biosciences, Inc., Plymouth, MN) and were purchased from TIBMOLBIOL (Berlin, Germany). Primer pairs designed for the amplification of *β-actin, PC1, PC2,*

Cathepsin-L, Aminopeptidase B, Pomc, Sfrp1, Dicer, and *IL-10*, were exon-intron spanning.

2.2.10.5 Real-time quantitative reverse-transcription PCR (qRT-PCR) analysis

Quantitative real-time PCR was performed using the FastStart DNA Master PLUS SYBR Green 1 kit according to the manufacturers' instructions (Roche). Real-time PCR was performed using the Mastercycler ep realplex (Eppendorf). The final reaction volume of 20 µl contained 25 pM antisense primer, 25 pM sense primer, 1 × PCR buffer with 2.0 mM $MgCl_2$, 0.8 mM dNTPs, 1U AMV polymerase and either 2 µl template or RT^- control. Positive controls contained 2 µl pituitary (P) or placenta (PL) cDNA; negative controls (NC) were supplemented with 2 µl ddH_2O. Each assay started with an initial denaturation cycle of 10 min at 95 °C, followed by 40-45 amplification cycles (8 sec/95 °C denaturation, 8 sec/55-68 °C annealing, and 8-20 sec/72 °C for extension). Detailed PCR conditions for *Pomc*, *Dicer*, *PC1*, *PC2*, *Sfrp1*, and *β-actin* mRNA are listed in table 2.8.

Table 2.8 RT-PCR conditions for different gene transcripts

Gene	AT (annealing temperature) ºC / sec	Elongation	TM (melting temperature)	Fragment size
β-Actin	68	72 ºC / 10	85	191
POMC	63	72 ºC / 27	89	668
PC1	55	72 ºC / 10	82	254
PC2	69	72 ºC / 10	87	207
Cathepsin L	62	72 ºC / 13	83	312
Aminopeptidase B	62	72 ºC / 13	85	312
Dicer	67	72 ºC / 11	82	251
IL-10	60	72 ºC / 10	86	241
Sfrp1	60	72 ºC / 20	91	492

Data were analysed using the master cycler software (Eppendorf, Hamburg, Germany). The excess of background emission by specific amplification was automatically determined as a crossing point (CP). The relative expression of target mRNAs was evaluated in treated vs. control conditions and relative to the

expression of β-Actin as housekeeping gene by applying the delta-delta CP method previously described by PE Applied Biosystems (Perkin Elmer, Foster City, CA). Samples were always analysed as a set that was amplified together in the same qRT-PCR run. The 'relative expression ratio' of target mRNAs was calculated following the equations previously described by de Longueville and colleagues (2003):

$$\Delta CP = CP_{POMC} - CP_{Actin}$$

$$\Delta\Delta CP = \Delta CP \text{ treated} - \Delta CP \text{ control}$$

$$\text{Relative expression ratio} = 2^{-\Delta\Delta CP}$$

2.2.10.6 Melting curve analysis

Subsequent to amplification, qRT-PCR products were heated from 65 °C to 95-99 °C using a temperature transition rate of 0.1 °C / sec following the manufacturers' instructions. The level of fluorescence (F) was measured continuously during heating, changing relative to (1) the presence or absence of PCR products and (2) to the temperature (T). Melting curves – providing information about product specificity – were automatically calculated by the Eppendorf system and plotted as the ratio of changes of fluorescence to temperature changes [$-\Delta F1/ \Delta T$] over temperature. Curves obtained from pituitary material were used as a positive control to evaluate LN-derived qRT-PCR products with the exception of Sfrp1 expression, which is not expressed in the pituitary. Control cDNA was used from placenta instead. Products were cooled down to 4 °C thereafter.

2.2.10.7 Agarose gel electrophoresis

Electrophoresis was run at 110 volts constantly for 40 min in 1 x TBE buffer (100 mM Tris base, 100 mM boric acid, 2.5 mM EDTA). Therefore, 20-25 µl PCR products were mixed with 4-5 µl agarose gel sample buffer (0.25% bromphenol blue, 50 mM Tris pH 7.6, 60% glycerol, H_2O) and transferred to 1% agarose gels (1 x TBE, 1% agarose, 1 µl Midori green or 4 µl Midori green advanced/100ml).

A 100 bp DNA ladder (Roche, Germany) was run in parallel to estimate sizes of PCR products. PCR products were imaged with a Biorad documentation system.

2.2.11 Bisulfite sequencing

2.2.11.1 Bisulfite modification

Bisulfite modification of DNA occurs in three steps including sulphonation, deamination and desulphonation (Hayatsu et al., 1976; Shapiro et al., 1973; Shapiro et al., 1970). After these processes all unmethylated cytosine bases are converted into uracil, while methylated cytosine bases do not change. During PCR amplification uracil bases are replaced by thymine (Roux et al., 1995). This allows methylated cytosines to be distinguished from unmethylated cytosines during downstream analysis.

2.2.11.2 Process of bisufite modification

An EZ DNA methylation kit was used for bisulphite modification. The protocol used followed the manufacturers' instructions without modifications. According to this protocol, 5 µl of M-dilution buffer was added to genomic DNA (1 µg). The total reaction volume was 50 µl in each tube with nanopure water. Solutions were mixed by pipetting up and down. Sample tubes were incubated at 37 ˚C for 15 min in a PCR thermal cycler. After incubation, 100 µl freshly prepared CT conversion reagent was added to each tube and mixed well. These sample tubes were kept in a PCR machine and 20 PCR cycles were programmed. Each cycle consisted of 95˚C for 30 seconds and 50 ˚C for 15 min. Following cycling, the samples were cooled to 6 ˚C. They were then added to 400 µl of M-binding buffer in Zymo-Spin™ IC columns and these columns were placed into collection tubes. The solutions were mixed by gently pipetting up and down. The columns with collection tubes were centrifuged at >10,000 x *g* for 1 min. Flow-through was discarded after every centrifuge step unless otherwise stated. 200 µl M-wash buffer was added to each column and centrifuged at full speed for 1 minute. 200 µl M-desulphonation buffer was added to the columns and left at room temperature (20 ˚C to 30 ˚C) for 15 min in the dark. The columns were centrifuged at full speed for 1 min. 200 µl M-wash buffer was added and centrifuged at full speed for 1 min. This step was

repeated, followed by another centrifugation for 2 min. Then the columns were placed into 1.5 ml microcentrifuge tubes and 10 µl dH_2O was added. The tubes were centrifuged for 1 min at full speed, and bisulphite-modified DNA was eluted. Bisulphite-modified DNA is not stable and has to be stored at –80 °C.

2.2.11.3 PCR conditions

Usually we used 35 to 45 cycles for successful PCR amplification of bisulfite-converted DNA. The protocol includes 5-10 cycles for priming, followed by 35 to 40 amplification cycles. Annealing temperatures were 50-70°C. UTR primers were designed for the untranslated regions of the sequence. C-free primers were designed to bind to both the untranslated and bisulfite-converted sequences, as they are independent of cytosine residues. Bisulfite-specific primers (BSP) were designed to amplify converted DNA. Different BSP primers were designed to amplify regions with different product sizes and nested BSP primers were also designed. Methylation-specific primers (MSP) bind specifically to methylated sites that could virtually appear at any CpG sites in a CpG island, but those primers were also based on the converted DNA sequence. We designed such primers to distinguish methylated from unmethylated sites of the *Pomc* locus, taking advantage of the sequence differences resulting from bisulphite modification. MSP primers were designed using the methyl primer express design tool from Applied Biosystems.

Table 2.9 List of UTR and C-free primers – sequences, length and PCR conditions are given

Name	**Sequence (5`- to -3`)**	**bp**	**Tm (°C) 5 cycles / 40 cycles**	**Primer type**
UTRrPOMCse1(234)	CTGCCTTGGGCTGCCATGATTCT	23	65/70	sense
UTRrPOMCse2 (235)	CTCTGTCCAGTCCTGAGTGGAG	22	65/70	sense
UTRrPOMCas (236)	GGTTAAGGAGCAGTGACTAAGAGAGGC	27	65/70	antisense
C-free POMC FW	TTGGAATAAGTATTGGGGATGGAGA	25	55/65	sense
C-free POMC RV1	GGAGGAGAAAAGAGGTTAAGGAG	23	55/65	antisense
C-free POMC RV2	AGGTATAAAAGAAGAGAGAAGAGTGA	26	55/65	antisense

Table 2.10 List of BSP primers – sequences, length, and PCR conditions are given

Name	Sequence (5`- to -3`)	bp	Tm (°C) 5 cycles / 40 cycles	Primer type
BSP (FW) 116	TTGTTTTGGGTTGTTATGATTTT	23	55/65	sense
BSP (FW) 118	AGGTAGTTTGTTTTGGGTTGTT	22	55/65	sense
BSP (FW) 120	TTTTGTTTAGTTTTGAGTGGAG	22	55/65	sense
BSP (RV) 117, 119, 121	GGTTAAGGAGTAGTGATTAAGAGAGGT	27	55/65	antisense

Table 2.11 List of MSP primers – sequences, length, and PCR conditions are given

Name	Sequence (5`- to -3`)	bp	Tm (°C) 5 cycles / 40 cycles	Primer type
MSP_1_FW 261	TAATATTGGGGAAATTTGATGT	22	50/62	sense
MSP_1_RV 801	AACCAAAACACCCTTACCTATC	22	50/62	antisense
MSP_2_FW 199	TGTTGTTTTTTTTTTTGAAAT	21	50/62	sense
MSP_2_RV 621	CCTTCCTAACAACACTTCTAC	21	50/62	antisense
MSP_3_FW 261	TATTGGGGAAATTTGATGC	19	50/62	sense
MSP_3_RV 801	AACCGAAACACCCTTACCTA	20	50/62	antisense
MSP_4_FW 199	GTTGTTTTTTTTTTCGAAAC	20	50/62	sense
MSP_4_RV 621	CTTCCTAACAACGCTTCTAC	20	50/62	antisense

2.2.11.4 Purification of PCR products via gel extraction

After electrophoretic separation, PCR product bands were cut out, and DNA was extracted from the gel by using the QIAGEN gel extraction kit according to the manufacturers' instructions. DNA was eluted in 30-40 µl H_2O and was sent for sequence analysis to LGC Genomics GmbH (Berlin, Germany).

2.2.12 Immunohistochemistry (IHC) of arthritic mouse knees

Animals were killed and both knee joints were fixed in 4% buffered formaldehyde, decalcified with EDTA, and embedded in paraffin. Serial sections (4–5 µm thick) were cut and stained with haematoxylin eosin (HE) for microscopic evaluation. Dr. Uta Baddack scored the knee sections in a blinded manner, examining three sections per knee joint. A three parameter scoring system was

used, where individual scores comprise the following: acute score (exudate: 1–3 points, granulocytes infiltrating the synovial membrane: 1–3 points, fibrin exudates: 1 point), chronic score (synovial hyperplasia: 1–3 points, mononuclear cells infiltrating the synovial membrane: 1–3 points, fibrosis: 1–3 points), cartilage and bone destruction (1–3 points).

For immunohistochemistry, paraffin sections were deparaffinised using xylol acetone and unmasked by heat. For staining, the following primary antibodies were used: anti-CD3e (goat, Santa Cruz Biotechnology, Santa Cruz, CA), anti-β-endorphin (Bachem Group, Peninsula Laboratories, UK). For detection, biotinylated donkey anti-goat, donkey anti-rat or peroxidase-coupled donkey anti-goat antibodies were added, followed by streptavidin-conjugated alkaline phosphatase (all from Jackson ImmunoResearch, Newmarket, UK). Enzyme reactions were developed with AECþSubstrate Kit (DAKO) or Fast Blue substrate (Sigma-Aldrich).

2.2.13 Statistical analysis

All data were processed using Microsoft Excel 2003 for Windows (Microsoft Corporation) and GraphPad Prism Version 5.01 for Windows (GraphPad Software, Inc.). GraphPad Prism was used for the statistical analysis. Data were analysed for equal variance and for normal distribution using the D'Agostino & Pearson omnibus normality test. Normally distributed data were analysed by Student t-test and nonparametric data by Mann-Whitney-U-Test if two independent groups were compared. In case of dependent data, the paired t-test and the Wilcoxon signed rank test were used to analyse normally distributed and non-parametric data, respectively. Multiple measurements of normally distributed, independent data were analysed with the One-Way ANOVA test or the Kruskal-Wallis test in case of not normally distributed data. Dependent data were analysed using the One-Way Repeated Measurers ANOVA or the Friedman test to compare more than two groups with a normal or non-parametric distribution, respectively. Post hoc comparisons were performed with Dunnett's multiple comparison test for normally distributed data and with Dunn's method for not normally distributed data. For all tests, statistical significance was considered if $P < 0.05$. Data represent the mean ± the standard error of the mean (SEM).

3 Results

3.1 Regulation of pro-opiomelanocortin (*Pomc)* mRNA expression

Full-length *Pomc* mRNA is difficult to detect in naïve lymphocytes. Therefore we hypothesized that it may be repressed under unstimulated conditions. We studied different mechanisms that may either interfere with *Pomc* gene expression or strengthen the degradation of *Pomc* mRNA.

3.1.1 Possible repressive mechanisms regulating *Pomc* mRNA expression in lymphocytes

3.1.1.1 Repression by methylation or acetylation

To investigate the possible role of DNA methylation in the expression of *Pomc*, primary naïve LN cells were treated *in vitro* with IL-4 in order to stimulate *Pomc* expression as previously described (Busch-Dienstfertig et al, 2012) or were left untreated (see section 2.2.5.1), and genomic DNA was isolated from separated T and B cells thereafter. DNA strands were subjected to bisulfite treatment (see section 2.2.11), which normally results in the conversion of unmethylated cytosines (C) into uracils (U) while methylated cytosines remain unaffected. A sequence of approximately 700 bp in total, comprising the 5`-upstream untranslated region (UTR) and exon 1 of the *Pomc* gene, was amplified using RT-PCR and different primer combinations (see section 2.2.11.3). Before bisulfite conversion, the DNA strands were amplified using UTR primers to test the integrity of the *Pomc* locus and were inspected electrophoretically. The PCR products generated from bisulfite converted DNA strands were also separated via agarose gel electrophoresis (see section 2.2.10.7), selected by size, and directly sequenced to screen for cytosine replacements by uracil. Sequence analyses after bisulfite treatment showed no clear peaks, which indicates that either nucleotides were unreadable or nucleotides were not successfully converted and were identical to unconverted genomic DNA. Therefore, the results were inconclusive.

Next, we tried to address the question about DNA methylation by using DNA methyltransferase inhibitors based on the paper by Brueckner and colleagues (2005). The authors used 2-(1,3-Dioxo-1,3-dihydro-2H-isoindol-2-yl)-3-(1H-indol-3-yl)propionic acid (RG108), a small molecule that was shown to effectively block DNA methyltransferases *in vitro* in human cancer cell lines. We supplemented media with

RG108 and kept primary LN-derived cells from healthy animals in culture. The inhibitor was added at a final concentration of 10 µM, and cells were harvested after 5, 10, and 15 days followed by RT-PCR analysis (see section 2.2.10.5). *β-Actin* levels confirming the quality of cDNA and RT PCR are given in (Fig. 3.1 A). As a positive control, we amplified *Sfrp*1 mRNA. The *Sfrp*1 gene is known to be suppressed by methylation and upregulated upon RG108 treatment in HCT116 cells (HCT 116 Cell Line human colon carcinoma). *Sfrp*1 mRNA was not expressed in untreated LN cells but was detectable in RG108-treated LN cells after 15 days (Fig. 3.1 B). No *Pomc* mRNA expression was detected in untreated or RG108-treated cells at the time points investigated (Fig. 3.1 C). Together, these results suggest that *Pomc* mRNA is not expressed after DNA demethylation in these cells.

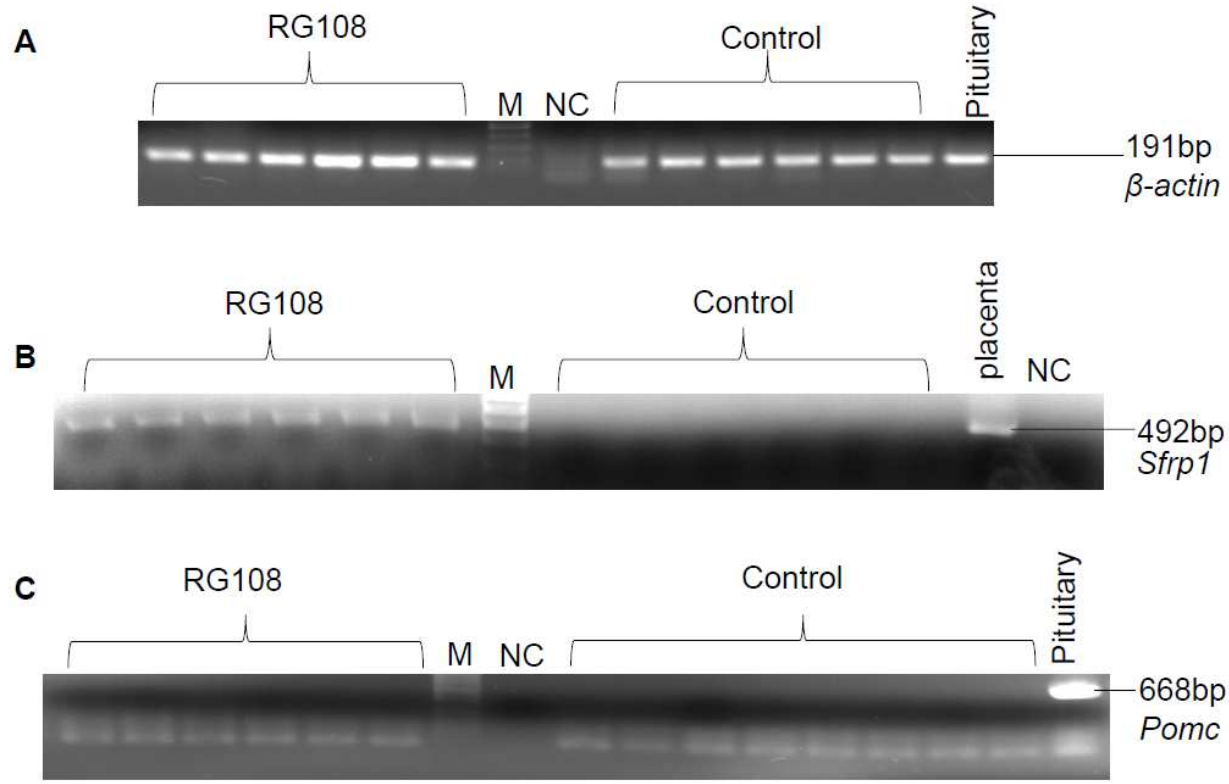

Figure 3.1 Effect of RG108 on *Pomc* and *Sfrp1* gene expression in lymphocytes Unseparated primary, naïve LN-derived cells were treated with 10 µM RG108, harvested after 15 days, and followed by RNA isolation, cDNA synthesis, and PCR. Number of independent experiments: n = 6. **A** shows the expression of *β-actin*; pituitary cDNA served as positive control. **B** shows *Sfrp1* mRNA expression; placenta cDNA served as positive control. **C** shows *Pomc* gene expression (*Pomc* mRNA transcripts); pituitary cDNA served as positive control. All PCR products were electrophoretically separated by size by using agarose gel electrophoresis. A DNA marker (M) was run in parallel to estimate the product size. NC = water control. Control = untreated cells kept under otherwise identical conditions.

A reduced transcriptional activity can also be related to the deacetylation of histones, which increases the affinity of histone proteins to DNA. The histone deacetylase inhibitor trichostatin A produces an accumulation of acetylated histones, which is expected to enhance transcription by decreasing the histones' affinity to DNA. However, treatment of lymph node cells with 1 µM trichostatin A for 24 h did not increase *Pomc* gene expression (Fig. 3.2 A). *β-Actin* was used as an internal control (housekeeping gene) to confirm cDNA quality and RT-PCR efficacy.

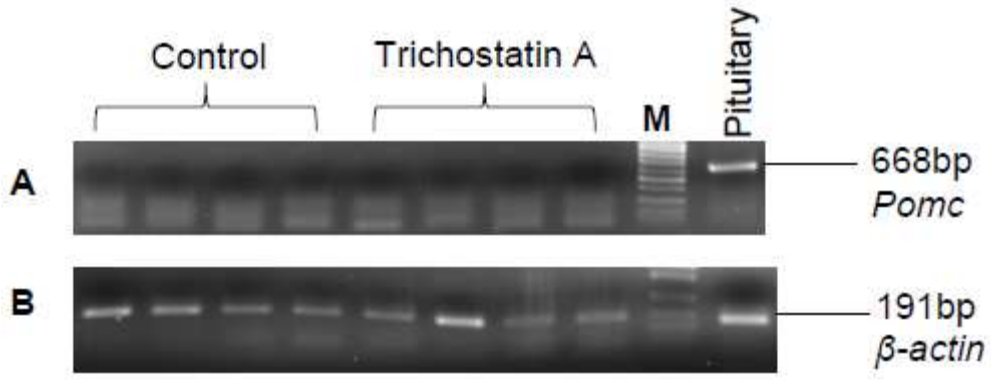

Figure 3.2 Effect of trichostatin A on *Pomc* gene expression in lymphocytes Unseparated primary, naïve LN-derived cells were treated with 1 µM of trichostatin A, harvested after 24 h, followed by RNA isolation, cDNA synthesis, and PCR. Number of independently performed experiments: n = 4. PCR products were electrophoretically separated by size using agarose gel electrophoresis. **A**: *Pomc* gene expression (*Pomc* mRNA transcripts). **B**: *β-actin* expression. Pituitary cDNA served as positive control. M = DNA marker. Control = untreated cells kept under otherwise identical conditions.

Finally, cells were treated with both 10 µM RG108 and 1 µM trichostatin A. The cells were incubated in the presence of RG108 for 5, 10, and 15 days as in the previous experiments, and trichostatin A was added on the 4th, 9th, and 14th day (24 h before harvesting the cells). *Sfrp1* expression was observed only in the cells treated with RG108 and trichostatin A (Fig. 3.3 A), confirming that *Sfrp1* expression is suppressed by DNA methylation. *β-Actin* expression attested to the RT efficiency and cDNA quality of the samples (Fig. 3.3 B). No increase in *Pomc* gene expression was detectable in treated versus untreated cells (Fig. 3.3 C). Together these results indicate that *Pomc* gene repression in lymphocytes is not diminished by demethylation or increased acetylation.

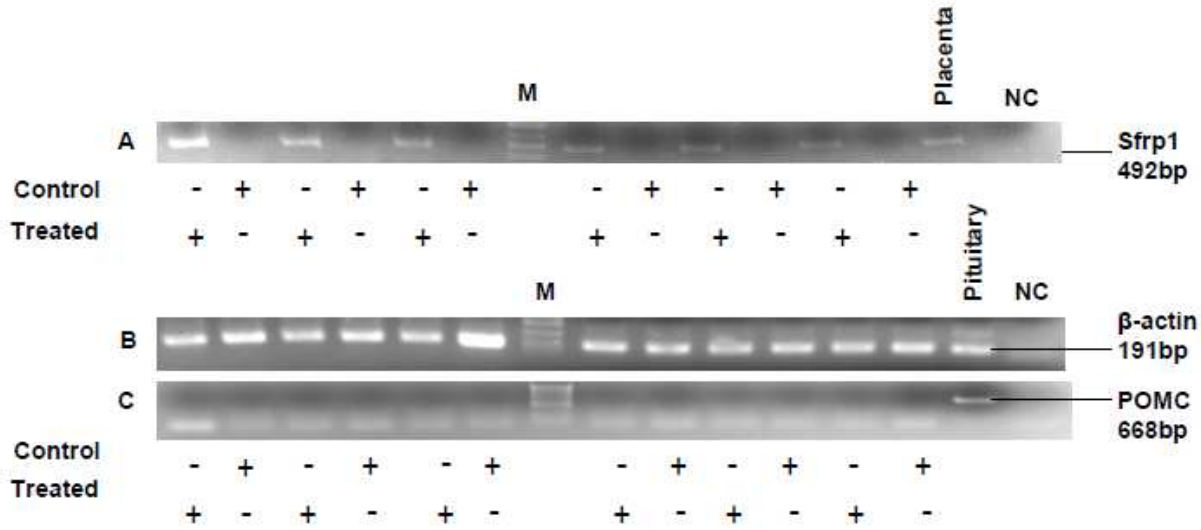

Figure 3.3 Effect of combined RG108 and trichostatin A treatment on *Pomc* and *Sfrp1* gene expression in lymphocytes Unseparated primary, naïve LN-derived cells were treated with 10 µM of RG108, harvested after 5, 10, and 15 days. Only the 15 day treatment is shown. Moreover, cells were treated with 1 µM trichostatin A for 24 h prior to harvesting, followed by RNA isolation, cDNA synthesis, and PCR. Number of independent experiments: n = 6. **A**: *Sfrp*1 mRNA expression; placenta cDNA served as positive control. **B**: *β-actin* mRNA amplicons. **C**: *Pomc* mRNA transcripts; pituitary cDNA served as positive control. Treated = RG108 + trichostatin A. Control = untreated cells kept under otherwise identical conditions. M = DNA marker. NC = water control.

3.1.1.2 Repression by miRNAs

Many genes are post-transcriptionally regulated by miRNAs. To assess the relevance of miRNAs for *Pomc* regulation in lymphocytes, primary naïve LN cells were transfected with Dicer siRNAs *in vitro* and Dicer knockdown was investigated using qRT-PCR. We tested different methods of chemical siRNA transfer (Lipofectamine 2000, Fugene, etc.) using a fluorescent control siRNA. The uptake was investigated using flow cytometry, but no conclusive results were obtained. We therefore used electroporation (see section 2.2.5.3), although this approach can be accompanied by massive cell death. We chose to deliver siRNA using two different electrical devices as described in (section 2.2.5.3). The conditions were optimized for the uptake of approximately 80% of the fluorescent control siRNA and for at least 40% cell viability as determined by flow cytometry using the apoptotic marker propidium iodide. A significant *Dicer* mRNA knockdown was observed after 48 h of electroporation using the double-pulse strategy when compared to electroporation with non-target (scrambled) siRNA (Fig. 3.4 A). Non-electroporated cells of the same animal were always investigated in parallel to determine baseline gene expression. As a positive control, we amplified *IL10* mRNA, which is known to be regulated upon knockdown of Dicer (Sharma et al., 2009). *IL-10* mRNA was detectable in non-

electroporated and scrambled siRNA-pulsed cells but was undetectable in Dicer siRNA-pulsed cells (Fig. 3.4 C). Dicer knockdown had no effect on *Pomc* mRNA expression (Fig. 3.4 B).

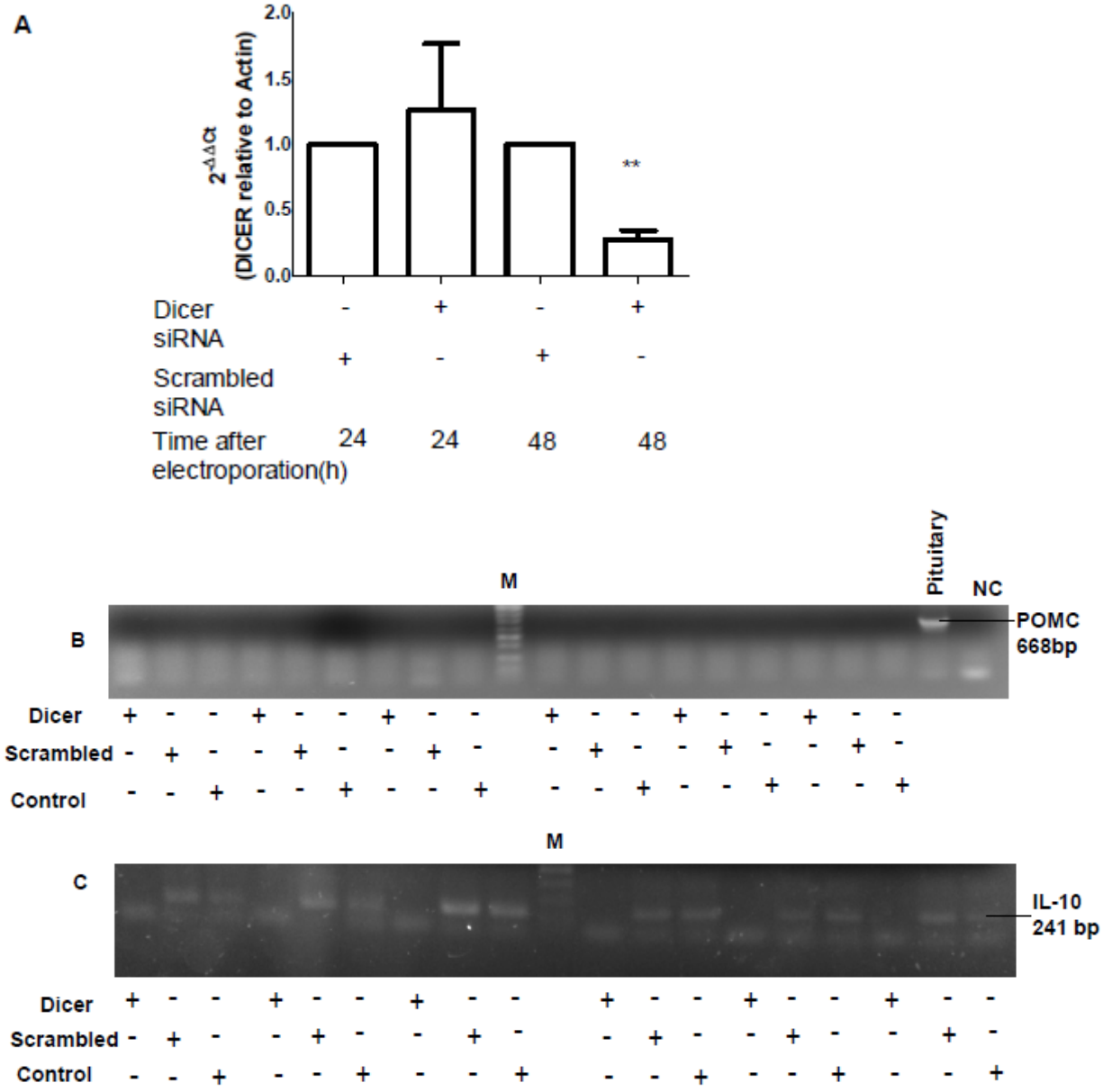

Figure 3.4 *Dicer* knockdown using electroporation A: Primary, naïve LN cells were treated with 100 µl of transfection buffer and 100 µM Dicer or non-target siRNA. Cells were harvested after 24 or 48 h followed by qRT-PCR analysis. Data were calculated using the delta-delta CP method and represent the mean ± SEM fold change in *Dicer* mRNA levels in relation to treatment with scrambled siRNA (these levels were set to 1). Statistical analysis was performed using the Kruskal-Wallis test and Dunn's multiple comparison test. ** $P < 0.01$ ($n = 6$). Gel electrophoresis of *Pomc* mRNA (**B**) and *IL-10* mRNA (**C**) transcripts in electroporated and non-electroporated samples after 48 h. Control = unpulsed/non-electroporated cells kept under otherwise identical conditions.

To further examine the effect of Dicer knockdown on *Pomc* mRNA expression, we used soft pulse technology as described (in section 2.2.5.3) and harvested the cells after 5, 6, and 7 days of electroporation for analysis via PCR and immunocytochemistry. Only the results after 5 d of electroporation are shown (Fig. 3.5), since cell viability at 6 and 7 days was strongly impaired. (Fig. 3.5 A) shows that none of the treatments had any effect on *Pomc* mRNA expression.(Fig. 3.5 B) shows successful knockdown of *Dicer* mRNA in *Dicer* siRNA-pulsed cells. (Fig. 3.5 C) shows *β-actin* levels confirming the quality of cDNA and PCR. Control experiments showed a loss of *IL-10* mRNA expression in *Dicer* siRNA-pulsed cells (Fig. 3.5 D). The knockdown of Dicer protein at day 5 post electroporation is shown in (Fig. 3.6). The mean fluorescence intensity per cell was significantly decreased in *Dicer* siRNA electroporated cells as compared to basal levels determined in cells electroporated with scrambled siRNA (Fig. 3.6). Together, these results indicate no definite relevance of miRNA in the regulation of *Pomc* mRNA.

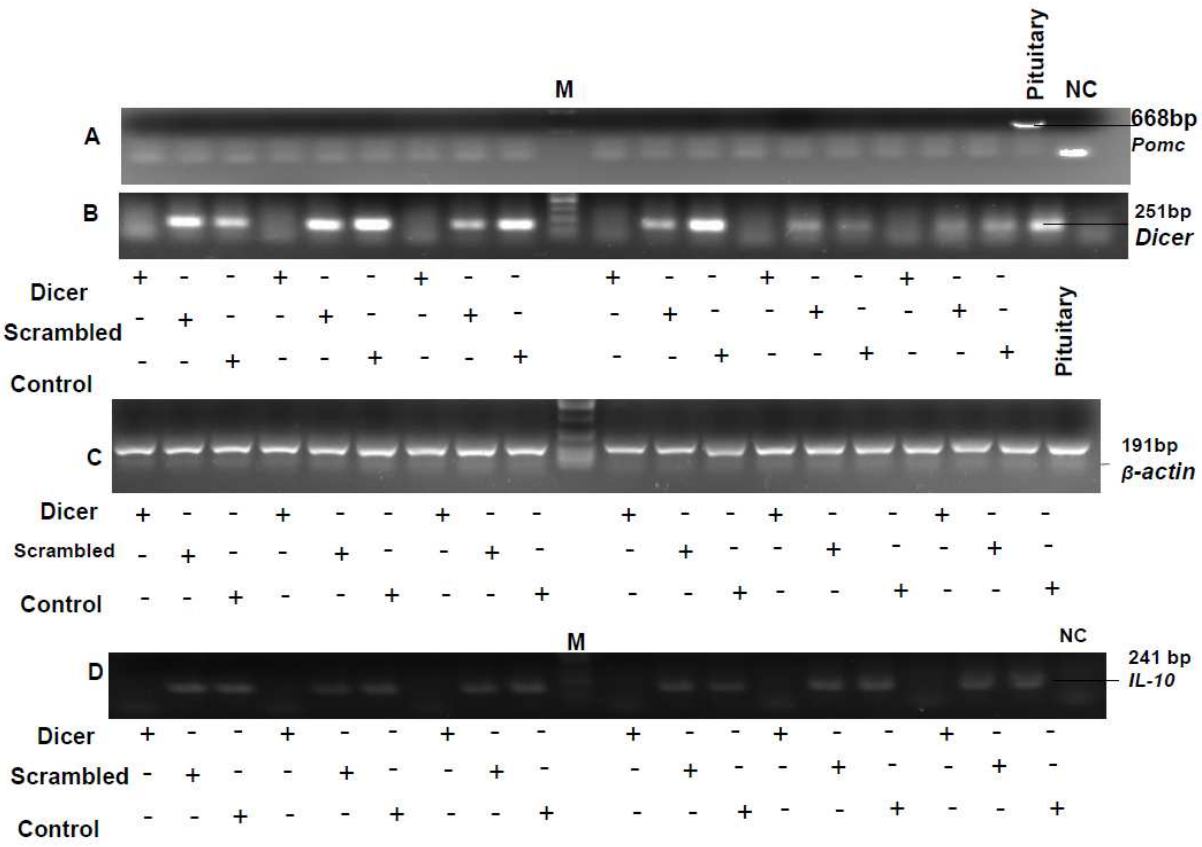

Figure 3.5 Effects of *Dicer* siRNA on mRNA expression of *β-actin*, *Pomc, Dicer*, and *IL-10* using soft pulse technology Primary, naïve LN cells were treated with 100 µl of transfection buffer and 100 µM Dicer or non-target siRNA. Cells were harvested after 5 days, followed by PCR. **A**: *Pomc* mRNA transcripts, pituitary cDNA served as positive control. **B**: *Dicer* mRNA; pituitary cDNA served as positive control. **C**: *β-actin* mRNA. **D**: *IL-10* mRNA. A DNA marker was run in parallel to estimate the product size. Number of independent experiments n=6 per group.

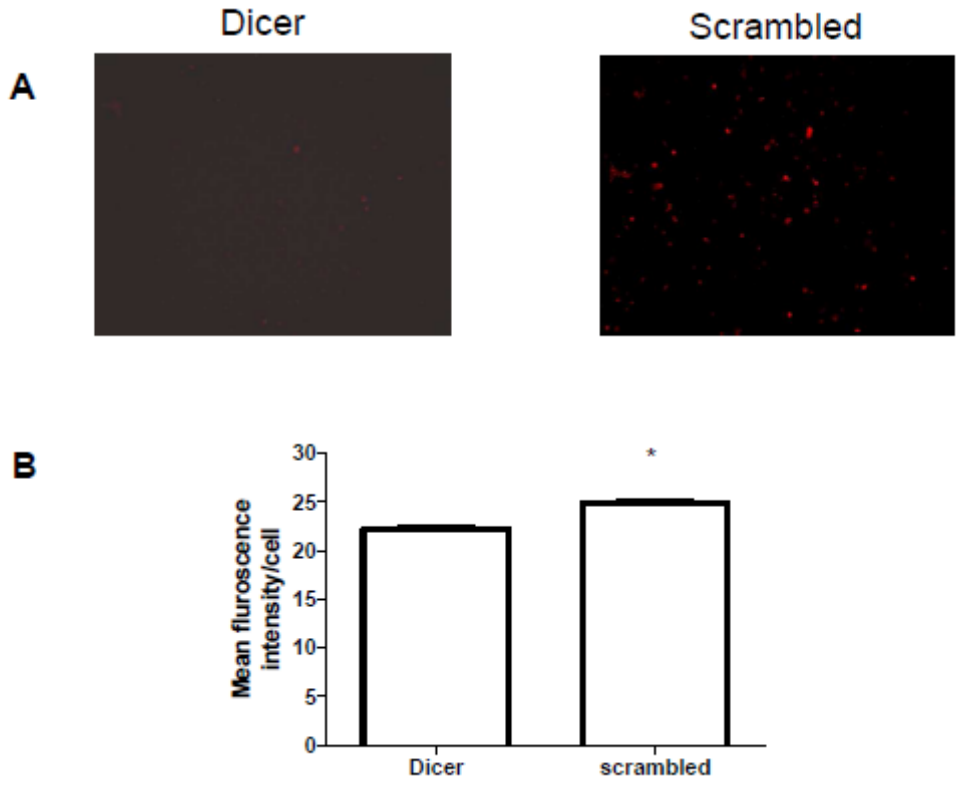

Figure 3.6 *Dicer* siRNA-induced Dicer protein knockdown using electroporation Primary, naïve LN cells were treated with 100 µl transfection buffer and 100 µM *Dicer* or non-target siRNA. Cells were harvested after 5 days. Isolated cells were transferred to object trays after centrifugation for immunofluorescence analysis. **A**: representative anti-Dicer stainings of cytospin preparations after treatment with *Dicer* siRNA and scrambled siRNA. **B**: mean fluorescence intensity per cell after treatment with *Dicer* siRNA and scrambled siRNA (n = 6 animals per group). Statistical analyses were performed using the Wilcoxon signed rank test. * $P < 0.05$.

3.1.2 Expression of *Pomc* mRNA after cytokine stimulation in subsets of T and B lymphocytes.

Previous studies indicated that *Pomc* is not expressed in naïve lymphocytes but is expressed upon stimulation. It was shown that *Pomc* gene expression is stimulated by IL-4 *in vitro* (Busch-Dienstfertig et al., 2012) and is upregulated in the draining LN after induction of complete Freund's adjuvant (CFA) paw inflammation *in vivo* (Sitte et al., 2007). Here we investigated *Pomc* mRNA expression in separated T and B cells of dissociated popliteal LNs dissected 2-4 h after injection of CFA into the rat hind paw. (Fig. 3.7), *Pomc* mRNA transcripts were present in B ($CD45RA^+$) but not in T cells ($CD45RA^-$). *In vitro* IL-4 treatment for 2 h increased *Pomc* mRNA expression in B cells only (data not shown), while both cell populations derived from naïve LNs expressed *pomc* mRNA after 24 h of cytokine stimulation. After 24 h exposure to IL-4, B cells showed a significantly stronger relative elevation than T cells (Fig. 3.8).

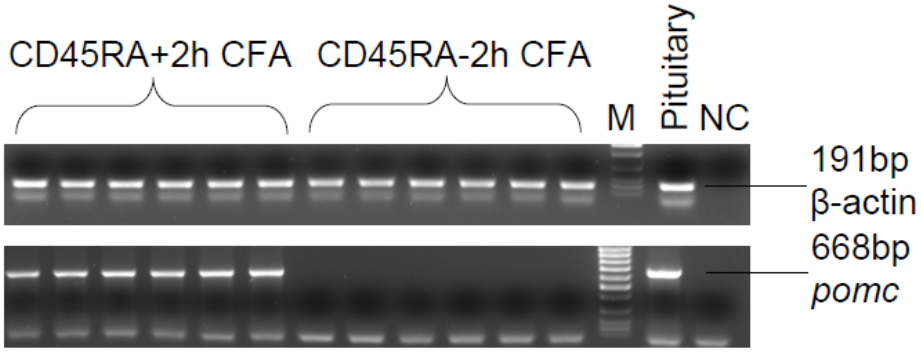

Figure 3.7 *In vivo* expression of *Pomc* mRNA in T and B cells from rat lymph nodes Popliteal LNs were dissected and separated using anti-CD45RA microbeads into T ($CD45RA^-$) and B cells ($CD45RA^+$) 2h after induction of hind paw inflammation by an i.pl. CFA injection. *Pomc* mRNA transcripts were analyzed using PCR (n = 6 nodes). *β-Actin* mRNA transcripts, pituitary cDNA served as positive control. *pomc* mRNA transcripts, pituitary cDNA served as positive control.

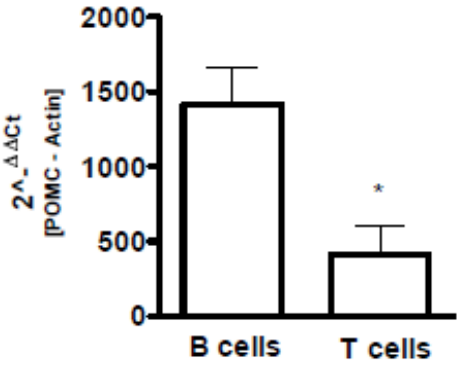

Figure 3.8 *In vitro* expression of *Pomc* mRNA in IL-4-treated T and B cells Primary, naïve LN cells were stimulated *in vitro* with IL-4 for 24 h and subsequently separated using anti-CD45RA microbeads into T ($CD45RA^-$) and B cells ($CD45RA^+$); the target gene expression was normalised to *β-actin* gene expression. Number of independently performed experiments: n = 7. Data were calculated using the delta-delta CP method and represent the mean ± SEM fold change. Pairwise comparison was performed using the Wilcoxon signed rank test, *$p < 0.05$.

3.1.2.1 Signaling pathways and interactions between T and B cells *in vitro*

Previous studies showed that IL-4 induces *Pomc* mRNA expression in lymphocytes, which is partially mediated via the JAK/STAT pathway involving tyrosine-phosphorylated STATs 1 and 3 but not STAT 6 or MAP kinases such as ERK 2 or p38 (Busch-Dienstfertig et al., 2012). As described in the previous paragraph, an upregulation of *Pomc* mRNA expression was detected in B cells, when T and B cells were incubated together for 2 h in the presence of IL-4. However, when T and B cells were incubated separately with IL-4, no elevation of *Pomc* mRNA expression was observed (in either T or B cells, data not shown), indicating that

interaction between the two cell types is required. Since *in vivo* activation of LN cells following paw inflammation also resulted in *Pomc* gene expression in B but not in T cells (Fig. 3.7), more attention was hereupon directed to B cells. When the supernatant of IL-4-treated T cells was transferred to purified B cells, an upregulation of *Pomc* mRNA expression was detectable (Fig. 3.9). Together, these results show that B cells express *Pomc* mRNA in a T cell-dependent manner, which is contrary to our initial hypothesis.

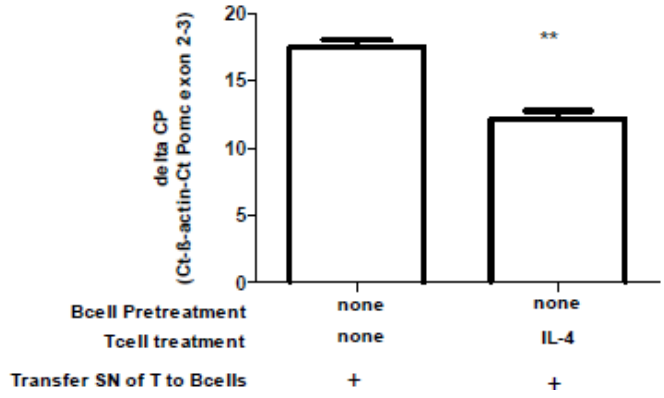

Figure 3.9 IL-4–stimulated *Pomc* mRNA expression in B cells Primary, naïve T and B cells were separated from dissociated LN cells using anti-CD45RA microbeads and MACS columns. T cells were untreated or pre-treated with IL-4. After 2 h, the supernatant (SN) from T cells was collected and transferred to untreated B cells. Number of independently performed experiments: n = 5. B cells were harvested 2 h after SN transfer and pellets were processed for the analysis of *Pomc* mRNA levels. Data were calculated using the delta CP method and represent the mean ±SEM *Pomc-β-actin* mRNA levels. Statistical analysis was performed to compare delta CP values determined in untreated B cells exposed to the SN of unstimulated *versus* IL-4-treated T cells using Mann Whitney test. **P < 0.01. Lower delta CP values indicate higher *Pomc* mRNA expression.

Next we used cell permeable inhibitors to interfere with the JAK/STAT pathway activated by IL-4. Pyridon 6 is a pan-JAK inhibitor, whereas JAKII and STAT-5 inhibitors are selective. The experiments shown in (Fig. 3.10) demonstrate that previously untreated B cells express *Pomc* mRNA when stimulated with the supernatant of IL-4-treated T cells. This effect was inhibited by pre-treatment of T cells with pyridon 6 and with STAT-5 inhibitor (Fig. 3.10 A); the JAKII inhibitor had no significant effect. Pre-treatment of B cells with pyridon 6 and STAT-5 inhibitor resulted in significantly decreased *Pomc* mRNA levels after adding supernatants from T cells treated with IL-4 (Fig. 3.10 B), while pre-treatment of B cells with JAK II inhibitor seemed to increase this gene expression.

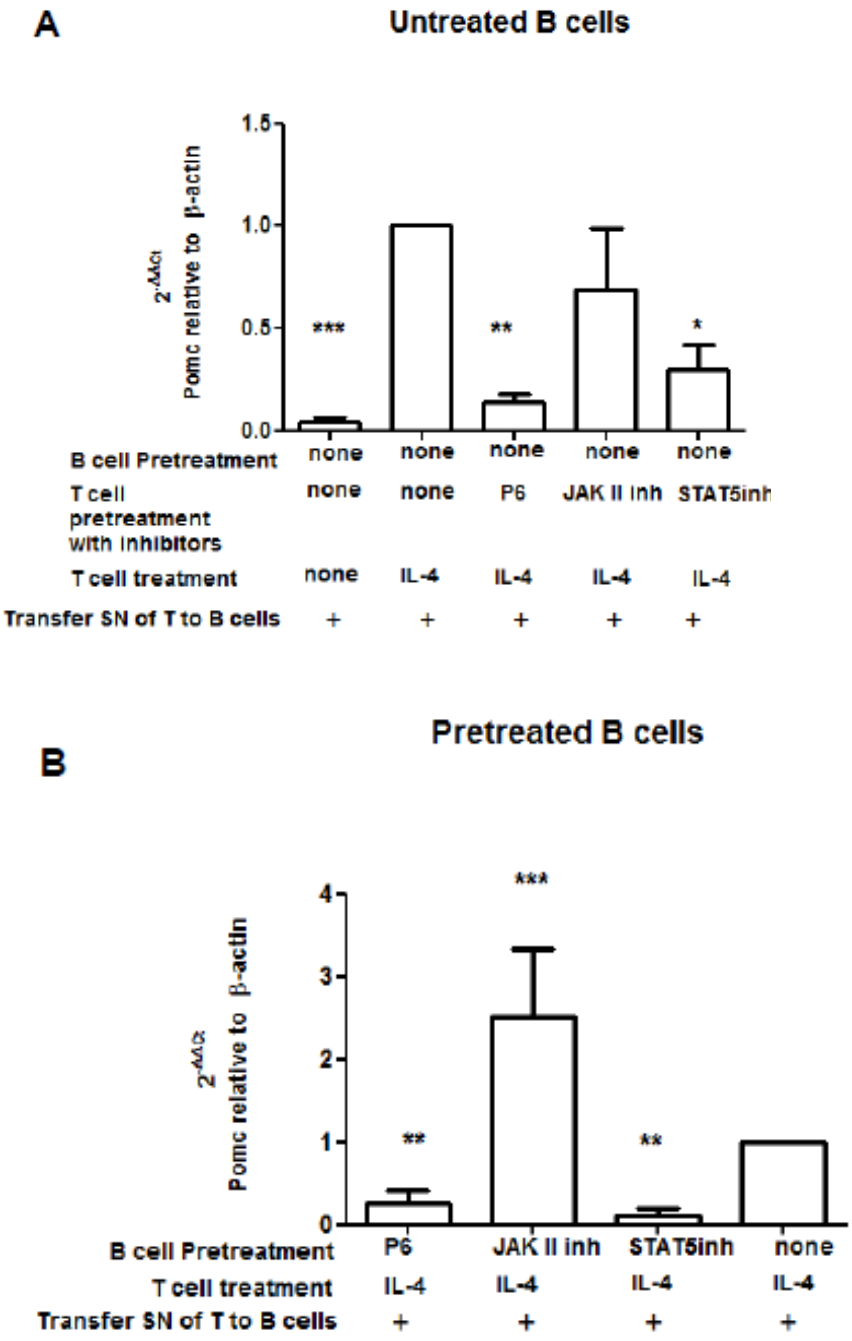

Figure 3.10 Effect of JAK/STAT inhibitors on IL-4–stimulated *Pomc* mRNA expression in B cells
Naïve T and B cells were separated from dissociated LN cells using anti-CD45RA microbeads and MACS columns. **A**: T cells were pre-treated for 30 min with/without inhibitors prior to the addition of IL-4. Controls were left untreated. After 2 h, the supernatant (SN) from the T cells was transferred to untreated B cells. Number of independent experiments: n = 5. **B**: B cells were pre-treated for 30 min with inhibitors, controls were left untreated. T cells were stimulated with IL-4 and after 2 h the SN was transferred to the pre-treated B cells. Number of independent experiments: n = 5. In both setups B cells were harvested 2 h after SN transfer, and pellets were processed for the analysis of *Pomc* mRNA levels. Data were calculated using the delta-delta CP method and represent the mean ± SEM fold change of *Pomc* mRNA expression over levels determined in untreated B cells exposed to the supernatant of IL-4-treated T cells that were set to 1. Statistical analysis was performed using Friedman test and Dunn's multiple comparison test. *P < 0.05; **P < 0.01; *** P < 0.001. Inhibitors: P6 = pyridon 6, JAKII inhibitor, STAT-5 inhibitor.

These findings indicated that IL-4, via JAK/STAT activation, leads to the release of a factor from T cells, which in turn mediates *Pomc* gene expression in B cells. The results in (Fig. 3.10 B), indicate that the JAK/STAT pathway mediates this *Pomc* mRNA expression in B cells. To find this factor, cytokine array analyses were performed with supernatants of *in vivo* and *in vitro* activated T cells. Of 34 analysed cytokines, almost all were significantly upregulated in the supernatants of T cells derived from inflamed LNs in comparison to naïve T cells from non-inflamed LNs. In the supernatants of *in vitro* IL-4-stimulated T cells, IL-2, IL-4, IL-6, IL-10, ciliary neurotrophic factor (CTNF), IL-1β, and IFN-gamma were significantly elevated over untreated controls (Fig. 3.11).

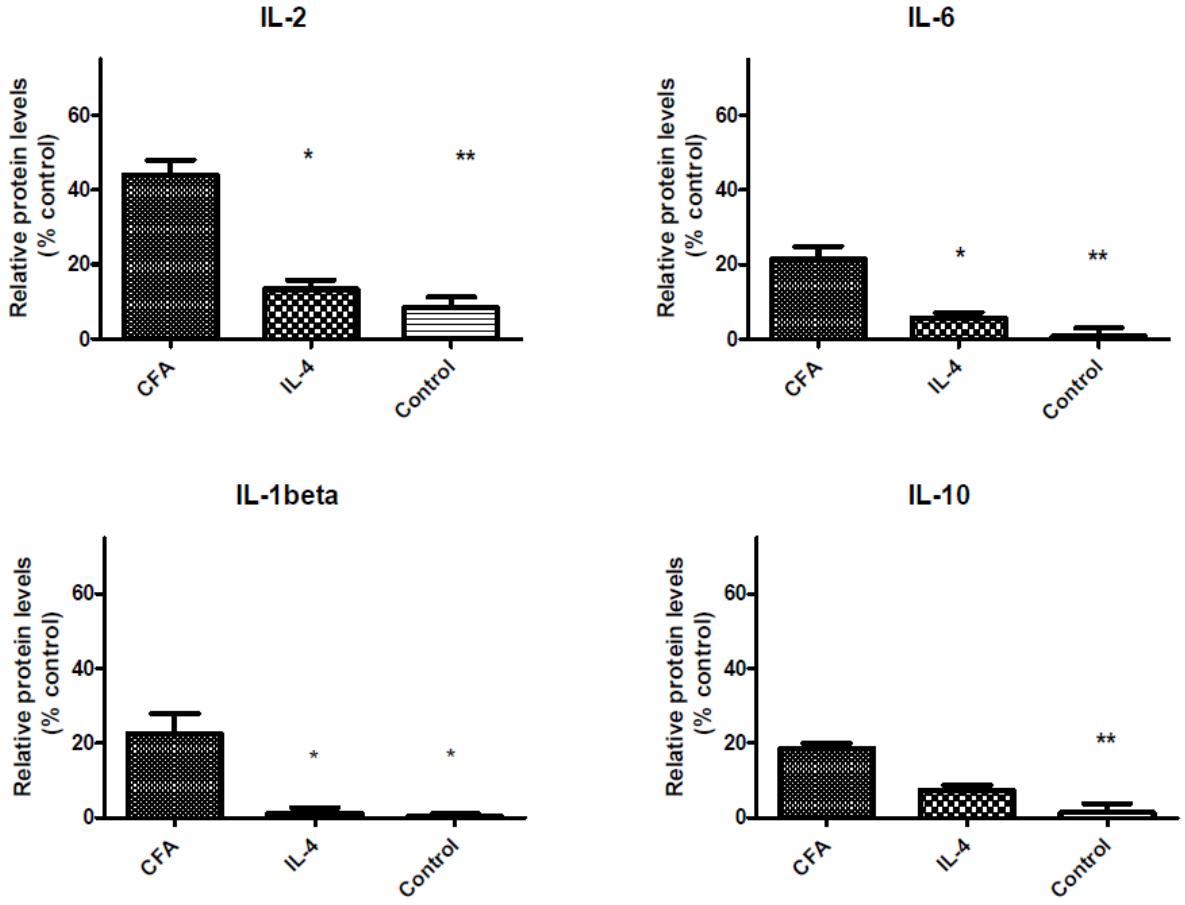

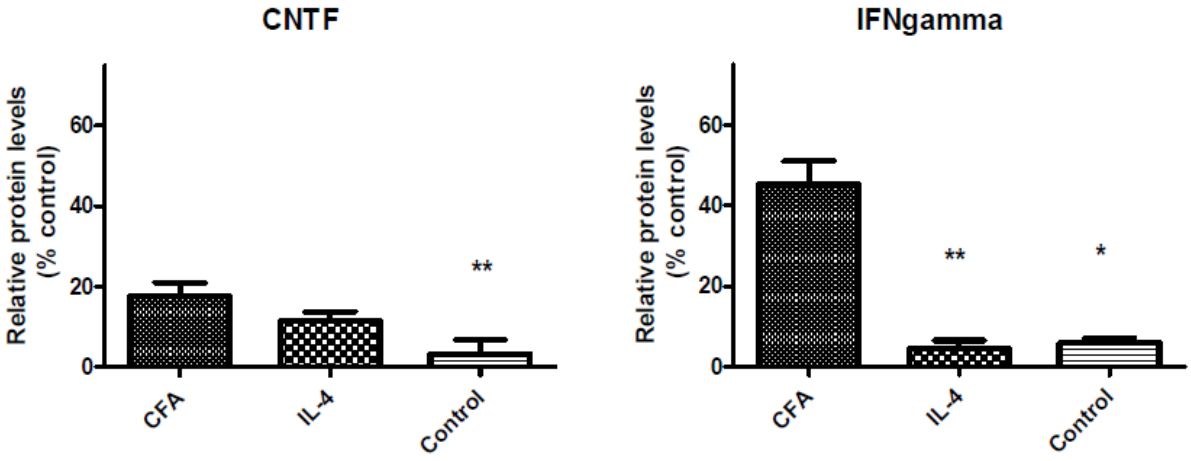

Figure 3.11 (previous and present page) Cytokine secretion changes in stimulated T cells Naïve T and B cells were separated from dissociated LNs using anti-CD45RA microbeads and MACS columns. B cells were discarded, and T cells were treated with/without IL-4 for 2 h, harvested, and the supernatant was analyzed by cytokine array. Similarly, T and B cells were separated by draining LNs of i.pl. CFA-treated animals were isolated (2 h after CFA injection). B cells were discarded and T cells were kept in the medium for 2 h at 37 ºC, harvested, and the supernatant was analyzed via cytokine array. Control (unstimulated) cells were kept under similar conditions. Number of independent experiments: n = 6 per group. Densitometry analyses of the array blots were done. Data represent mean ± SEM fold change over levels determined in unstimulated controls. Statistical analyses were performed using Kruskal-Wallis test and Dunn's multiple comparison test. *P < 0.05; **P < 0.01.

Naïve B cells were then treated for 2 h with the upregulated cytokines as identified by the cytokine array and with various combinations of cytokines (IL-2, IL-6, IL-6Rα IL-10), but no upregulation of *Pomc* mRNA expression was observed (Fig. 3.12). At this point it is still an open question as to what the factor is that is released from T cells and stimulates B cells to produce *Pomc*.

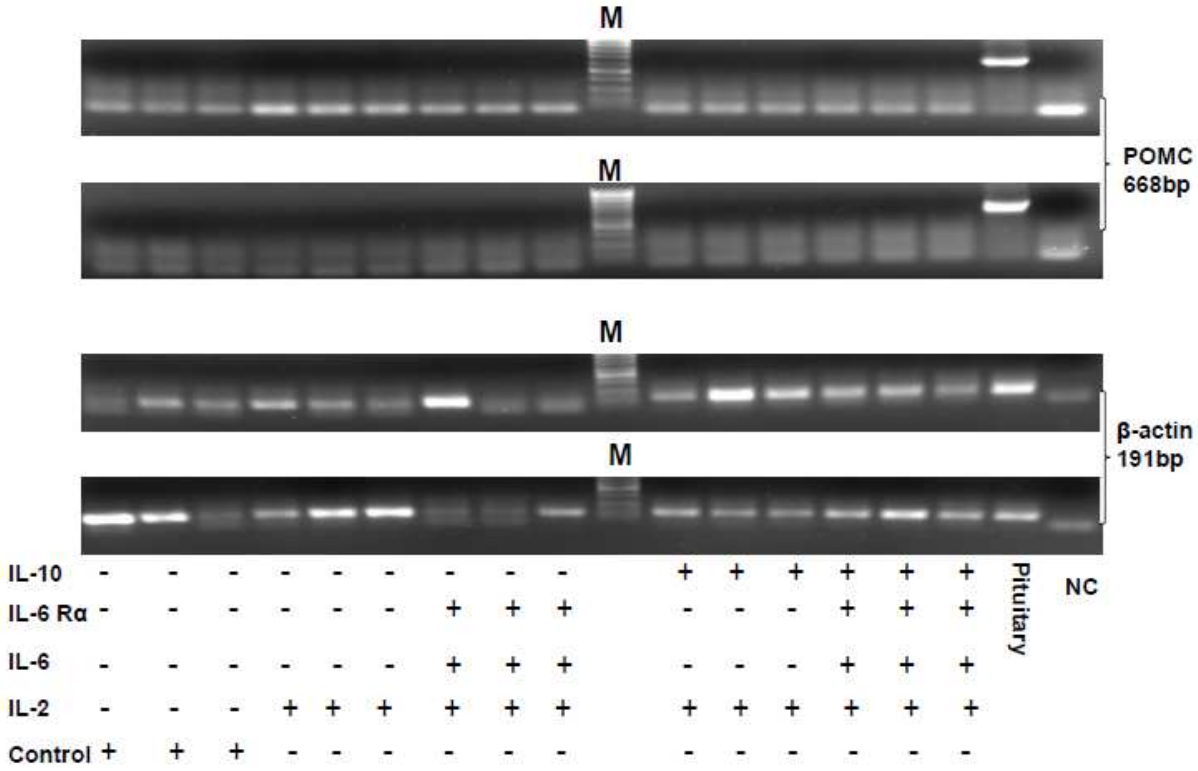

Figure 3.12 Effect of cytokine treatments on *Pomc* mRNA expression in naïve B cells B cells were stimulated with IL-2, IL-2 + IL-6 + IL-6Rα, IL-2 + IL-10 and with IL-2 + IL-6 + IL-6Rα + IL-10. After 2 h cells were centrifuged and pellets were processed for the analysis of *Pomc* mRNA levels using PCR. Number of independently performed experiments: n = 6 per group.

3.2 POMC-processing enzymes

3.2.1 Prohormone convertase 1 (PC1) in lymph node cells

Next we addressed the post-translational regulation of Pomc by examining the presence of *PC1* mRNA and protein in popliteal LN cells from rats with and without CFA-induced hind paw inflammation. In unseparated cells, *PC1* mRNA was upregulated within 6 h after i.pl. CFA injection vs. control values (Fig. 3.13).

Immunofluorescence analysis of PC1 protein is shown in (Fig. 3.14). The mean fluorescence intensity per cell and the number of cells above threshold were determined and calculated using Image J as described in (2.2.9). PC1 protein was significantly increased within 24 h after the onset of CFA-induced paw inflammation when compared to basal levels determined in LNs from healthy rats (Figs. 3.14 B and C). No significant differences in comparison to control levels were found at 96 and 120 h (Fig. 3.14 A-C). To verify antibody specificity, preabsorption experiments with recombinant PC1 and PC2 peptides were performed (Figs. 3.14 D-E). Staining the LN cells with anti-PC1 after 24 h of paw inflammation demonstrated a significant

reduction inmean fluorescence intensity per cell after preabsorption with recombinant PC1 but not with PC2 (Fig. 3.14 E).

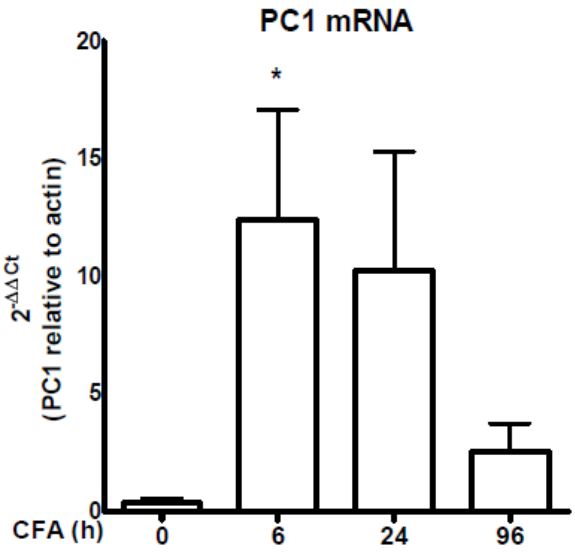

Figure 3.13 ***In vivo PC1*** **mRNA expression in lymph nodes** Rats received an i.pl. CFA injection and popliteal LNs were harvested after 6, 24, and 96 h and from untreated control rats (0 h). *PC1* transcripts were amplified by qRT-PCR. Data were calculated using the delta-delta CP method and represent mean ± SEM fold change of *PC1* mRNA over levels determined in cells from naïve LNs relative to *β-actin* expression. Statistical analysis was performed using the Kruskal-Wallis test and Dunn's multiple comparison test. *P < 0.05, n = 12 per group.

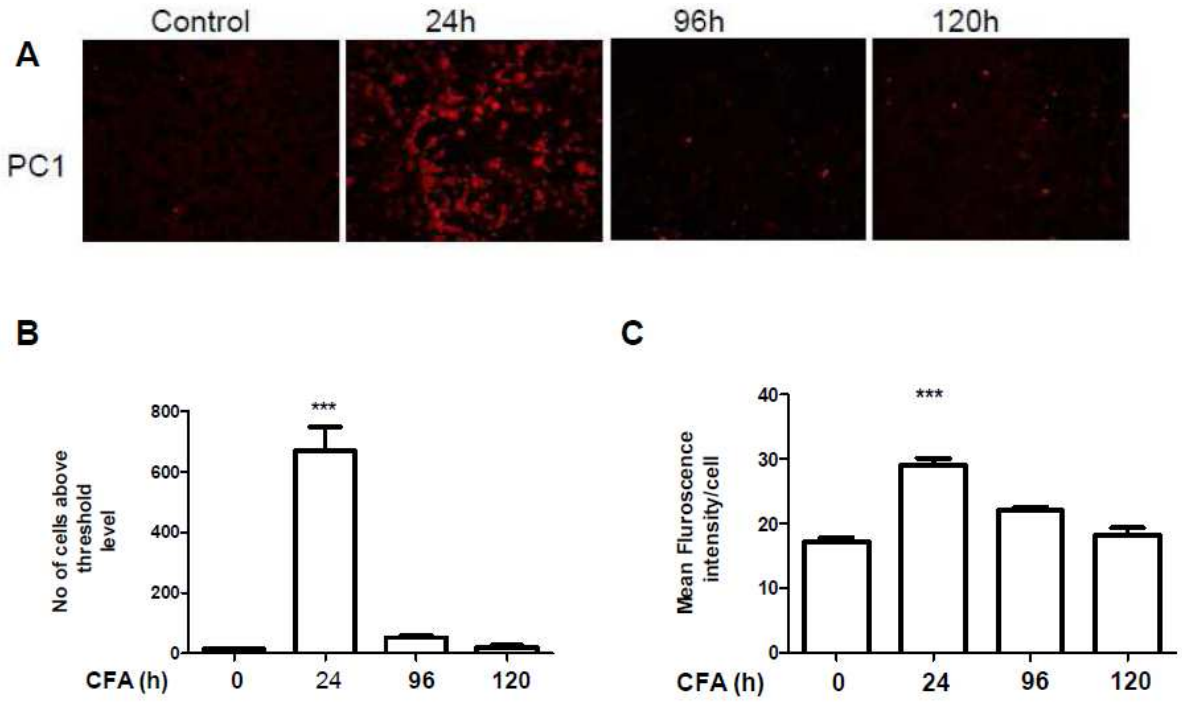

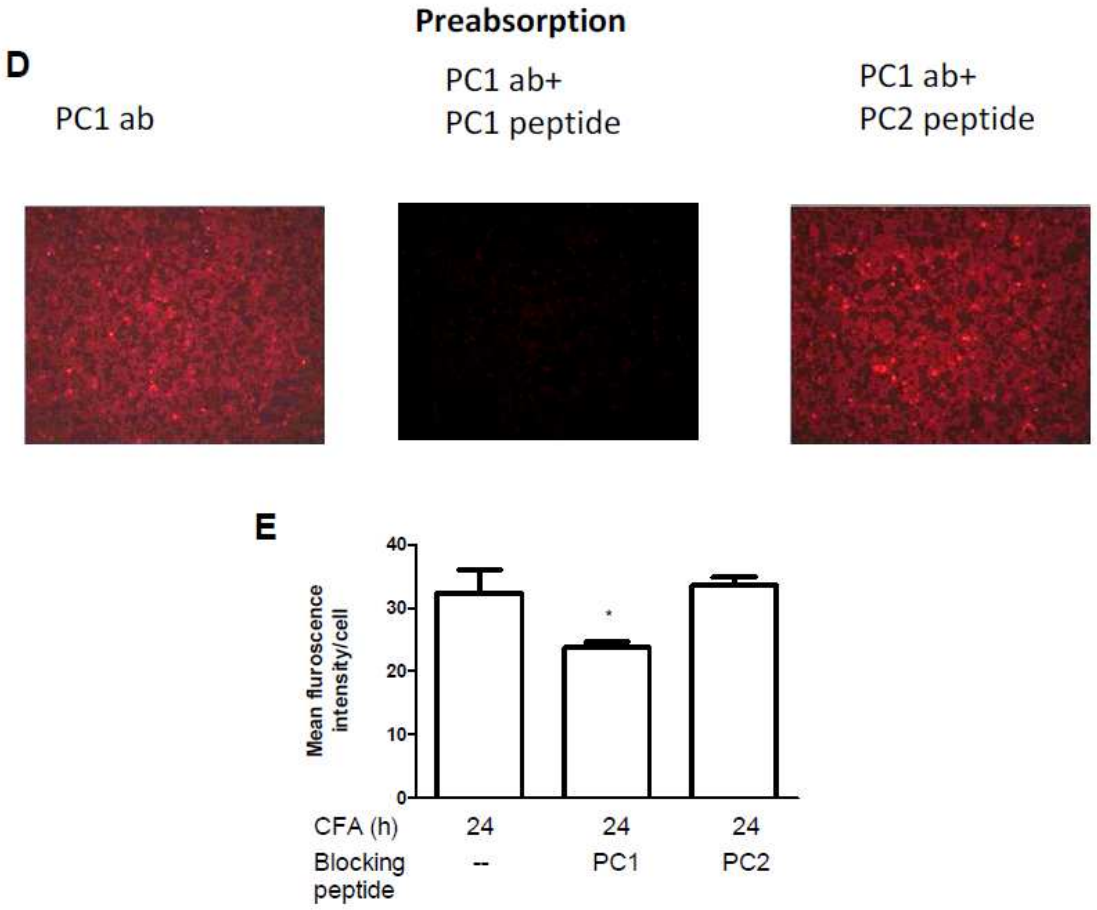

Figure 3.14 ***In vivo*** **PC1 expression in lymph node cells** Rats received an i.pl. CFA injection and popliteal LNs were harvested after 24, 96, and 120 h; control nodes were taken from untreated rats. **A (previous page)**: Representative anti-PC1 staining of cytospin preparations at the indicated time points (n=6 animals per time point). In **B (previous page)** the number of PC1-positive cells is represented in mean ± SEM. **C (previous page)**: Mean fluorescence intensity per cell ± SEM (n = 6 per group). **D**: Preabsorption with PC1 but not with PC2 peptide diminished the staining of anti-PC1. **E**: Mean fluorescence intensity per cell ± SEM (n = 4 per group). Statistical analyses were performed using the Kruskal-Wallis test and Dunn's multiple comparison test (compared to PC1 staining without preabsorption). *P < 0.05; **P < 0.01; *** P < 0.001.

To study the expression of *PC1* in the subsets of lymphocytes, popliteal LNs were dissected and separated using anti-CD45RA microbeads into T ($CD45RA^-$) and B cells ($CD45RA^+$) 24 h after the induction of hind paw inflammation. *PC1* mRNA transcripts were analysed using PCR. *β-Actin* transcripts confirming the quality of cDNA and RT-PCR are shown in (Fig. 3.15 A). (Fig. 3.15 B) shows that *PC1* mRNA was below detection limit in separated B and T cells from normal LNs. At 24 h of CFA-induced paw inflammation, *PC1* transcripts were observed in $CD45RA^+$ (B cells) and $CD45RA^-$ (T cells) of the draining LNs (Fig. 3.15 B).

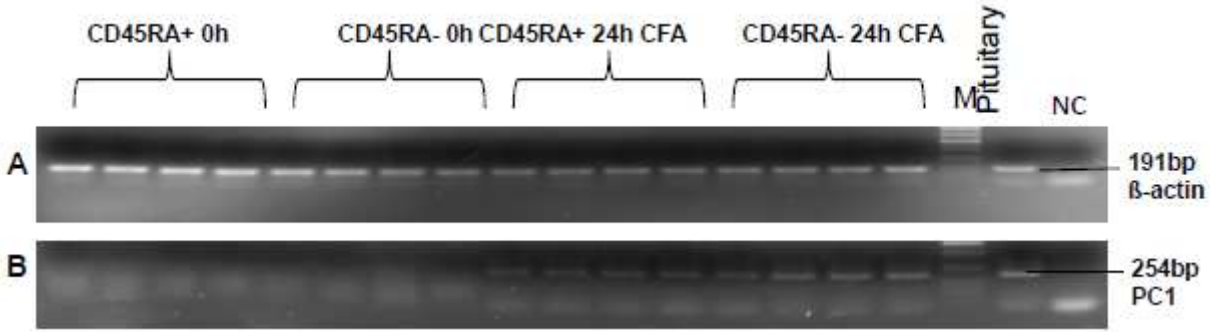

Figure 3.15 *In vivo PC1* mRNA expression in B and T cells Rats received an i.pl. CFA injection; popliteal LNs were harvested after 24 h and separated into CD45RA$^-$ (T cells) and CD45RA$^+$ (B cells) using anti-CD45RA microbeads followed by PCR. **A**: *β-Actin* mRNA transcripts, pituitary cDNA served as positive control. **B**: *PC1* mRNA transcripts, pituitary cDNA served as positive control. Nodes from healthy rats served as controls (0 h). A DNA marker was run in parallel to estimate the product size in bp. Number of independent experiments: n = 6 per group, n = 4 are represented.

Dissociated LN cells were also separated into CD8$^+$ (cytotoxic T cells) and CD8$^-$ (mixed B and T helper cells) using anti-CD8a microbeads. *β-Actin* transcripts confirming the quality of cDNA and RT-PCR are shown in (Fig. 3.16 A). At 24 h after i.pl. CFA, *PC1* mRNA was detected in all CD8$^-$, but not in CD8$^+$ cells from inflamed LNs (Fig. 3.16 B). *PC1* mRNA was undetectable in CD8$^+$ and CD8$^-$ fractions of non-inflamed LNs.

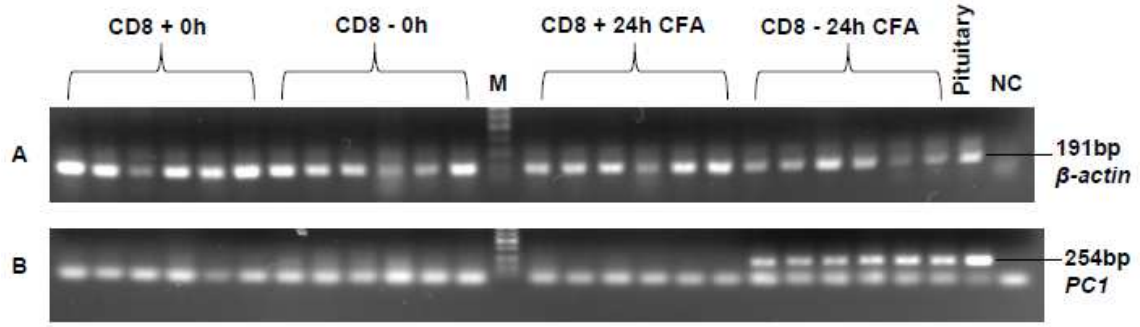

Figure 3.16 *In vivo PC1* mRNA expression in cytotoxic T cells and mixed B and T helper cell fractions Rats received an i.pl. CFA injection; popliteal LNs were harvested after 24 h and separated into CD8$^+$ (cytotoxic T cells) and CD8$^-$ (mix of B- and T-helper cells) fractions using anti-CD8 microbeads followed by PCR. **A**: *β-Actin* mRNA transcripts, pituitary cDNA served as positive control. **B**: *PC1* mRNA transcripts, pituitary cDNA served as positive control. Lymph nodes from healthy rats served as controls (0 h). A DNA marker was run in parallel to estimate the product size in bp. Number of independent experiments: n = 6 per group, n = 4 are represented.

3.2.2 Prohormone convertase 2 (PC2) in lymph node cells

PC2 mRNA was significantly upregulated in unseparated LN cells at 96 h after i.pl. CFA injection in comparison to 6 h (Fig. 3.17).

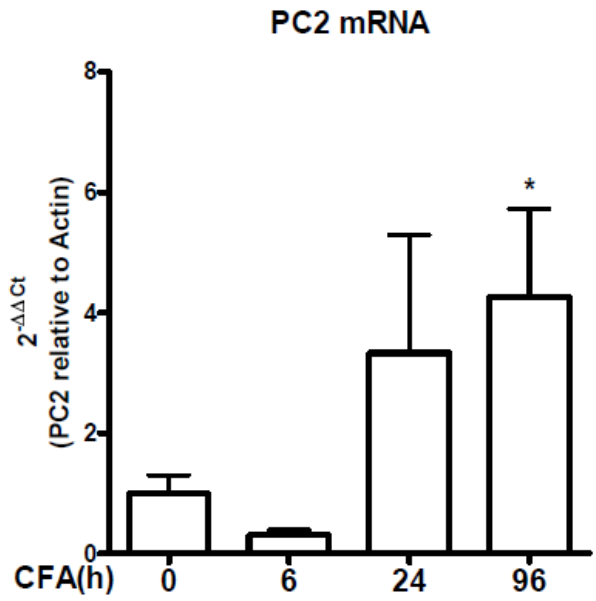

Figure 3.17 *In vivo PC2* mRNA expression in lymph node cells Rats received an i.pl. CFA injection and popliteal LNs were harvested after 6, 24, and 96 h and from untreated control rats (0 h). *PC2* transcripts were amplified by qRT-PCR. Data were calculated using the delta-delta CP method and represent mean ± SEM fold change of *PC2* mRNA over levels determined in cells from naïve LNs relative to *β-actin* mRNA expression. Statistical analysis was performed using the Kruskal-Wallis test and Dunn's multiple comparison test. *P < 0.05, n = 8-10 per group.

Immunofluorescence analysis of PC2 protein is shown in (Fig. 3.18 A). The mean fluorescence intensity per cell and the number of cells above threshold were determined and calculated using Image J as described in (section 2.2.9). PC2 protein was significantly increased within 24 h after the onset of CFA-induced paw inflammation when compared to basal levels determined in LNs from healthy rats. No significant differences in comparison to control levels were found at 96 and 120 h (Fig. 3.18 B).

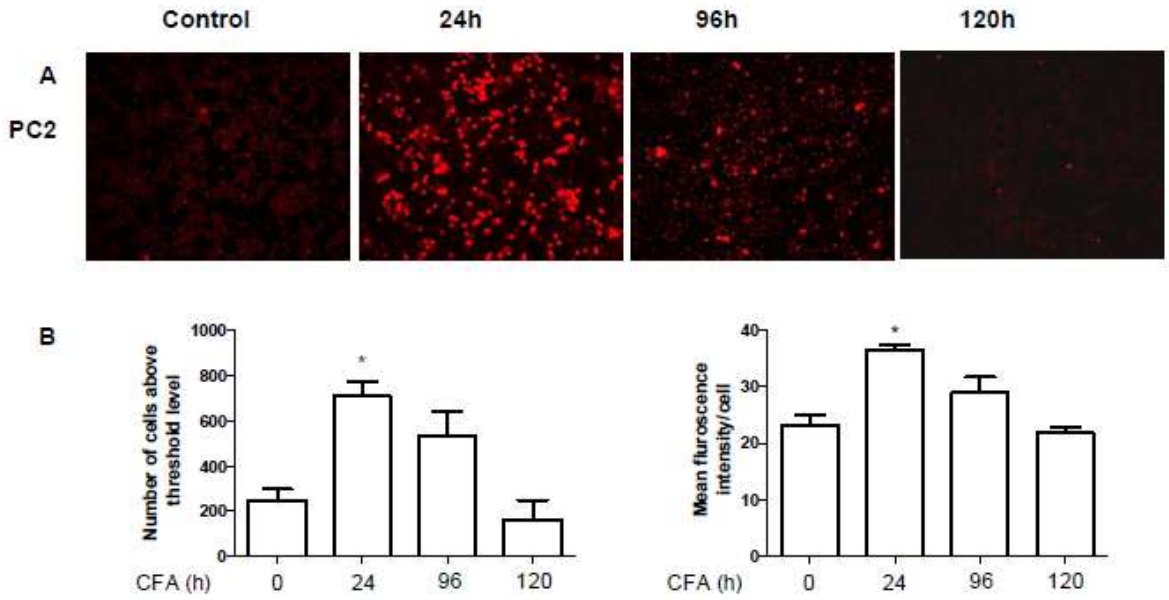

Figure 3.18 *In vivo* PC2 expression in lymph node cells draining healthily and CFA-inflamed hind paws of rats Rats received an i.pl. CFA injection and popliteal LNs were harvested after 24, 96, and 120 h; control nodes were dissected from untreated rats. **A**: Representative anti-PC2 stainings of LN cells. **B**: Mean number of cells above threshold ± SEM (left) and mean fluorescence intensity ± SEM (right) of anti-PC2 stained cells are shown. Number of independently performed experiments: n = 6 per group. Statistical analysis was performed using the Kruskal-Wallis test and Dunn's multiple comparison test (comparison against basal levels). *P < 0.05.

To verify antibody specificity, the PC2 antibody was preabsorbed with recombinant PC1 and PC2 peptides. Staining LN cells at 24 h after CFA injection demonstrated a significant reduction of the mean fluorescence intensity per cell in the presence of PC2 but not of PC1 peptide in comparison to controls (Fig. 3.19).

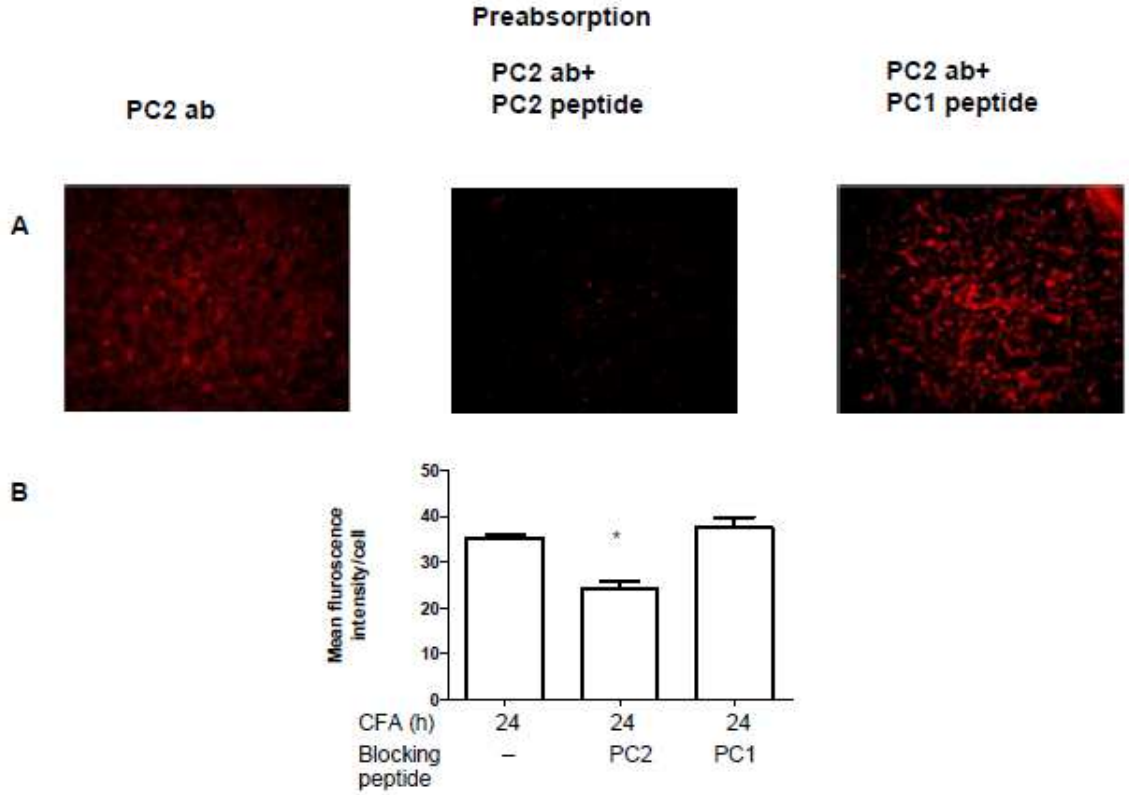

Figure 3.19 Preabsorption experiments with anti-PC2 **A**: preabsorption with PC2 peptide diminished the staining of anti-PC2; staining was unaffected by preabsorption with PC1 peptide. **B**: Mean fluorescence intensity per cell represented in ± SEM. n = 6. Statistical analyses were performed using the Kruskal-Wallis test and Dunn's multiple comparison test. *P < 0.05.

To study the expression of *PC2* in the subsets of lymphocytes, popliteal LNs were dissected and separated using anti-CD45RA microbeads into T ($CD45RA^-$) and B cells ($CD45RA^+$) at 24 h after induction of hind paw inflammation. *PC2* mRNA transcripts were analysed using PCR. *β-Actin* transcripts confirming the quality of cDNA and RT-PCR are shown in (Fig. 3.20 A). *PC2* mRNA was seen in $CD45RA^+$ (B cells) and $CD45RA^-$ fractions (T cells), both in naïve and inflamed LNs (Fig. 3.20 B).

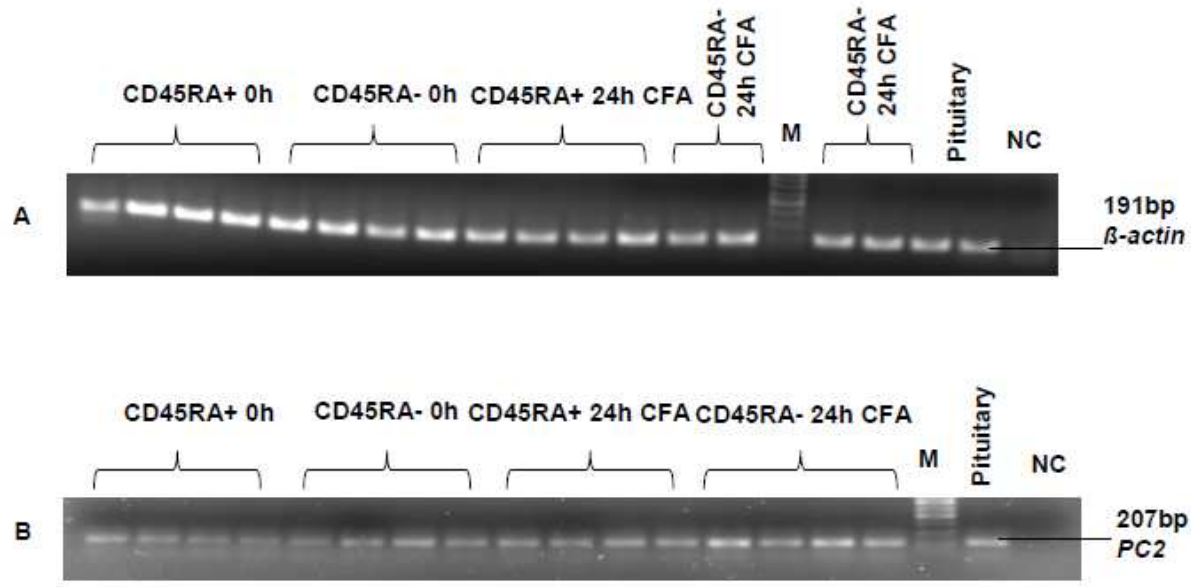

Figure 3.20 ***In vivo PC2*** **mRNA expression in B and T cells**. Rats received an i.pl. CFA injection; popliteal LNs were harvested after 24 h and separated into CD45RA$^-$ (T cells) and CD45RA$^+$ (B cells) using anti-CD45RA microbeads followed by PCR. **A**: *β-Actin* mRNA transcripts, pituitary cDNA served as positive control. **B**: *PC2* mRNA transcripts, pituitary cDNA served as positive control. Nodes from healthy rats served as controls. A DNA marker was run in parallel to estimate the product size in bp. Number of independent experiments: n = 6 per group, n = 4 are represented.

Dissociated LN cells were also separated into CD8$^+$ (cytotoxic T cells) and CD8$^-$ (mixed B and T helper cells) using anti-CD8a microbeads. *PC2* mRNA was detected in both CD8$^-$ and CD8$^+$ cells from non-inflamed and inflamed LNs (Fig. 3.21 A). *β-Actin* transcripts confirming the quality of cDNA and RT-PCR are shown in (Fig. 3.21 B).

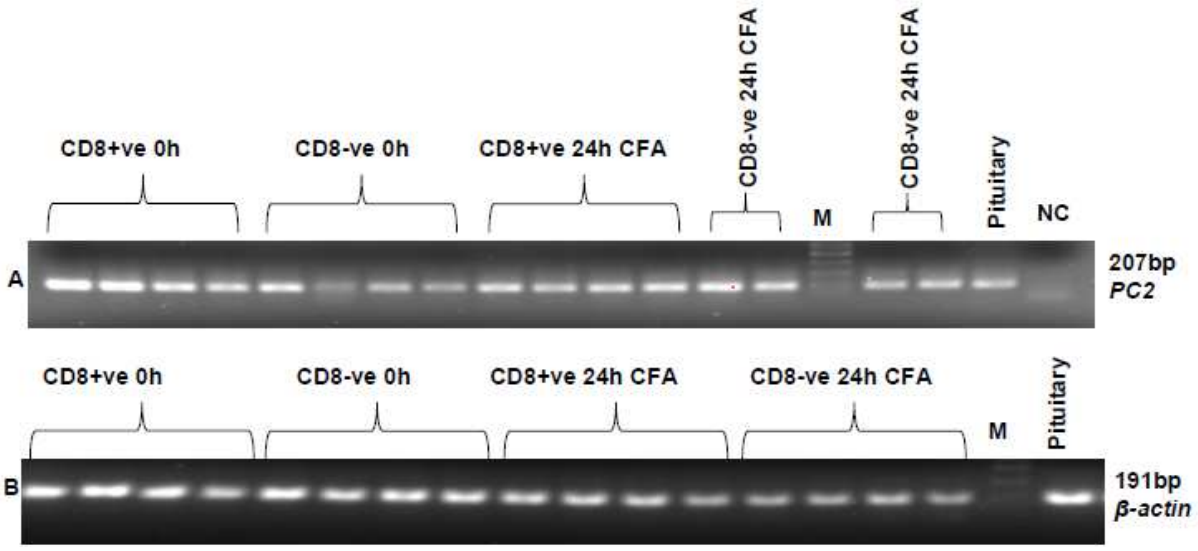

Figure 3.21 (bottom previous page) *In vivo PC2* mRNA expression in cytotoxic T cells and mixed B and T helper cell fractions Rats received an i.pl. CFA injection; popliteal LNs were harvested after 24 h and separated into $CD8^+$ (cytotoxic T cells) and $CD8^-$ (mix of B and T helper cells) fractions using anti-CD8 microbeads followed by PCR. **A**: *PC2* mRNA transcripts, pituitary cDNA served as positive control. Nodes from healthy rats served as controls (0 h). **B**: *β-Actin* mRNA transcripts, pituitary cDNA served as positive control. A DNA marker was run in parallel to estimate the product size in bp. Number of independent experiments: n = 6 per group, n = 4 are represented.

3.2.3 *Cathepsin L* and *aminopeptidase B* mRNA in lymph node cells

Several studies demonstrated an additional protease pathway for the conversion of POMC into ACTH, β-END, and α-MSH mediated by cathepsin L and aminopeptidase B in secretory vesicles (Yasothornsrikul et al., 2003; Funkelstein et al., 2008). We observed that *cathepsin L* mRNA was downregulated in unseparated LN cells at 24 h after i.pl. CFA injection in comparison to non-inflamed node cells (0 h) and was upregulated at 96 h after i.pl. CFA injection (Fig. 3.22). *Aminopeptidase B* mRNA was upregulated at 96 h after i.pl. CFA injection in comparison to 0, 6, and 24 h (Fig. 3.23).

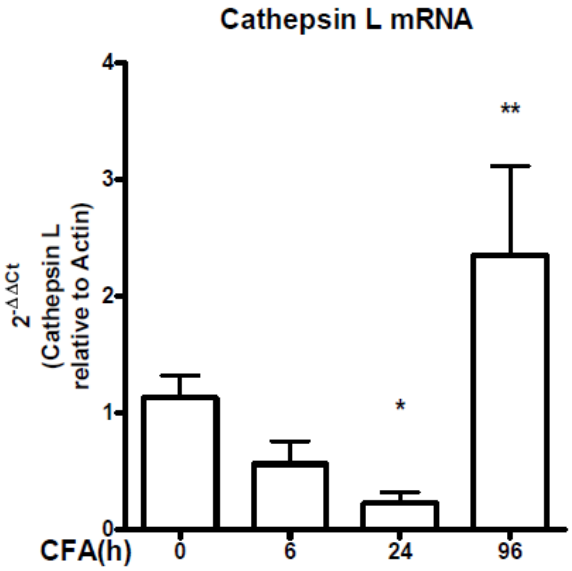

Figure 3.22 *In vivo cathepsin L* mRNA expression in lymph nodes Rats received an i.pl. CFA injection and popliteal LNs were harvested after 6, 24, and 96 h and from untreated control rats (0 h). *Cathepsin L* transcripts were amplified by qRT-PCR. Data were calculated using the delta-delta CP method and represent the mean ± SEM fold change of c*athepsin L* mRNA levels after CFA injection over levels determined in cells from naïve LNs relative to the *β-actin* levels. Statistical analysis was performed using the Kruskal-Wallis test and Dunn's multiple comparison test. *P < 0.05, n = 8-10 per group.

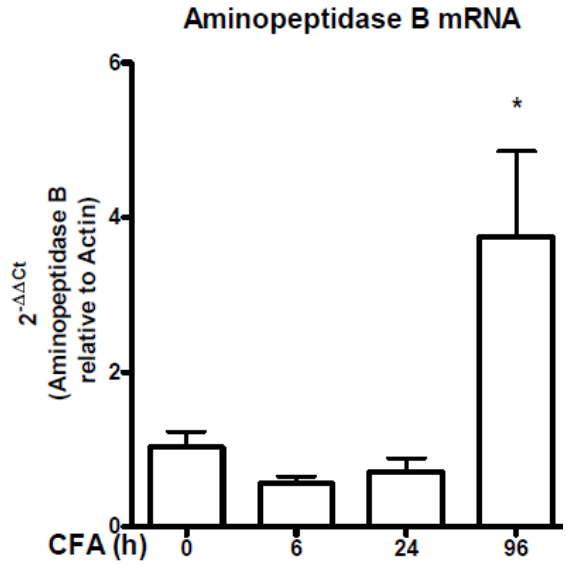

Figure 3.23 ***In vivo aminopeptidase B*** **mRNA expression in lymph nodes** Rats received an i.pl. CFA injection and popliteal LNs were harvested after 6, 24, and 96 h and from untreated control rats (0 h). *Aminopeptidase B* transcripts were amplified by qRT-PCR. Data were calculated using the delta-delta CP method and represent the mean ± SEM fold change of *aminopeptidase B* mRNA levels after CFA injection over levels measured in cells from naïve LNs relative to the *β-actin* levels. Statistical analysis was performed using the Kruskal-Wallis test and Dunn's multiple comparison test. *P < 0.05, n = 8-10 per group.

3.2.4 *In vitro* PC1 and PC2 protein in lymph node cells

LN cells were stimulated with IL-4, conA, and IL-4 plus conA separately. Immunofluorescence analysis of PC1 and PC2 protein is shown in Fig. 3.24. The mean fluorescence intensity per cell in anti-PC1 stained preparations was significantly increased within 24 h after stimulation with IL-4 plus conA as compared to basal levels in LN cells from healthy rats (n = 6). In anti-PC2-stained preparations no significant differences were observed between stimulated and unstimulated LN cells.

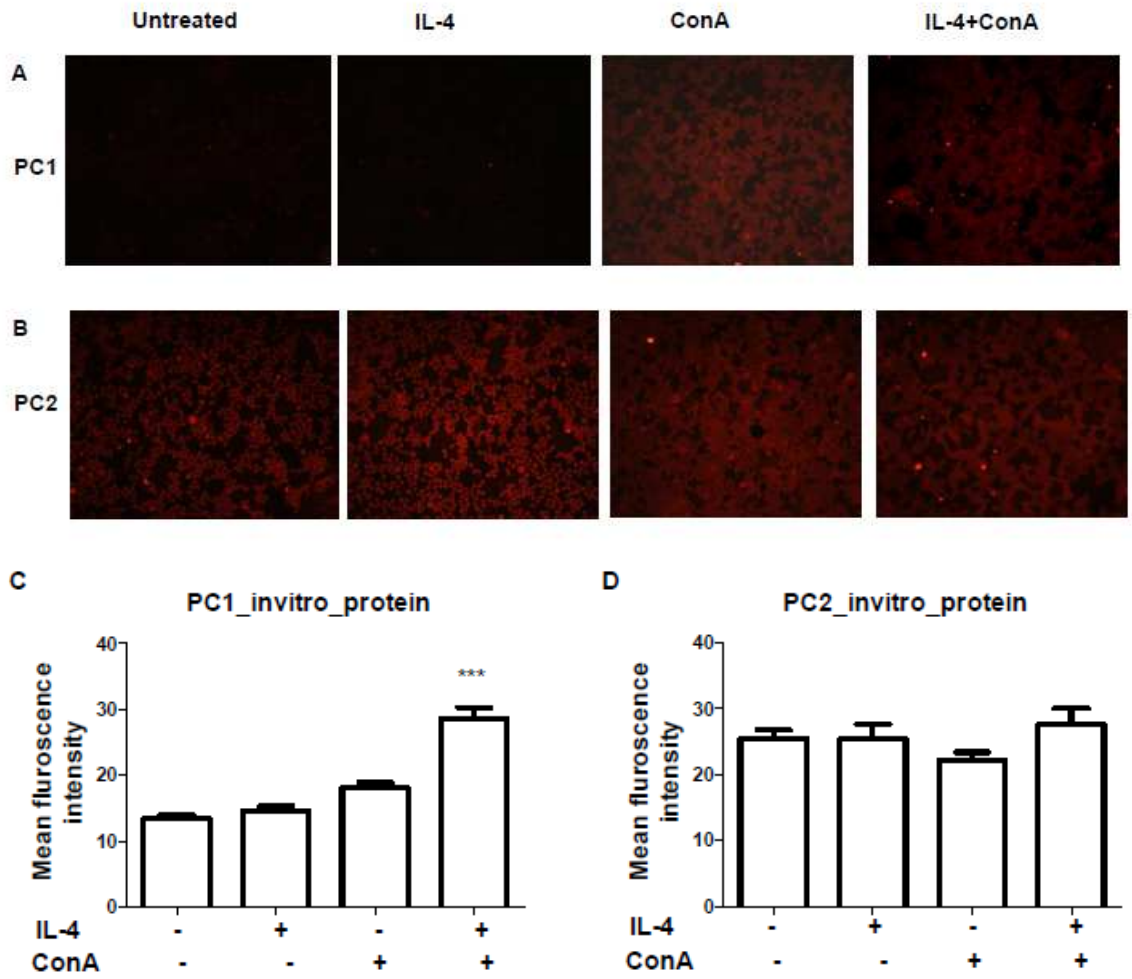

Figure 3.24 *In vitro* PC1 and PC2 expression in IL-4 and mitogen treated LN cells Primary, naïve LN cells were stimulated *in vitro* with IL-4 and conA for 24 h, and LNs were subsequently harvested. Control cells were processed identically but were left without treatment. **A+B**: Representative anti-PC1 and PC2 stainings of untreated and stimulated LN cells. **C+D**: Mean fluorescence intensities ± SEM of anti-PC1 and anti-PC2 stained cells are shown. Number of independently performed experiments: n = 6 per group. Statistical analyses were performed using the Kruskal-Wallis test and Dunn's multiple comparison test. ***P < 0.001.

3.3 Measurement of β-endorphin (β-END)

The detection of β-END was established using immunofluorescence (see section 2.2.9). The mean β-END fluorescence intensity per cell increased significantly over control levels in LN cells treated with conA and conA plus IL-4 (n = 6, Fig. 3.25 C). IL-4 treatment alone had no effect. The mean number of β-END-positive cells above threshold intensities increased significantly over control levels after treatment with conA and conA plus IL-4 (n = 6, Fig. 3.25 D), while IL-4 alone had no significant effect. In cells treated with conA plus IL-4 the mean number of β-END-positive cells was significantly higher than in cells treated only with conA (n = 6, Fig. 3.25 D). To verify antibody specificity, the β-END antibody was preabsorbed with

recombinant Met-enkephalin (MENK) and β-END peptides. Anti-β-END staining of LN cells at 24 h after CFA demonstrated a significant reduction of the mean fluorescence intensity per cell in the presence of β-END but not of MENK peptide in comparison to cells treated with the antibody only (Fig. 3.26).

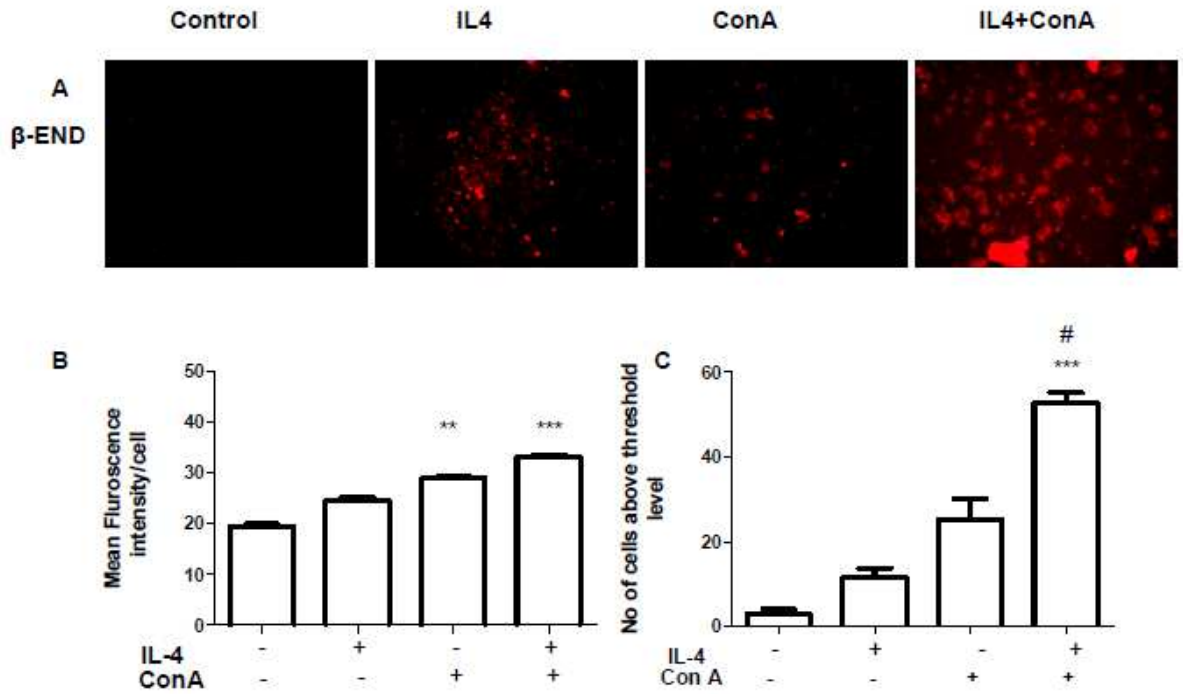

Figure 3.25 *In vitro* stimulation of β-endorphin in naïve lymph node cells LNs from healthy rats were dissected and cells were incubated with IL-4, conA, and IL-4+conA for 24 h. **A**: Representative anti- β-END staining of stimulated and unstimulated LN cells. **B+C:** Mean fluorescence intensity ± SEM (left) and mean number of cells above threshold ± SEM (right) (n = 6 per group). Statistical analysis was performed using the Kruskal-Wallis test and Dunn's multiple comparison test. **P < 0.01 and ***P < 0.001: treatments in comparison to untreated control; $^{\#}$P < 0.05: conA compared to conA+IL-4.

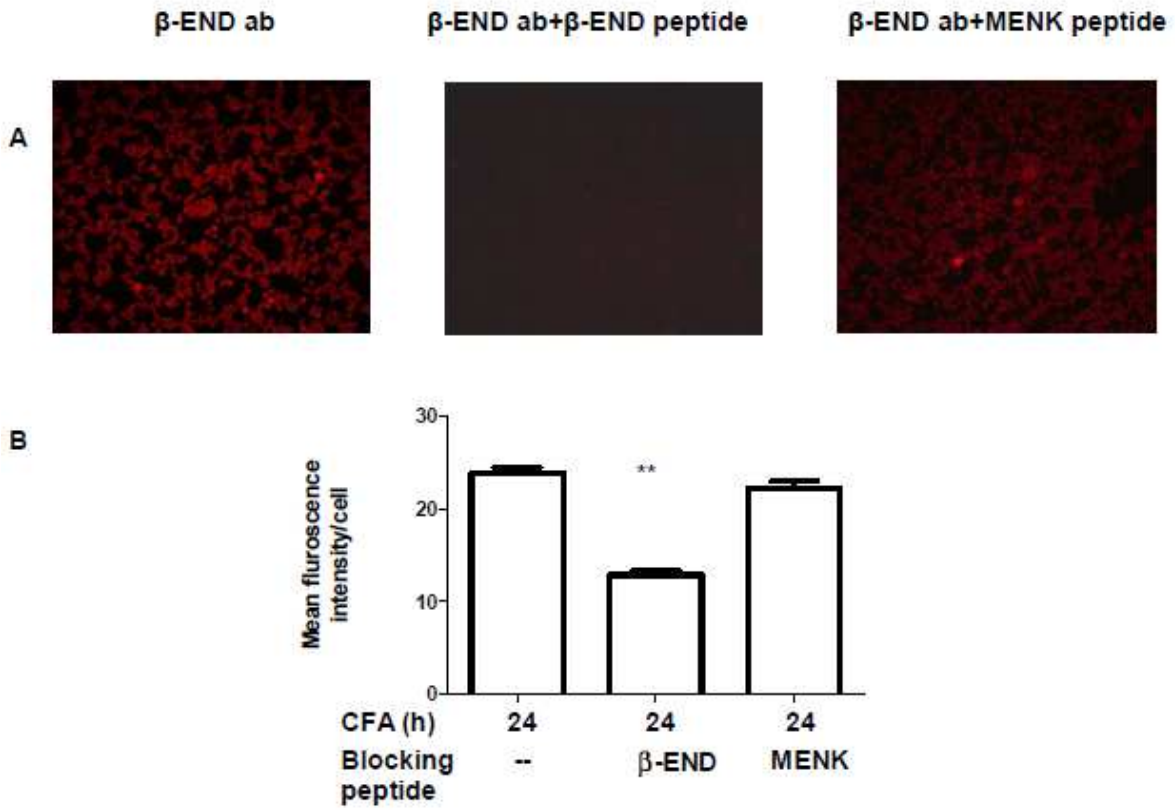

Figure 3.26 Preabsorption experiments of anti-β-END A: Preabsorption with β-END diminished the staining of anti-β-END, while the staining was unaffected by preabsorption with MENK. **B**: Mean fluorescence intensity per cell ± SEM; n = 4 per group. Statistical analysis was performed using the Kruskal-Wallis test and Dunn's multiple comparison test. **P < 0.01.

Next, cellular β-END amounts were determined in B and T cells. We found that the amount of β-END in B cells was more than in T cells. These new data extend previous findings showing increased cellular β-END levels in lymph node cells stimulated *in vivo* (CFA) and *in vitro* (IL-4/ConA) (Sitte et al., 2007 and Busch-Dienstfertig et al., 2012).

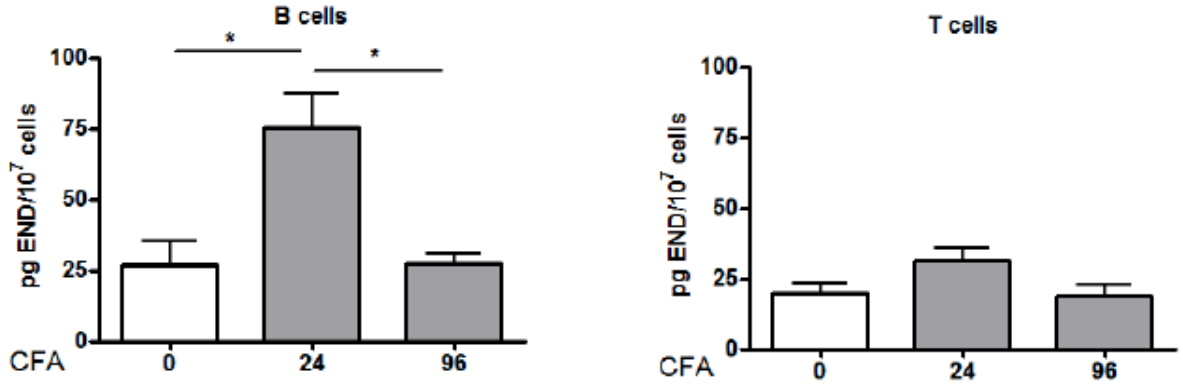

Figure 3.27 *In vivo* stimulation of β-END production in lymph node cell subsets by CFA injection. Rats received an i.pl. CFA injection, popliteal LNs were harvested after 24 and 96 h and separated into $CD45RA^-$ (T cells) and $CD45RA^+$ (B cells) using anti-CD45RA microbeads. Nodes from healthy rats served as controls (0 h). In cell lysates the β-END-immunoreactivity was determined by RIA. Values are given as mean pg END per 10^7 cells ± SEM. Statistical analyses were performed using the Kruskal-Wallis test and Dunn's multiple comparison test. *P < 0.05; n = 6-8 nodes per time point.

3.4 Opioid peptides in mice with chronic arthritis

In order to extend our studies to chronic inflammation, the presence of endogenous opioid peptides was investigated in a new mouse model of rheumatoid arthritis (ACIA-model) (Baddack et al., 2013). Similar to our previous studies in inflamed paws (Stein et al., 1990), immunocytes; (Przewlocki et al., 1992), we first examined opioid peptide production at the site of primary inflammation (joint), and then in the draining LNs. (Fig. 3.28 A), gives an overview of a representative arthritic knee joint and the surrounding tissues. The severity of chronic inflammation and joint destruction was evaluated by semi-quantitatively scoring hematoxylin and eosin (HE)-stained paraffin sections of the inflamed (left) knee joint. The score for chronic inflammation reflects synovial hyperplasia, infiltration of the synovium by mononuclear cells, and fibrosis. Joint destruction scores were based on pannus formation and cartilage and bone erosion.

Anti-β-END and anti-CD3 staining was first done on paraffin sections to examine opioid peptides in periarticular and popliteal LNs and to investigate the localization of β-END. Since the stainings were inconsistent, we subsequently studied opioid peptides using RIA.

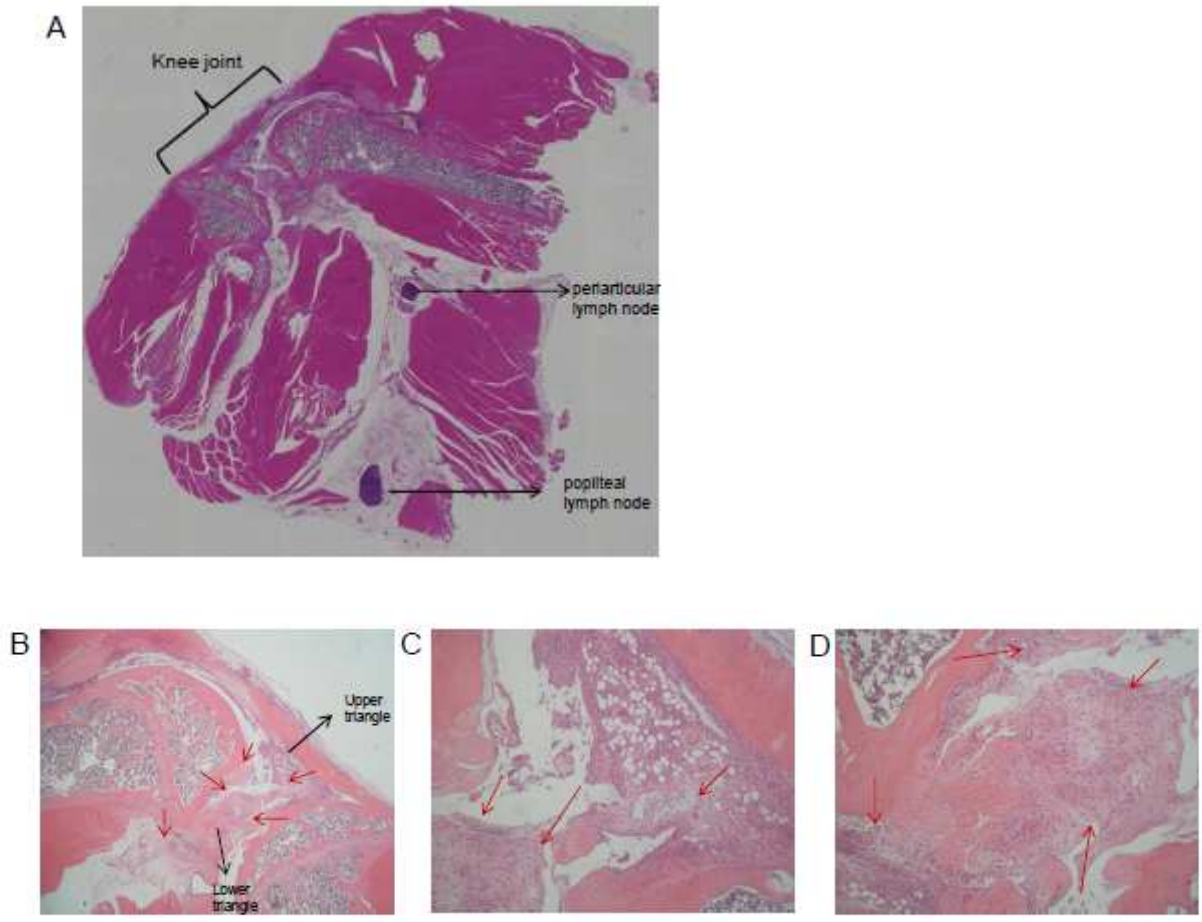

Figure 3.28 HE-staining of the arthritic mouse knee Chronic arthritis was induced by unilateral intraarticular injection of methylated bovine serum albumin (mBSA) in Balb/c mice immunized against antigen (mBSA) and collagen (bovine collagen II). Ipsilateral knees were collected 64 days after induction. Paraffin sections were stained with HE yielding red coloration of soft tissues (muscles, tendon, connective tissue, cartilage) and blue staining of cell nuclei. **A**: Knee joint with popliteal and periarticular LNs. **B**: Magnification of the knee joint with upper triangular and lower triangular region of the synovial space. **C**: Magnification of upper triangular region. **D**: Magnification of lower triangular region. Red arrows in **B-D** point to sites of dense nuclear staining caused by cellular infiltration.

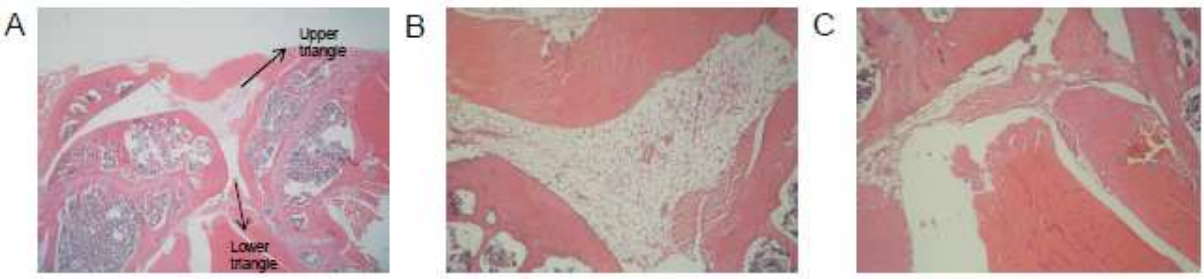

Figure 3.29 HE-staining of healthy knee joint Paraffin sections were prepared from healthy knees and those stained with HE. **A**: Section of the knee joint with upper triangular and lower triangular region of the synovial space. **B**: Magnification of upper triangular region. **C**: Magnification of lower triangular region.

Cell subsets of the LNs draining the arthritic knee were analysed in analogy to our investigations of popliteal LNs draining CFA-inflamed rat hind paws. The numbers of CD4+ T cells, CD8+ cells, and CD8- cells started to increase after the second immunization step, followed by a stronger expansion of all subsets after intraarticular (i.a.) injection of mBSA. In the chronic phase, however, cell numbers dropped back to the values determined before arthritis induction by i.a. mBSA. Next, immunoreactive Met-enkephalin (ir-MENK) levels were determined in cell subsets of the draining LNs. The total amount of ir-MENK showed an elevation over baseline levels within 24 h after induction of arthritis by i.a. mBSA in all cell fractions analysed (CD4+ T cells, CD4- cells, CD8+ T cells, and CD8- cells). When ir-MENK levels were calculated per cell, no substantial changes were observed for the different subsets comparing the different time points of ACIA. The baseline values detected per cell in CD8+ and CD8- cells were higher than those in CD4+ T cells and CD4- cells.

Furthermore, we used RIA and EIA measurements to study opioid peptide liberation from the cellular infiltrate of arthritic knee joints. The knee cells were explanted and prepared as described (in section 2.2.6). (Fig. 3.30), shows the amount of peptides released per knee. The amounts of MENK and β-END peptides released into the supernatant were similar as determined by both RIA and EIA. The release of Met-enkephalin was not correlated to the cell numbers explanted from arthritic knees. The release of β-END was strongly correlated with the cell numbers explanted from arthritic knees but showed no correlation with numbers of $CD45^+$ cells.

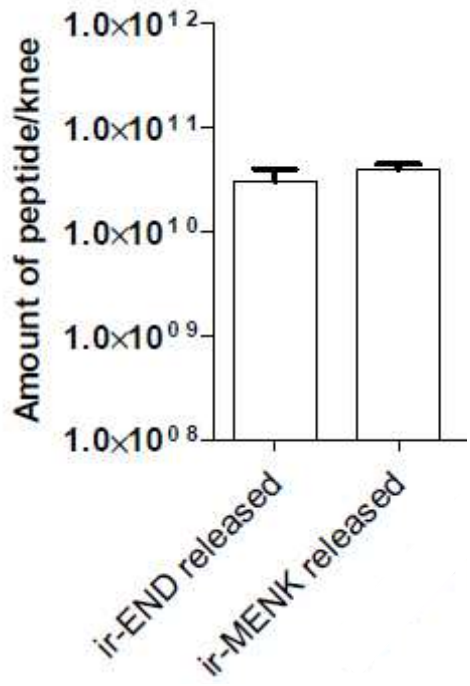

Figure 3.30 MENK and β-END liberated from arthritic knee cells Knees were collected 64 days after induction of arthritis, and the cellular infiltrate was isolated after tissue digestion. Single cell suspensions were kept for 1.5 h at 37 °C and supernatants were harvested to determine the opioid peptide release thereafter (MENK with RIA, β-END with EIA). Cells were counted and some animals were pooled in case the cell numbers were below 3.0E+06. From the pg-amount of ir-MENK and ir-β-END determined in RIA and EIA, respectively, the number of biologically active particles was calculated based on their molecular mass and on the Avogadro number. The Wilcoxon signed rank test was used for a pairwise comparison of ir-β-END released vs. ir-MENK released. The level of significance was $P < 0.05$.

Table 3.1 Correlations between opioid peptide release and cell numbers of explanted knee cells Analyses were performed using Spearman correlation; Spearman r is given. *P < 0.05, **P < 0.01.

Opioid peptide	Number of explanted knee cells	Number of $CD45^-$ knee cells in explants	Number of $CD45^+$ knee cells in explants
ir-MENK released	0.3	0.46	0.15
ir-β-END released	0.69*	0.76*	0.24

4 Discussion

The major findings of this study are the following:

1. *Pomc* mRNA expression in naïve lymphocytes seems to be regulated exclusively by neither DNA methylation and acetylation nor by miRNA.
2. Signal sequence-encoding *Pomc* mRNA is selectively expressed in B cells from LNs draining inflamed paws as early as 2 h after inflammation onset. This is mimicked by an *in vitro* cell stimulation model using IL-4.
3. IL-4 stimulated T cells release a factor that stimulates B cells to express *Pomc* mRNA in a JAK/STAT-mediated manner.
4. T helper and B cells express *PC1* mRNA during inflammation; *PC2* mRNA is expressed in all cell subsets in inflamed and non-inflamed LN cells. Both processing enzymes are upregulated on the protein level in inflammation, while only the PC1 protein level increases after combined IL-4 plus conA treatment *in vitro*.
5. β-END synthesis is elevated in LN cells during paw inflammation *in vivo* and also after combined IL-4 plus conA treatment *in vitro*.

4.1 Repressive mechanisms

The human *pomc* promoter was previously found to be methylated in non-*POMC*-expressing tissues and tumours as well as in normal lymphocytes (Newell-Price et al., 2001). However, *POMC*-expressing tissues and tumours showed less or no *Pomc* gene methylation. Taken together, these findings indicate a regulatory role of DNA methylation in *Pomc* gene expression. To elucidate a possible suppression of *Pomc* expression in naïve rat lymphocytes, we started looking at DNA methylation in naïve and stimulated cells from LNs draining rat paws. This question was addressed using bisulfite conversion by applying a commercial kit. However, according to our sequencing data, the conversion was not efficient. One cause might have been the instability of the chemical modification. However, the same or similar kits were used with success by others (Hansmann T et al., 2012; Lisanti S et al. 2013). Another possibility could be a loss of information due to the conversion (by erasing all non-methylated cytosines and their replacement by uracil). This could have decreased the specificity of PCR primers, even though special methylation primer design software was used. Moreover, the PCR products generated

simultaneously from different cell types most probably represented amplicons from DNAs with different methylation statuses. (Lisanti et al.,2013), used four different surrogate assays for global DNA methylation analysis (LUMA Alu, LINE 1, and HPLC). In the LUMA assay, DNA samples were digested in parallel with the isoschizomer restriction enzymes MspI (unaffected by methylation) and HpaII (methylation sensitive). Both recognize the same sequence (CCGG) but cut differentially according to the methylation state of the internal cytosine residue. The digestion ratio of HpaII/MspI can be determined by pyrosequencing, and the resulting ratio is inversely proportional to the methylation content of the sample. In the Alu and LINE1 assays, the methylation status of specific cytosine residues in bisulfite-converted DNA is also quantified by pyrosequencing. Hansmann and colleagues (2012) cloned the bisulphite-converted DNA into a vector followed by pyrosequencing. Menschikowski and colleagues (2012) used bisulphite conversion followed by sequencing and also quantified the methylation status using methylation-sensitive high-resolution melting analysis. This is a relatively new post-PCR analysis used to identify variations in nucleic acid sequences. The method is based on detecting small differences in PCR melting (dissociation) curves. The success of these studies suggests that it is of advantage not only to directly sequence PCR products, but to include further steps, such as cloning and single colony sequencing to obtain reliable results. However, in the time frame of the present thesis and for financial reasons it was not possible to go for such costly and time consuming approaches.

Due to the limitations of bisulfite conversion, alternative strategies to study the effects of DNA methylation on *Pomc* gene expression were sought. Menschikowski and colleagues (2012) have shown that under control conditions no *PLA2R1*-mRNA (Secretory phospholipase A2 receptor) was detectable after qRT-PCR and agarose gel electrophoresis in Jurkat cells (immortalized line of human T lymphocytes) and U937 cells. Furthermore, no amplification occurred while using real-time qRT-PCR. After exposure of the cells to 5-aza-2´-deoxycytidine(5-aza-dC), which inhibits DNA methyltransferase activity and results in DNA demethylation (hypomethylation) and gene activation by ‘opening’ chromatin, significant *PLA2R1* transcript levels were detectable Brueckner and colleagues (2005) investigated the expression of Secreted frizzled-related protein 1 (*Sfrp1*), a gene that is known to be regulated by methylation, in human colon carcinoma cells (HCT 116) and human leukaemic pre-B cells (NALM-

6) using the DNA methyltransferase inhibitor 2-(1,3-Dioxo-1,3-dihydro-2H-isoindol-2-yl)-3-(1H-indol-3-yl) propionic acid (RG108). In our study RG108 was used to investigate the *Pomc* methylation status because it specifically inhibits CpG methylases and is not cytotoxic. In LN cells RG108 failed to elevate *Pomc* expression, but the control gene *Sfrp1* was elevated after 15 d of treatment with this inhibitor. Besides *Sfrp1* there are several genes under control of DNA methylation. Another example is the extracellular matrix protein SPARC (secreted protein, acidic, rich in cysteine), which showed decreased expression levels in intervertebral discs in correlation with increased levels of DNA methylation of the *SPARC* promoter (Tajerian et al., 2011). Brueckner and colleagues (2005) also showed that RG108 treatment resulted in the demethylation of the tissue inhibitor of metalloproteinases (*TIMP)-3 gene* and the cyclin-dependent kinase inhibitor 2A multiple tumour suppressor 1 (*P16*) gene in HCT 116 cells. *Timp-3* mRNA was constitutively expressed in LN cells, which indicates that this gene is unmethylated in this cell system. Therefore, the *Timp-3* gene was not suitable as a control in our experiments, and P16 was not tested. Together, our findings suggest that the expression of POMC mRNA cannot be induced by interfering with the methylation of the gene, but further studies should be undertaken using alternative approaches.

Moreover, the mechanism affecting gene expression via histone acetylation and deacetylation was investigated. This mechanism relates to the condensation of chromatin, which modulates the accessibility of the DNA for transcription factors, etc. The histone deacetylase inhibitor trichostatin A was used to treat the LN cells, resulting in no upregulation of *Pomc* mRNA expression. Studies showed that the DNA methyltransferase inhibitor 5-aza-2′-deoxycytidine and the histone deacetylase inhibitor trichostatin A synergistically upregulate the expression of *Maspin* in human breast cancer cells (MCF-7) (Liao et al., 2014). To rule out that histone deacetylation and DNA methylation might act synergistically in the inhibition of *Pomc* gene expression, LN cells were treated with both RG108 and trichostatin A. Nevertheless, *Pomc* mRNA expression in naïve lymphocytes was unaffected by the combined treatment, which is similar to the single inhibitor treatments. These findings lead to the conclusion that the suppression of the *Pomc* gene expression in naïve lymphocytes cannot be overcome by interfering with the DNA methylation and histone acetylation status, indicating that other mechanisms seem to be involved.

To study the possible relevance of miRNA in the repression of *Pomc* mRNA expression, knockdown of *Dicer* was performed using siRNA. Dicer is an important endoribonuclease for the processing of most miRNAs. Several transfection reagents such as Lipofectamin 2000 and Fugene were tested, but none resulted in a reliable uptake of a fluorescent control siRNA (scrambled) by LN cells (data not shown). Others demonstrated that the majority of cationic liposome-delivered siRNAs enter cells via endocytosis (Lu et al., 2009). In immune cells, the endosomal detention of siRNA can result in immune responses via toll-like receptor activation (Sioud et al., 2005; Yoo et al., 2006). Therefore, immune cells are considered especially hard to transfect. Moreover, primary and suspension cells such as our LN cells are generally difficult to transfect. An alternative approach to introduce siRNA into cells is the use of electroporation. The application of an external electrical field temporarily increases cell membrane permeability (Neumann et al., 1982) and delivers siRNA directly into the cell cytoplasm. Thus, electroporation can resolve some of the cell-specific limitations associated with liposome-based transfection, like the immune response induced by siRNA (Sioud et al., 2005). This technique has successfully been used to introduce siRNA into primary murine bone marrow-derived macrophages, resulting in a target gene knockdown (Wiese et al., 2010). Therefore, the electroporation of primary LN cells to knock down *Dicer* expression using siRNA was established.

In the beginning an electroporation system designed and constructed by Thorsten Stroh from the group of Prof. Sigmund (Department of Gastroenterology, Charité, Berlin) was used, but as this system was not accessible in the long term, the experiments were transferred to the Eppendorf Multiporator system with a different pulse profile. Similar results were obtained using the two systems. A reliable knockdown of *Dicer* mRNA was achieved after 48 h of electroporation using the Eppendorf Multiporator system, 1 µM siRNA, and a pulse of 600 V/25 µs. Studies have shown that despite the high efficiency of nucleic acid transfer, electroporation can induce high cell mortality (Tsong et al., 1991) Therefore, the number of transfected cells was increased from 1 to 10 million, which improved the survival rate and the uptake of siRNA. These experimental conditions were comparable to the conditions used in other studies (Jensen et al., 2014). Dicer protein knockdown was achieved after 5 d using the Eppendorf Multiporator system. At later time points the cells were less vital (as determined from microscopic observation of cell shape and via the trypan blue exclusion method), and *β-actin* mRNA levels were decreased (6

and 7-day experiments). Thus, the cells might have gone into apoptosis. However, knockdown of *Dicer* at the mRNA and protein level did not result in an upregulation of *Pomc* mRNA levels. As a positive control *IL-10* mRNA was investigated, as its expression has been shown to be regulated by miRNA. In macrophages for example, innate *IL-10* expression is promoted by miR-145 through targeting the epigenetic *IL-10* gene silencer histone deacetylase 11 (Lin et al., 2013). In this work, *IL-10* mRNA levels were undetectable in electroporated LN cells upon Dicer knockdown, while untreated and scrambled siRNA-electroporated cells displayed basal *IL-10* mRNA expression. On the other hand, there are several miRNAs that downregulate *IL-10* expression. For example, the *IL-10* level was shown to be inversely correlated with the level of Egr 1 (ETS-related gene, an oncogene) induced by has-miR-106a expression in Jurkat (immortalized line of human T lymphocytes) and Raji cells (lymphoblast-like cells) (Sharma et al., 2009). In $CD4^+$ T cells, *IL-10* mRNA levels are reduced by let-7 miRNA (Swaminathan et al., 2012). These findings indicate a complex regulation of *IL-10* mRNA by diverse miRNAs. *Pomc* mRNA, however, does not seem to be affected by this post-transcriptional regulatory mechanism. These results lead to the conclusion that miRNA does not play a suppressive role in naïve lymphocytes in our setup.

4.2 Expression of POMC

Next, we investigated the transcriptional inducers of *Pomc* expression. It was previously shown that under inflammatory conditions there was an upregulation of *Pomc* mRNA in LN cells (Sitte et al., 2007). In addition, treatment of naïve mixed LN cells with IL-4 also resulted in an upregulation of *Pomc* mRNA levels and this effect seemed to be mediated by STAT3 (Busch-Dienstfertig et al., 2012). Moreover, STAT3 was also found to be upregulated in a mixed population of LN cells draining inflamed paw tissue. Based on these findings, we postulated that cytokines are important activators of *Pomc* mRNA expression in lymphocytes and that the JAK-STAT pathway is the critical signalling cascade mediating this effect. As these earlier studies were performed in a mixed population of LN cells, the present study aimed to investigate the effect of cytokine stimulation in subsets of LN cells.

To identify the LN cell subsets expressing *Pomc* mRNA after CFA-induced paw inflammation *in vivo* or after IL-4 exposure *in vitro*, the mixed LN cell cultures were subsequently separated into B and T cells using MACS columns. Two time points were investigated (2 h and 24 h). Both treatments induced *Pomc* mRNA expression in B cells after 2 h, while T cells were found to transcribe the *Pomc* gene only after 24 h post IL-4 exposure and not at all after paw inflammation. These findings were in contrast to our hypothesis of a predominant *Pomc* mRNA expression in effector T cells. The analysis of peripheral blood leukocytes from healthy donors by Anderson and co-workers showed highest *Pomc* mRNA levels in T helper (Th) cells, while cytotoxic T cells, B cells, natural killer cells, monocytes, and granulocytes expressed lower levels (Andersen et al., 2005). In contrast to the present study, Anderson and colleagues did not measure *Pomc* exon 2-3 spanning primers but determined the level of exon 3 transcripts only. This not only holds the risk of amplifying DNA traces instead of mRNA but also touches a long-standing discussion on *Pomc* transcription in non-pituitary tissues. Several previous studies detected so-called truncated *Pomc* transcripts in naïve lymphocytes (Buzzetti et al., 1989; Cabot et al., 1997; DeBold et al., 1988; Lacaze-Masmonteil et al., 1987; Oates et al., 1988; Przewlocki et al., 1992). Others argued that the translation products of truncated *Pomc* transcripts lacking the signal sequence encoded by exon 2 are not processed to authentic peptides (Clark et al., 1990; Rees et al., 2002). In the present study, all PCR measurements focused on the amplification of exons 2-3. There are not many appropriate studies to compare to our findings. (Lansac et al., 2006), investigated proenkephalin mRNA expression in the spleen of LPS-treated rats and found an elevation in the marginal zone, which harbours B cells, macrophages, and dendritic cells. However, no detailed analysis of the proenkephalin mRNA-expressing cell subsets in the marginal zone was performed. β-END is expressed by peripheral blood B cells after culture with corticotropin-releasing factor and arginine vasopressin (Kavelaars et al., 1989). These findings indicate that full-length *Pomc* mRNA was expressed in B cells, which is in line with our data. This is also supported by the findings that a mouse B cell line produced and secreted ACTH (Weigentet al., 1987) and that the production of ACTH and β-END in B cells is stimulated with corticotropin-releasing factor and lipopolysaccharide (Harbour et al., 1987; 1991). However, these studies did not show *Pomc* gene expression.

After we identified B cells as the main *Pomc*-expressing LN cell subset, they were isolated again and directly stimulated with IL-4. However, in the absence of T cells no elevation of *Pomc* mRNA was observed. To detect if this lack of response to IL-4 was due to the missing cell-cell contact of B and T cells, T cells were stimulated with IL-4, and the supernatant was then added to B cells. These supernatant transfer experiments resulted in the expression of *Pomc* mRNA in B cells, indicating that a soluble T cell-derived factor was mediating this gene expression in B cells. In order to identify which cytokines were elevated in CFA and IL-4-stimulated T cells and which could be responsible for B cell activation, cytokine arrays were performed. The cytokines that were elevated in both cases (IL-2, IL-6, and IL-10) were then used to stimulate isolated B cells individually and in various combinations, but no *Pomc* mRNA expression was observed. In line with these findings, IL-2 also did not elevate *Pomc* mRNA in AtT-20 cells (a mouse corticotroph cell line) (Katahira et al., 1998; Fukata et al., 1989) and had no effect on mixed LN cell cultures (Busch-Dienstfertig et al., 2012). In T cell clones, however, Stephanou and colleagues (Stephanou et al., 1991) found an IL-2-induced elevation of *Pomc* mRNA expression after 18-24 h, which resembles the time span of the IL-4-induced *Pomc* mRNA expression in LN-derived T cells shown here. In contrast to our findings in B cells, a combination of LIF and IL-6 has been shown to increase the *Pomc* precursor in corticotroph cells (Li et al., 1999). In summary, we found that IL-4 induces *Pomc* mRNA expression in B cells indirectly in a T cell-dependent manner. However, we could not identify the factor released by T cells that stimulated B cells to induce *Pomc* mRNA.

4.2.1 Pathway and transcription factors

To identify the relevant signalling pathway and active transcription factors involved in the IL4-induced, T cell-mediated *Pomc* mRNA expression in B cells, we used cell permeable inhibitors of the JAK-STAT pathway. The IL-4 effect was substantially blocked by pyridon 6, a Janus kinase blocker, and by a STAT5 inhibitor, but it was not affected using a JAK II inhibitor. These findings indicate that *Pomc* exon 2–3 mRNA upregulation by IL-4 is largely mediated via the JAK-STAT pathway involving STAT5, JAK 1, and JAK 3. There are several studies showing that the JAK-STAT pathway is also involved in regulating pituitary *Pomc* gene expression. In pituitary corticotrophs, LIF induced *Pomc* gene expression by binding phosphorylated

STAT1 and -3 homo- and heterodimers to the promoter (Mynard et al., 2002). LIF was found to stimulate *Pomc* promoter activity through STAT1 and STAT3 transcription factors (Ray et al., 1996; Bousquet et al., 1997). Li and coworkers (Li et al., 1999) demonstrated coordinated regulation of both *Pomc* and *PC1* by LIF and IL-6. Mouse AtT-20 cells have also been reported to display LIF-induced enhancements in ACTH secretion and *Pomc* transcription (Ray et al., 1996). It was also shown that LIF induced *Pomc* transcription in the placenta of pregnant rats. When differentiated rat choriocarcinoma cells (Rcho-1) were treated with LIF or IL-6, they also increased the expression of *Pomc* (Simamura et al., 2010). Besides JAK-STAT, IL-4 also activates the phosphoinositide 3-kinase / protein kinase B (Akt) pathway (Keegan et al., 1994). This pathway was not addressed in the present study, since it mainly regulates translational activity, cell growth, proliferation, differentiation, motility, and survival, while transcriptional regulation is not amongst its principal functions. Previous studies indicated that the MAPK pathway, which is activated by theAkt pathway, is not essential for IL-4-induced *Pomc* gene expression in lymphocytes (Busch-Dienstfertig et al., 2012). This resembles the findings of others in AtT-20 cells (Bousquet et al., 1999).

In the present study, STAT5 as a transcription factor in B cells was found to be important for *Pomc* gene expression after supernatant transfer from IL-4 stimulated T cells. In our previous study the role of STATs was also investigated but with another approach (Busch-Dienstfertig et al., 2012). By competing with STAT1/3 and STAT5 binding using decoy oligonucleotides, the IL-4-induced *Pomc* gene expression was reduced, but only STAT1/3 decoy oligonucleotides produced a significant effect. STAT5, in addition to STAT6, becomes directly activated by IL-4 in human B (Rolling et al., 1996) and murine pro-B cells (Friedrich et al., 1999). This suggests that the STAT5 activation in our experiments was not related to the unidentified T cell factor but was induced by IL-4. This raises the question of why direct IL-4 stimulation of B cells was insufficient for inducing *Pomc* gene expression if STAT5 is the key transcription factor. It seems that STAT5 is not the only critical factor determining *Pomc* transcription. Other factors, including STAT3, may play a concomitant role.

At this point the exact mechanism or factor that suppresses *Pomc* expression in naïve lymphocytes is unclear. For LN cells stimulated *in vitro* by IL-4 or *in vivo* by paw inflammation, the current and previous data suggest that STAT3 and -5 have the potential to enhance *Pomc* gene expression in lymphocytes. However, the identity of

the regulatory factor inducing *Pomc* mRNA expression in B cells remains to be determined. The present study excluded IL-2, IL-6, and IL-10. However, various cytokines were upregulated after CFA and IL-4 treatments, leaving several candidates to be investigated. The current findings demonstrated the importance of the JAK-STAT pathway for the expression of *Pomc* mRNA in lymphocytes, which is supported by the fact that this is also a crucial pathway in the pituitary and hypothalamus.

4.3 POMC-processing enzymes

Another aim of the present study was to demonstrate that lymphocytes express the POMC-processing enzymes PC1 and PC2. We hypothesized that their expression is upregulated during hind paw inflammation. *PC1* mRNA transcripts and protein were detectable in LNs draining inflamed paws *in vivo*. In the *in vitro* experiments, protein expression in IL-4 plus conA-treated cells, but not in non-inflamed LNs, was observed. Cell subsets expressing *PC1* mRNA under inflammatory conditions were B and T helper cells, while cytotoxic T cells did not express such transcripts. *PC2* transcripts were expressed in non-inflamed and inflamed LNs, and its protein was significantly upregulated in cells from inflamed LNs, although *PC2* mRNA expression levels decreased after the induction of inflammation. PC2 was expressed with or without IL-4 plus conA treatment, while PC1 was expressed only when LN cells were treated. The present findings extend previous findings of a co-expression of PC1 and PC2 protein with POMC and β-END in circulating leukocytes and inflammatory paw cells (Mousa et al., 2004). Differential expression of *PC1* and *PC2* mRNA was also shown in human pituitary tumours (Tateno et al., 2007). In general, basal PC1 and PC2 expression seems to be more common in other immune cells than lymphocytes. (LaMendola et al., 1997) detected *PC1* mRNA in differentiated macrophages derived from human blood cells. (Vindrola et al., 1994), found PC1 protein in alveolar macrophages and in splenic mononuclear cells, and PC2 protein was present in polymorphonuclear leukocytes. The present findings of an expression of the two PCs in lymphocytes under inflammatory conditions are largely in line with findings shown by (Lansac et al., 2006), who investigated *PC1* and *PC2* mRNA expression in rat spleens after LPS treatment. They found basal *PC1* mRNA expression only in macrophage-rich regions such as

the splenic red pulp and the dense paracortical regions of LN tissue. Basal *PC2* mRNA was observed in LN follicles containing densely packed lymphoblasts and B-lymphocytes but was absent in normal spleen tissue. *PC1* and *PC2* mRNAs were induced after LPS-injection in the germinal centres of spleens, while we found *PC1* mRNA induction but *PC2* mRNA downregulation in the LNs draining paw inflammation. (Nakashima et al., 2001), investigated the expression of PCs in the spleen of diabetic rats. Their analysis showed basal PC1 in both the white (T lymphocytes) and red (monocytes and macrophages) pulps and demonstrated an increase after streptozotocin-induced diabetes in the white pulp, which is similar to the observations of this study.

As has been shown by others, the expression of *PC1* and *PC2* in corticotroph cells is strongly associated with JAK/STAT pathway activation and can be induced by different cytokines. However, IL-4 treatment of naïve LN cells did not result in an upregulation of PC1 and PC2 in our experiments. This may be because IL-4 mainly activates STAT6. On the other hand, we observed PC1 protein expression after conA treatment of LN cells, which was amplified by combined IL-4 plus conA treatment. PC2 protein expression remained unaffected by all *in vitro* treatments. The question of whether conA induces PC1 expression via STAT3 activation was not addressed but may be of interest in future studies. In summary, the present study demonstrated *Pomc* gene expression and the presence of processing enzymes in LN-derived B cells under stimulated conditions, which strongly suggests that such cells are a source of bioactive peptides in inflammation.

Other extracellular signals may explain the downregulation of *PC2* mRNA levels under inflammatory conditions (Espinosa et al., 2008). For example, in the hypothalamus *PC2* promoter activity can be regulated by a cAMP response element (Espinosa et al., 2008). These authors demonstrated that, by binding to inhibitory G-protein coupled receptors, morphine induced a decrease in cAMP, resulting in the downregulation of *PC2* mRNA. A potential inflammatory cytokine that binds to the inhibitory G-protein-coupled receptor CCR6 is the chemokine CCL20 (Yang et al., 2005; Tanaka et al., 1999; Dieu-Nosjean et al., 2000).

In the present study the mRNA expression of *PC1* but not of *PC2* coincided with the respective protein expression. Others showed that both *PC1* and *PC2* mRNA and protein levels coincided in primary hypothalamic neuronal cultures stimulated with leptin (Sanchez et al., 2004). There are several reasons for the poor correlations.

First, there are many post-transcriptional mechanisms involved in turning mRNA into protein that are not yet sufficiently defined; second, proteins may differ in their *in vivo* half-lives; third, there is a significant amount of noise in both protein and mRNA experiments (Baldi et al., 2001; Szallasi et al., 1999). Protein turnover can vary significantly depending on a number of different conditions (Glickman et al., 2002). A cell can control the rates of degradation or synthesis for a given protein, and there is significant heterogeneity, even within proteins that have similar functions (Pratt et al., 2002; Anderson et al.,1997; Orntoft et al., 2002) found significant correlations. However, (Lichtinghagen et al., 2002) found no significant relationship between mRNA and protein levels. The discrepancy between *PC2* mRNA and protein expression may as well suggest that translation is repressed. Such repression has previously been reported for the PC2 chaperone 7B2 (Tadros et al., 2011). Moreover, the discrepancy between mRNA and protein expression could also be due to false positive results. Here, the specificity of PCR products was confirmed via melting curve analysis and agarose gel electrophoresis, using pituitary cDNA as a positive control. The melting peaks of LN-derived amplicons were identical to those obtained from pituitary transcripts. Furthermore, electrophoretic separation of PCR products revealed that *PC1* and *PC2* amplicons detected in LNs matched the expected length of the nucleotide sequences and were equal in size to pituitary transcripts. These qualitative controls strongly suggest that our PCR products were valid. Although the antibody (PC1 and PC2) specificity/sensitivity was previously verified by the provider using transfected cells (Ugleholdt et al., 2006), we verified their specificity for our method and our cell type using preabsorption assays. Anti-PC1 staining was reduced by preabsorbing the antibody with PC1 peptide, but the staining was unaffected by preabsorption with PC2 peptide. Similarly, anti-PC2 staining was reduced by preabsorbing the antibody with PC2 peptide, while preabsorption with PC1 peptide had no effect. Additionally, we also performed specificity tests using western blot analysis of the pituitary lysates of PC1 and PC2 knockouts (data not shown).

In addition to PC1 and PC2, there are other enzymes of importance for POMC processing. One of them is carboxypeptidase E (CPE), which functions as a regulated secretory pathway sorting receptor for several prohormones, including proopiomelanocortin, proenkephalin, and proinsulin. (Zhang et al., 2003) showed by mutational studies that full length CPE C-terminal residues are required for the regulated secretory pathway. They also showed that sorting CPE to the regulated

secretory pathway in endocrine cells is mediated by lipid rafts and that the four C-terminal residues of CPE, i.e. Thr(431) to Leu-Asn-Phe(434), are required for raft association and sorting. In the present study, *CPE* mRNA and protein expression was undetectable in non-inflamed and inflamed LNs as well as in IL-4-stimulated LN cells. Since neither *CPE* mRNA nor protein was detected, we assume that full-length *CPE* is absent in rat LN cells. How lymphocytes compensate for the lack of CPE function remains to be determined.

Other studies demonstrated an additional protease pathway for converting prohormones into active peptides mediated by cathepsin L in secretory vesicles (Yasothornsrikul et al., 2003) and Arg/Lys aminopeptidase (Yasothornsrikul et al., 1998). Cathepsin L cleaves proteins at the NH_2-terminal side of dibasic sites or between the dibasic residues (Yasothornsrikul et al., 1998). In contrast, PC1 and PC2 cleave proteins at the COOH-terminal side of dibasic sites, which then requires carboxypeptidase E/H (CPE/H) in order to remove COOH-terminal basic residues (Azaryan et al.,1994; Zhou et al., 1999; Seidah et al., 2002; Fugère et al., 2005). Different aminopeptidases such as cathepsin H (Lu et al., 2012) and aminopeptidase B (Yasothornsrikul et al., 2003; Hwang et al., 2007b) have been shown to remove the N-terminal basic residues Arg and Lys from peptide intermediates. The investigation of cathepsin L knockout mice revealed that cathepsin L is involved in processing POMC to produce ACTH, β-END, and α-MSH (Funkelstein et al., 2008). Cathepsin L knockout mice have decreases in pituitary ACTH, β-END, and α-MSH, while levels of POMC increased. Others showed a co-localization of cathepsin L with β-END, α-MSH, and ACTH in pituitary secretory vesicles (Hook et al., 2012). We found c*athepsin L* and *aminopeptidase B* mRNA expression in LNs from healthy rats and from animals with paw inflammation. Future studies will have to examine cathepsin L and aminopeptidase B proteins. Together these findings indicate that cathepsin L and aminopeptidase B may also be involved in POMC cleavage in lymphocytes.

4.4. Measurement of β-endorphin (β-END)

To match the processing of POMC with the presence of PC1 and PC2 in lymphocytes we analysed whether our *in vivo* and *in vitro* stimulation models resulted in enhanced cellular β-END contents. Immunofluorescence experiments with antibodies to β-END showed no elevation of β-END when naïve LN cells were

treated with IL-4 alone. To obtain significant opioid peptide levels and cell numbers expressing β-END *in vitro*, we had to prime naïve cells with the mitogen conA, similar to others (Hermanussen et al., 2004). An elevation of β-END was observed under the same conditions that produced upregulation of PC1 protein expression. These results extend our previous findings where increased β-END levels of LN cells were measured after *in vitro* stimulation with IL-4 plus conA (Busch-Dienstfertig et al., 2012). Then we set out to investigate β-END production in cell subsets of the draining LNs of rats with paw inflammation. We found a strong upregulation in B cells of inflamed nodes, while the amount of β-END in T cells only slightly increased. These data extend our previous findings showing increased cellular β-END levels in mixed LN cells *in vivo* (Sitte et al., 2007) and indicate that B cells are the predominant *Pomc* gene expressing subtype in inflammation. Since these cells were found to express PC1 and PC2 alike, it is consistent that β-END elevation was determined in B but not in T cells. Nevertheless, these findings were unexpected. Previous double-staining experiments with antibodies to β-END and different cell phenotypes demonstrated that β-END is mostly present in memory T cells (Cabot et al., 1997). However, in line with our findings, others investigated the cleavage products of POMC in B cells (Harbour et al., 1991; 1987). These authors found that stimulating B cells with corticotropin-releasing hormones or viruses produced ACTH 1-39 and β-END, while in LPS-stimulated cells cleavage products of ACTH 1-39 (ACTH 1-22 to 1-26) and β-END (gamma-END) predominated. LPS activated an additional processing enzyme with an activity pH of 5, which resembles the optimal pH of PC2 (Li et al., 2003). Together, these findings suggest that B cells are a source of β-END production, and they support that *Pomc* gene expression and precursor processing are independently regulated in lymphocytes.

4.5 Opioid peptides in arthritis

In order to compare the above findings to a different model of inflammation (ACIA), the expression of opioid peptides in explanted cells of arthritic knees was investigated. As expected, the amount of β-END determined in the supernatant of such cells was generally related to the cell number, but it surprisingly did not correlate with the number of immune cells in the preparation. This is in contrast to previous findings obtained in acutely inflamed hind paws (Rittner et al., 2001; Brack

et al., 2004). It is possible that β-END may be expressed in other cells under chronic conditions than in acute inflammation. Mousa and colleagues have shown that, besides macrophages and T cells, fibroblast-like synoviocytes also stained positive for β-END in tissue biopsies from patients with chronic rheumatoid arthritis. In some biopsies, fibroblast-like synoviocytes and plasma cells represented the predominant β-END-containing cell populations (Mousa et al., 2007). Our data suggest that in ACIA the expression of β-END also occurs in non-immune cells.

The cellular levels of met-enkephalin correlated significantly with cell numbers from explanted knee cells. Correlations with the number of CD45+ cells were also strong but not statistically significant; the strongest correlation was found for the number of non-immune cells. Overall, the presence of this opioid peptide in immune and non-immune cells is in agreement with previous findings of met-enkephalin-positive lymphocytes, macrophages, and plasma cells in tissue biopsies from rheumatoid arthritis patients and with met-enkephalin-positive fibroblasts in tissue biopsies from osteoarthritis patients (Mousa et al., 2007). The liberation of met-enkephalin, however, did not correlate with cell numbers of explanted knee cells. It is possible that the extent of met-enkephalin release differs between the cell subsets (lymphocytes, macrophages, plasma cells, and fibroblasts). However, relative to the molecular mass of the two peptides (571.65 Da for met-enkephalin and 3466.07 Da for β-END), the net amount of biologically active peptides determined here was similar.

Finally, we compared opioid peptides in explanted cells of arthritic knees and LNs. In knee cells we found that the amount of Met-enkephalin increased after induction of arthritis but decreased at later stages. This is in contrast to LN cells, where no substantial changes were observed between early and later stages. This may indicate that opioid peptides in the knee joint are stimulated by different mechanisms in comparison to LNs. Previous studies from (Baddack et al., 2013) showed the formation of a new LN in close proximity to the knee joint in this model. Therefore, we investigated opioid peptides in the synovial space, popliteal LNs, and periarticular LNs. The tissue slices were deparaffinised for antigen retrieval. Various parameters were altered, but the results were inconsistent. There could be various reasons for this. Proteolytic digestion of fixed paraffin sections can increase the stainability chances of cytoplasmic antigens (Nemes et al., 1983; Tanaka et al., 1984) demonstrated that pre-treatment with hyaluronidase was necessary for

staining surface antigens of lymphocytes, whereas (Sato et al., 1986) demonstrated that pre-treatment with the enzyme was not necessary. The staining also largely depends on the fixation procedure (Fisher et al., 1994). Some reports suggest that antigen retrieval immunohistochemistry gives good results (Shi et al., 1997) but standardization is required for this method (Taylor et al., 1994, 2006; Shi et al., 2013). For example, standardization of temperature, duration of heating, and pH value of the buffer are major factors that influence the effectiveness of staining (Shi et al., 2007). Future experiments will have to be performed to optimize these conditions.

4.6 Conclusion

From the present studies we can conclude that the regulation of *Pomc* in lymphocytes differs from the pituitary. *Pomc* in lymphocytes is expressed only in B cells under conditions such as paw inflammation and *in vitro* stimulation of LN cells with IL-4. Our experiments suggest that neither DNA methylation, acetylation, nor miRNA are involved in the repression of the *Pomc* gene in naïve cells. Although the key factor triggering *Pomc* mRNA expression in B cells remains unknown, there is an indication that it is a cytokine acting through the JAK/STAT pathway. Both *in vitro* and *in vivo* experiments show that the proteolytic processing of POMC into β-END in lymphocytes involves PC1, PC2, cathepsin L, and aminopeptidase B. However, unlike in the pituitary, it does not show involvement of CPE. We found that both β-END and POMC are produced in B cells. These findings may help develop novel strategies for pain therapy in inflammatory diseases by boosting the innate opioid peptide production in immune cells.

4.7 Future experiments

Future experiments will have to address remaining questions regarding the exact mechanism that suppresses *Pomc* gene expression in naïve lymphocytes, the factor released by T cells that stimulates B cell production of *Pomc* mRNA, the role of cathepsin L and aminopeptidase B in POMC cleavage in lymphocytes, the lack of CPE in lymphocytes, the cellular expression of β-END in chronic arthritis, and the differential production and release of β-END and Met-enkephalin.

5 References

Abrams GM, Nilaver G, Hoffman D, Zimmerman EA, Ferin M, Krieger DT, Liotta AS (1980). Immunocytochemical distribution of corticotropin (ACTH) in monkey brain. Neurology 30(10):1106-10.

Anderson L, Seilhamer J (1998). A comparison of selected mRNA and protein abundances in human liver. Electrophoresis 18:533-537.

Asa S, Kovacs K, Melmed S (1995). The hypothalamic-pituitary function. In: Melmed S, ed. The Pituitary. Cambridge, MA: Blackwell Science; p. 3.

Azaryan AV and Hook VYH. (1994) Unique cleavage specificity of prohormone thiol protease' related to proenkephalin processing. FEBS Lett 341:197-202.

Baddack U, Hartmann S, Bang H, Grobe J, Loddenkemper C, Lipp M, and Muller G. (2013). A chronic model of arthritis supported by a strain-specific periarticular lymph node in BALB/c mice. Nat Commun 4:1644.

Bai G, Wei D, Zou S, Ren K, Dubner R (2010). Inhibition of class II histone deacetylases in the spinal cord attenuates inflammatory hyperalgesia. Mol Pain 7:6-51.

Baldi P, Long AD (2001). A Bayesian framework for the analysis of microarray expression data: regularized t-test and statistical inferences of gene changes. Bioinformatics 17:509-519.

Barber A, Gottschlich R (1992). Opioid agonists and antagonists: an evaluation of their peripheral actions in inflammation. Med Res Rev 12(5):525-62.

Bardin CW, Chen CL, Morris PL, Gerendai I, Boitani C, Liotta AS, Margioris A, Krieger (1987). Proopiomelanocortin-derived peptides in testis, ovary, and tissues of reproduction. Recent Prog Horm Res 43:1-28.

Benjannet S, Rondeau N, Day R, Chretien M, Seidah NG (1991). PC1 and PC2 are proprotein convertases capable of cleaving proopiomelanocortin at distinct pairs of basic residues. Proc Natl Acad Sci U S A 88(9):3564-3568.

Benjannet S, Rondeau N, Paquet L, Boudreault A, Lazure C, Chretien M, Seidah NG (1993). Comparative biosynthesis, covalent post-translational modifications and efficiency of prosegment cleavage of the prohormone convertases PC1 and PC2: glycosylation, sulphation and identification of the intracellular site of prosegment cleavage of PC1 and PC2. Biochem J 294(Pt 3):735-743.

Benjannet S, Savaria D, Chretien M, Seidah NG (1995). 7B2 is a specific intracellular binding protein of the prohormone convertase PC2. J Neurochem 64(5):2303-2311.

Bennett DL, Bailyes EM, Nielsen E, Guest PC, Rutherford NG, Arden SD, Hutton JC (1992). Identification of the type 2 proinsulin processing endopeptidase as PC2, a member of the eukaryote subtilisin family. J Biol Chem 267(21): 15229-15236.

Bergeron F, Leduc R, Day R (2000). Subtilase-like pro-protein convertases: from molecular specificity to therapeutic applications. J Mol Endocrinol 24(1): 1-22.

Bicknell AB (2008). The tissue-specific processing of pro-opiomelanocortin. Journal of Neuroendocrinology 20:692–699.

Binder W, Mousa SA, Sitte N, Kaiser M, Stein C, Schafer M. (2004). Sympathetic activation triggers endogenous opioid release and analgesia within peripheral inflamed tissue. Eur J Neurosci 20(1):92-100.

Bost KL, Smith EM, Wear LB, Blalock JE (1987). Presence of ACTH and its receptor on a B lymphocytic cell line: a possible autocrine function for a neuroendocrine hormone. J Biol Regul Homeost Agents 1(1):23-7.

Boston BA. (2002).Peripheral effects of melanocortins. In: Cone RD editor. *The Melanocortin Receptors*. Totowa, NJ: Human Press. p. 143–69.Boudreault, A,

Gauthier D and Lazure C (1998). Proprotein convertase PC1/3-related peptides are potent slow tight-binding inhibitors of murine PC1/3 and Hfurin. J Biol Chem 273(47): 31574-31580.

Boué J, Blanpied C, Brousset P, Vergnolle N, and Dietrich G. (2011). Endogenous opioid-mediated analgesia is dependent on adaptive T cell response in mice. J Immunol 186:5078-5084.

Bousquet C, Melmed S. (1999). Critical role for STAT3 in murine pituitary adrenocorticotropin hormone leukemia inhibitory factor signaling. J Biol Chem. 274:10723–10730.

Brack A, Rittner HL, Machelska H, Shaqura M, Mousa SA, Labuz D, Zöllner C, Schäfer M, Stein C (2004). Endogenous peripheral antinociception in early inflammation is not limited by the number of opioid-containing leukocytes but by opioid receptor expression. Pain 108(1-2):67-75.

Braks JA, Van Horssen AM, Martens GJ. (1996). Dissociation of the complex between the neuroendocrine chaperone 7B2 and prohormone convertase PC2 is not associated with proPC2 maturation. Eur J Biochem 238(2):505-10.

Brueckner B, Garcia Boy R, Siedlecki P, Musch T, Kliem HC, Zielenkiewicz P, Suhai S, Wiessler M, Lyko F.(2005). Epigenetic reactivation of tumor suppressor genes by a novel small-molecule inhibitor of human DNA methyltransferases. Cancer Res. 65(14):6305-11.

Busch-Dienstfertig M, Labuz D, Wolfram T, Vogel NN, Stein C. (2012). JAK-STAT1/3-induced expression of signal sequence-encoding proopiomelanocortin mRNA in lymphocytes reduces inflammatory pain in rats. Mol Pain. 13;8:83.

Butler AA, Cone RD. (2003). Knockout studies defining different roles for melanocortin receptors in energy homeostasis. Ann N Y Acad Sci ;994:240-5.

Buzzetti R, McLoughlin L Lavender PM, Clark AJ and Rees LH. (1989). Expression of pro-opiomelanocortin gene and quantification of adrenocorticotropic hormone-like immunoreactivity in human normal peripheral mononuclear cells and lymphoid and myeloid malignancies. J Clin Invest 83(2): 733-737.

Cabot, PJ Carter L, Gaiddon C, Zhang Q, Schäfer M, Loeffler JP and Stein C. (1997). Immune cell-derived beta-endorphin. Production, release, and control of inflammatory pain in rats. J Clin Invest 100(1): 142-148.

Castro M, Gusovsky GF and Loh YP. (1989). Transmembrane signals mediating adrenocorticotropin release from mouse anterior pituitary cells. Mol Cell Endocrinol 65(1-2): 165-173.

Castro MG, Morrison E. (1997). Post-translational processing of proopiomelanocortin in the pituitary and in the brain. Crit Rev Neurobiol.11:35–57.

Che FY, Yan L, Li H, Mzhavia N, Devi LA and Fricker LD. (2001). Identification of peptides from brain and pituitary of Cpe(fat)/Cpe(fat) mice. Proc Natl Acad Sci U S A 98(17): 9971-9976.

Chen CL, Chang CC, Krieger DT and Bardin CW (1986). Expression and regulation of proopiomelanocortin-like gene in the ovary and placenta: comparison with the testis. Endocrinology 118(6): 2382-2389.

Chiechio S, Zammataro M, Morales ME, Busceti CL, Drago F, Gereau RW, Copani A, Nicoletti F. (2009). Epigenetic modulation of mGlu2 receptors by histone deacetylase inhibitors in the treatment of inflammatory pain. Mol Pharmacol. 75(5):1014-20.

Childers SR (1993). Opioids I. In Herz A, ed. Handbook of Experimental Pharmacology, Vol. 104. Berlin: Springer Verlag; pp. 189–216.

Christie DL Batchelor DC and Palmer DJ. (1991). Identification of kex2-related proteases in chromaffin granules by partial amino acid sequence analysis. J Biol Chem 266(24): 15679-15683.

Clark AJ Lavender PM, Coates P, Johnson MR and Rees LH. (1990). In vitro and in vivo analysis of the processing and fate of the peptide products of the short proopiomelanocortin mRNA. Mol Endocrinol 4(11): 1737-1743.

Coelho FM, Pinho V, Amaral FA, Sachs D, Costa V, Rodrigues D. (2008). The chemokine receptors CXCR1/2 modulate antigen-induced arthritis by regulating adhesion of neutrophils to the synovial microvasculature. Arthritis Rheum 58: 1329–2337.

Cool DR and Loh YP. (1994). Identification of a sorting signal for the regulated secretory pathway at the N-terminus of pro-opiomelanocortin. Biochimie 76(3-4): 265-270.

Cool DR Normant E, Shen F, Chen HC, Pannell L, Zhang Y and Loh YP. (1997). Carboxypeptidase E is a regulated secretory pathway sorting receptor: genetic obliteration leads to endocrine disorders in Cpe(fat) mice. Cell 88(1): 73-83.

Corbett AD, Paterson SJ, and Kosterlitz HW. (1993) in Handbook of Experimental Pharmacology: Opioids I (A.Herz, Ed.), Vol. 104, pp. 645–679, Springer Verlag, Berlin.

Cowley MA, Pronchuk N, Fan W, Dinulescu DM, Colmers WF, Cone RD.(1999). Integration of NPY, AGRP, and melanocortin signals in the hypothalamic paraventricular nucleus: evidence of a cellular basis for the adipostat. Neuron. 1:155-63.

Cunha TM, Verri WA Jr, Silva JS, Poole S, Cuha FQ, Ferreira SH (2005). A cascade of cytokines mediates mechanical inflammatory hypernociception in mice. Proc Natl Acad Sci U S A 102: 1755–1760.

Day R, Schafer MK, Watson SJ, Chretien M and Seidah NG. (1992). Distribution and regulation of the prohormone convertases PC1 and PC2 in the rat pituitary. Mol Endocrinol 6(3): 485-497.

DeBold CR, Menefee JK, Nicholson WE and Orth DN. (1988). Proopiomelanocortin gene is expressed in many normal human tissues and in tumors not associated with ectopic adrenocorticotropin syndrome. Mol Endocrinol. 2(9): 862-870.

DeBold CR, Nicholson WE and Orth DN. (1988). Immunoreactive proopiomelanocortin (POMC) peptides and POMC-like messenger ribonucleic acid are present in many rat nonpituitary tissues. Endocrinology 122(6): 2648-2657.

Dieu-Nosjean MC, Massacrier C, Homey B, Vanbervliet B, Pin JJ, Vicari A, Lebecque S, Dezutter-Dambuyant C, Schmitt D, Zlotnik A, Caux C.(2000). Macrophage inflammatory protein 3alpha is expressed at inflamed epithelial surfaces and is the most potent chemokine known in attracting Langerhans cell precursors. J Exp Med. 4;192(5):705-18.

Doehring A, Geisslinger G, Lötsch J. (2011). Epigenetics in pain and analgesia: an imminent research field. Eur J Pain. 15(1):11-6.

Douglass J Civelli O and Herbert E. (1984). Polyprotein gene expression: generation of diversity of neuroendocrine peptides. Annu Rev Biochem 53: 665-715.

Espinosa VP, Liu Y, Ferrini M, Anghel A, Nie Y, Tripathi PV, Porche R, Jansen E, Stuart RC, Nillni EA, Lutfy K, Friedman TC. (2008). Differential regulation of prohormone convertase 1/3, prohormone convertase 2 and phosphorylated cyclic-AMP-response element binding protein by short-term and long-term morphine treatment: implications for understanding the "switch" to opiate addiction. Neuroscience. 15;156(3):788-99.

Firestein GS. (2003). Evolving concepts of rheumatoid arthritis. Nature 423:356-361.

Firestein GS. (2005). Immunologic mechanisms in the pathogenesis of rheumatoid arthritis. J Clin Rheumatol 11: S39–S44.

Fisher CJ, Gillett CE, Vojtěsek B, Barnes DM, Millis RR.(1994).Problems with p53 immunohistochemical staining: the effect of fixation and variation in the methods of evaluation. J Cancer. (1):26-31.

Fortenberry Y, Hwang JR, Apletalina EV and Lindberg I. (2002). Functional characterization of ProSAAS: similarities and differences with 7B2. J Biol Chem 277(7): 5175-5186.

Friedrich K, Kammer W, Erhardt I, Brändlein S, Sebald W, Moriggl R.(1999). Activation of STAT5 by IL-4 relies on Janus kinase function but not on receptor tyrosine phosphorylation, and can contribute to both cell proliferation and gene regulation. Int Immunol.11(8):1283-94.

Fukata J, Usui T, Naitoh Y, Nakai Y, Imura H. (1989). Effects of recombinant human interleukin-1 alpha, -1 beta, 2 and 6 on ACTH synthesis and release in the mouse pituitary tumour cell line AtT-20. J Endocrinol.122:33–39.

Funkelstein L, Toneff T, Hwang SR, Reinheckel T, Peters C, Hook V.(2008). Cathepsin L participates in the production of neuropeptide Y in secretory vesicles, demonstrated by protease gene knockout and expression. J Neurochem. 106(1):384-91.

Funkelstein L . Toneff SR, Hwang F, Beuschlein UD, LichtenauerT, Reinheckel C, Peters, Hook VYH.. (2008). Major role of cathepsin L for producing the peptide hormones ACTH, β-endorphin, and α-MSH, illustrated by protease gene knockout and expression, J. Biol. Chem. (83)35652–35659.

Fuge`re M and Day R. (2005) Cutting back on pro-protein convertases: the latest approaches to pharmacological inhibition. Trends Pharmacol. Sci. 26, 294–301.

Gee CE, Chen CL, Roberts JL, Thompson R, Watson SJ.(1983). Identification of proopiomelanocortin neurones in rat hypothalamus by in situ cDNA-mRNA hybridization. Nature. 306(5941):374-6.

Glickman MH, Ciechanover A. (2002). The ubiquitin-proteasome proteolytic pathway: destruction for the sake of construction. Physiol Rev. 82:373-428.

Goetz CA, Harmon IR, O'Neil JJ, Burchill MA, Johanns TM, Farrar MA. (2005). Restricted STAT5 activation dictates appropriate thymic B versus T cell lineage commitment. J. Immunol. 174, 7753–7763.

Goodman LJ and Gorman CM.(1994). Autoproteolytic activation of the mouse prohormone convertase mPC1. Biochem Biophys Res Commun 201(2): 795-804.

Gorbman A, Dickhoff WW, Vigna SR, Clark NB, Ralph CL.(1983). Comparative Endocrinology. New York: John Wiley and Sons.

Greenbaum D, Colangelo C, Williams K, Gerstein M.(2003). Comparing protein abundance and mRNA expression levels on a genomic scale. Genome Biol.4(9):117.

Grigorakis SI, Anastasiou E, Dai K, Souvatzoglou A, Alevizaki M. (2000). Three mRNA transcripts of the proopiomelanocortin gene in human placenta at term. Eur J Endocrinol. 142(5):533-6.

Hakes DJ, Birch NP, Mezey A, Dixon JE. (1991). Isolation of two complementary deoxyribonucleic acid clones from a rat insulinoma cell line based on similarities to Kex2 and furin sequences and the specific localization of each transcript to endocrine and neuroendocrine tissues in rats. Endocrinology.129(6):3053-63.

Hansmann T, Pliushch G, Leubner M, Kroll P, Endt D, Gehrig A, Preisler-Adams S, Wieacker P, Haaf T. (2012).Constitutive promoter methylation of BRCA1 and RAD51C in patients with familial ovarian cancer and early-onset sporadic breast cancer. Hum Mol Genet. 21(21):4669-79.

Harbour DV, Galin FS, Hughes TK, Smith EM, Blalock JE. (1991). Role of leukocyte-derived pro-opiomelanocortin peptides in endotoxic shock. Circ Shock. 35(3):181-91.

Harbour DV, Smith EM, Blalock JE. (1987). Novel processing pathway for proopiomelanocortin in lymphocytes: endotoxin induction of a new prohormone-cleaving enzyme. J Neurosci Res. 18(1):95-101.

Harbour DV, Smith EM, Blalock JE. (1987). Splenic lymphocyte production of an endorphin during endotoxic shock. Brain Behav Immun. (2):123-33.

Hayatsu H. (1976). Bisulfite modification of nucleic acids and their constituents. Prog Nucleic Acid Res Mol Biol.16:75-124.

He L, Hannon GJ. (2004). MicroRNAs: small RNAs with a big role in gene regulation. Nat Rev Genet. (7):522-31.

Hermanussen S, Do M and Cabot PJ. (2004). Reduction of beta-endorphin-containing immune cells in inflamed paw tissue corresponds with a reduction in immune-derived antinociception: reversible by donor activated lymphocytes. Anesth Analg. 98:723-729.

Holm IA, Majzoub JA. Adrenocorticotropin. (1995). In: Melmed S editor. The Pituitary. Cambridge, MA: Blackwell Science 45 p.

Huscher D, Thiele K, Gromnica-Ihle E, Hein G, Demary W, Dreher R, Zink A and Buttgereit, F. (2009). Dose-related patterns of glucocorticoid-induced side effects. Ann Rheum Dis 68:1119-1124.

Huzen J, van Veldhuisen DJ, van Gilst WH, van der Harst P. (2008).Telomeres and biological ageing in cardiovascular disease. Ned Tijdschr Geneeskd.152(22):1265-70.

Jenks BG. (2009). Regulation of proopiomelanocortin gene expression: an overview of the signaling cascades, transcription factors, and responsive elements involved. Ann N Y Acad Sci.1163:17-30.

Jensen K, Anderson JA, Glass EJ. (2014). Comparison of small interfering RNA (siRNA) delivery into bovine monocyte-derived macrophages by transfection and electroporation. Vet Immunol Immunopathol.158(3-4):224-32.

Jiang Y, Genant HK, Watt I, Cobby M, Bresnihan B, Aitchison R. (2000). A multicenter, double-blind, dose-ranging, randomized, placebo-controlled study of recombinant human interleukin-1 receptor antagonist in patients with rheumatoid arthritis: radiologic progression and correlation of Genant and Larsen scores. Arthritis Rheum 43: 1001–1009.

Jin WD, Boutillier AL, Glucksman MJ, Salton SR, Loeffler JP and Roberts JL. (1994). Characterization of a corticotropin-releasing hormone-responsive element in the rat proopiomelanocortin gene promoter and molecular cloning of its binding protein. Mol Endocrinol 8(10): 1377-1388.

Jones CK, Eberle EL, Peters SC, Monn JA, Shannon HE. (2005).Analgesic effects of the selective group II (mGlu2/3) metabotropic glutamate receptor agonists LY379268 and LY389795 in persistent and inflammatory pain models after acute and repeated dosing. Neuropharmacology. 49 Suppl 1:206-18.

Jutras I, Seidah NG, Reudelhuber TL and Brechler V. (1997). Two activation states of the prohormone convertase PC1 in the secretory pathway. J Biol Chem 272(24): 15184-15188.

Katahira M Iwasaki Y, Aoki Y, Oiso Y and Saito H. (1998). Cytokine regulation of the rat proopiomelanocortin gene expression in AtT-20 cells. Endocrinology 139(5): 2414-2422.

Kavelaars A, Ballieux RE, Heijnen CJ. (1989). The role of IL-1 in the corticotropin-releasing factor and arginine- vasopressin-induced secretion of immunoreactive beta-endorphin by human peripheral blood mononuclear cells. J Immunol. ;142(7):2338-42.

Kavelaars A, Ballieux RE, Heijnen CJ.(1990). Differential effects of beta-endorphin on cAMP levels in human peripheral blood mononuclear cells. Brain Behav Immun.;4(3):171-9.

Keegan AD, Nelms K, Wang LM, Pierce JH, Paul WE.(1994). Interleukin 4 receptor: signaling mechanisms. Immunol Today;15(9):423-32.

Kim J, Bartel DP. (2009). Allelic imbalance sequencing reveals that single-nucleotide polymorphisms frequently alter microRNA-directed repression. Nat Biotechnol. 27(5):472-7.

Kobayashi Y, Sakamoto T, Iguchi K, Imai Y, Hoshino M, Lance VA. (2007). cDNA cloning of proopiomelanocortin (POMC) and mass spectrometric identification of POMC-derived peptides from snake and alligator pituitaries. Gen Comp Endocrinol 152:73–81.

Korner J, Chun J, O'Bryan L, and Axel R. (1991). Prohormone processing in Xenopus oocytes: characterization of cleavage signals and cleavage enzymes. Proc Natl Acad Sci U S A 88(24): 11393-11397.

Koscianska E, Starega-Roslan J, Krzyzosiak WJ. (2001).The role of Dicer protein partners in the processing of microRNA precursors. PLoS One. 6(12):e28548

Kroot EJ, de Jong BA, van Leeuwen MA, Swinkels H, van den Hoogen FH, van't Hof M,van de Putte LB, van Rijswijk MH, van Venrooij WJand van Riel PL. (2000). The prognostic value of anti-cyclic citrullinated peptide antibody in patients with recent-onset rheumatoid arthritis. Arthritis Rheum 43:1831-1835.

Labuz D, Schreiter A, Schmidt Y, Brack Aand Machelska H. (2010). T lymphocytes containing beta-endorphin ameliorate mechanical hypersensitivity following nerve injury. Brain Behav Immun 24:1045-1053.

Lacaze-Masmonteil T, de Keyzer Y, Luton JP, Kahn A and Bertagna X. (1987). Characterization of proopiomelanocortin transcripts in human nonpituitary tissues. Proc Natl Acad Sci U S A 84(20): 7261-7265.

Lamango NS Zhu X and Lindberg I. (1996). Purification and enzymatic characterization of recombinant prohormone convertase 2: stabilization of activity by 21 kDa 7B2. Arch Biochem Biophys 330(2): 238-250.

LaMendola J, Martin SK, Steiner DF.(1997).Expression of PC3, carboxypeptidase E and enkephalin in human monocyte-derived macrophages as a tool for genetic studies. FEBS Lett;404(1):19-22.

Lamolet B, Pulichino AM, Lamonerie T, Gauthier Y, Brue T, Enjalbert A and Drouin J.(2001). A pituitary cell-restricted T box factor, Tpit, activates POMC transcription in cooperation with Pitx homeoproteins. Cell 104(6): 849-859.

Lamonerie T, Tremblay JJ, Lanctot C, Therrien M, Gauthier Y and Drouin J.(1996). Ptx1, a bicoid-related homeo box transcription factor involved in transcription of the pro-opiomelanocortin gene. Genes Dev 10(10): 1284-1295.

Lansac G, Dong W, Dubois CM, Benlarbi N, Afonso C, Fournier I, Salzet M and Day R. (2006). Lipopolysaccharide mediated regulation of neuroendocrine associated proprotein convertases and neuropeptide precursor processing in the rat spleen. J Neuroimmunol 171(1-2): 57-71.

Lee RC, Feinbaum RL, Ambros V.(1993). The C. elegans heterochronic gene lin-4 encodes small RNAs with antisense complementarity to lin-14. Cell.75(5):843-54.

Lee SN Prodhomme E and Lindberg I. (2004). Prohormone convertase 1 (PC1) processing and sorting: effect of PC1 propeptide and proSAAS. J Endocrinol 182(2): 353-364.

Li CH, Chung D, Doneen BA.(1976). Isolation, characterization and opiate activity of beta-endorphin from human pituitary glands. Biochem Biophys Res Commun. ;72(4):1542-7.

Li CH, Chung D, Oelofsen W, Naudé RJ (1978). Adrenocorticotropin 53. The amino acid sequence of the hormone from the ostrich pituitary gland. Biochem Biophys Res Commun 81:900–6.

Li CH. (1981).β-Endorphin: synthetic analogs and structure-activity relationships. In: Li CH editor. Hormonal Proteins and Peptides. New York, NY: Academic Press. p. 2–34.

Li QL, Jansen E, Friedman TC (1999). Regulation of prohormone convertase 1 (PC1) by gp130-related cytokines. Mol Cell Endocrinol 158(1-2):143-52.

Li QL, Naqvi S, Shen X, Liu YJ, Lindberg I, Friedman TC (2003). Prohormone convertase 2 enzymatic activity and its regulation in neuro-endocrine cells and tissues. Regul Pept 110(3):197-205.

Liao XH, Li YQ, Wang N, Zheng L, Xing WJ, Zhao DW, Yan TB, Wang Y, Liu LY, Sun XG, Hu P, Zhou H, Zhang TC (2014). Re-expression and epigenetic modification of maspin induced apoptosis in MCF-7 cells mediated by myocardin. Cell Signal 26(6):1335-46.

Lian Z, Kluger Y, Greenbaum DS, Tuck D, Gerstein M, Berliner N, Weissman SM, Newburger PE. (2002). Genomic and proteomic analysis of the myeloid differentiation program: global analysis of gene expression during induced differentiation in the MPRO cell line. Blood.100:3209-3220.

Lichtinghagen R, Musholt PB, Lein M, Romer A, Rudolph B, Kristiansen G, Hauptmann S, Schnorr D, Loening SA, Jung K. (2002). Different mRNA and protein expression of matrix metallo proteinases 2 and 9 and tissue inhibitor of metalloproteinases 1 in benign and malignant prostate tissue. Eur Urol .42:398- 406.

Liew FY, McInnes IB (2005). A fork in the pathway to inflammation and arthritis. Nat Med 11: 601–602.

Lisanti S, Omar WA, Tomaszewski B, De Prins S, Jacobs G, Koppen G, Mathers JC, Langie SA.(2013). Comparison of methods for quantification of global DNA methylation in human cells and tissues. PLoS One. 18;8(11)

Litthauer D, Naudé RJ, Oelofsen W. (1984). Isolation, characterization and primary structure of two β-LPH variants from ostrich pituitary glands. Int J Pept Protein Res. 24:309–15.

Lodish H, Berk A, Zipursky SL, Matsudaira P, Baltimore D and Darnell JE. (2001). Molekulare Zellbiology: Prozessierung von mRNA bei Eukaryoten. Spectrum Akademischer Verlag GmbH Heidelberg - Berlin 4th ed: 447-459.

Loh YP. (1987).Peptide precursor processing enzymes within secretory vesicles. Ann N Y Acad Sci. 493:292-307.

Loh YP, Maldonado A, Zhang C, Tam WH and Cawley N. (2002). Mechanism of sorting proopiomelanocortin and proenkephalin to the regulated secretory pathway of neuroendocrine cells. Ann N Y Acad Sci 971: 416-425.

Lolait SJ, Clements JA, Markwick AJ, Cheng C, McNally M, Smith AI and Funder JW. (1986). Pro-opiomelanocortin messenger ribonucleic acid and posttranslational processing of beta endorphin in spleen macrophages. J Clin Invest 77(6): 1776-1779.

Lolait SJ, Lim AT, Toh BH and Funder JW.(1984). Immunoreactive beta-endorphin in a subpopulation of mouse spleen macrophages. J Clin Invest. 73(1): 277-280.

Lorincz A, Nusser Z. (2008). Specificity of immunoreactions: the importance of testing specificity in each method. J Neurosci. 28(37):9083-6.

Lötsch J, Geisslinger G, Tegeder I.(2009). Genetic modulation of the pharmacological treatment of pain. Pharmacol Ther.124(2):168-84.

Lu WD, Funkelstein L, Toneff T, Reinheckel T, Peters C, Hook V. (2012). Cathepsin H functions as an aminopeptidase in secretory vesicles for production of enkephalin and galanin peptide neurotransmitters. J Neurochem. 122(3):512-22.

Lyons PDand Blalock JE. (1995). The kinetics of ACTH expression in rat leukocyte subpopulations. J Neuroimmunol. 63(2): 103-12.

Lyons PD and Blalock JE. (1997). Pro-opiomelanocortin gene expression and protein processing in rat mononuclear leukocytes. J Neuroimmunol 78(1-2): 47-56.

Maier CC and Blalock JE. (1994). PCR-based cloning, sequencing, and exon mapping of lymphocyte-derived neuroendocrine peptides. Immunomethods 5(1): 3-7.

Mains RE, Eipper BA. (1990).The tissue-specific processing of Pro-ACTH/Endorphin recent advances and unsolved problems. Trends Endocrinol Metab. 1(8):388-94.

Marcinkiewicz M, Day R, Seidah NG and Chretien M (1993). Ontogeny of the prohormone convertases PC1 and PC2 in the mouse hypophysis and their colocalization with corticotropin and alpha-melanotropin. Proc Natl Acad Sci U S A 90(11): 4922-4926.

Martens GJ, Braks JA, Eib DW, Zhou Y and Lindberg I. (1994). The neuroendocrine polypeptide 7B2 is an endogenous inhibitor of prohormone convertase PC2. Proc Natl Acad Sci U S A 91(13): 5784-5787.

Mechanick JI, Levin N, Roberts JL and Autelitano DJ. (1992). Proopiomelanocortin gene expression in a distinct population of rat spleen and lung leukocytes. Endocrinology 131(1): 518-525.

Menschikowski M, Platzbecker U, Hagelgans A, Vogel M, Thiede C, Schönefeldt C, Lehnert R, Eisenhofer G, Siegert G. (2012). Aberrant methylation of the M-type phospholipase A(2) receptor gene in leukemic cells. BMC Cancer. 5;12:576.

Moreland LW, Baumgartner SW, Schiff MH, Tindall EA, Fleischmann RM, Weaver AL . (1997). Treatment of rheumatoid arthritis with a recombinant human tumor necrosis factor receptor (p75)-Fc fusion protein. N Engl J Med 337: 141–147.

Mountjoy KG, Wu CS, Cornish J, Callon KE. (2003). Alpha-MSH and desacetyl-alpha-MSH signaling through melanocortin receptors. Ann N Y Acad Sci. 994:58-65.

Mousa SA, Schäfer M, Mitchell WM, Hassan AH and Stein C. (1996). Local upregulation of corticotropin-releasing hormone and interleukin-1 receptors in rats with painful hindlimb inflammation. Eur J Pharmacol 311(2-3): 221-231.

Mousa SA, Machelska H, Schäfer M, Stein C. (2000). Co-expression of beta-endorphin with adhesion molecules in a model of inflammatory pain. J Neuroimmunol. 108(1-2):160-70.

Mousa SA, Zhang Q, Sitte N, Ji R, Stein C. (2001). beta-Endorphin-containing memory-cells and mu-opioid receptors undergo transport to peripheral inflamed tissue. J Neuroimmunol.115(1-2):71-8.

Mousa SA,Shakibaei M, Sitte N, Schafer M and Stein C. (2004). Subcellular pathways of beta-endorphin synthesis, processing, and release from immunocytes in inflammatory pain. Endocrinology. 145(3): 1331-1341.

Mousa SA, Straub RH, Schäfer M, Stein C. (2007). Beta-endorphin, Met-enkephalin and corresponding opioid receptors within synovium of patients with joint trauma, osteoarthritis and rheumatoid arthritis. Ann Rheum Dis.66(7):871-9.

Muller L and Lindberg I (1999). The cell biology of the prohormone convertases PC1 and PC2. Prog Nucleic Acid Res Mol Biol 63: 69-108.

Mynard V, Guignat L, Devin-Leclerc J, Bertagna X, Catelli MG. (2012). Different mechanisms for leukemia inhibitory factor-dependent activation of two proopiomelanocortin promoter regions. Endocrinology.143:3916–3924.

Nakanishi S, Inoue A, Kita T, Nakamura M, Chang ACY, Cohen SN.(1979) Nucleotide sequence of cloned cDNA for bovine corticotropin-β-lipotropin precursor. *Nature* **278**:423–7.

Naudé RJ, Chung D, Li CH, Oelofsen W. (1981). β-Endorphin: primary structure of the hormone from the ostrich pituitary gland. Biochem Biophys Res Commun. 98:108–14.

Naudé RJ, Chung D, Li CH, Oelofsen W. (1981).β-Lipotropin: primary structure of the hormone from the ostrich pituitary gland. Int J Pept Protein Res. 18:138–47.

Naudé RJ, Litthauer D, Oelofsen W, Chrétien M, Lazure C.(1993). The production of the ostrich NH2-terminal POMC fragment requires cleavage at a unique signal peptidase site. Peptides.14:519–29.

Naudé R, Oelofsen W, Takahashi A, Amano M, Kawauchi H. (2006). Molecular cloning and characterization of preproopiomelanocortin (prePOMC) cDNA from the ostrich (*Struthio camelus*). Gen Comp Endocrinol 146:310–7.

Nemes Z, Thomazy V, Szeifelt G. (1983). Demonstration of light chain monotypia in B cell non-Hodgkin's lymphomas using unfixed freeze-dried and formalin-fixed sections. J Clin Pathol.36:883-893

Neumann E, Schaefer-Ridder M, Wang Y, Hofschneider PH. (1982). Gene transfer into mouse lyoma cells by electroporation in high electric fields. EMBO J.1(7):841-5.

Newell-Price J, King P and Clark AJ. (2001). The CpG island promoter of the human proopiomelanocortin gene is methylated in nonexpressing normal tissue and tumors and represses expression. Mol Endocrinol 15(2): 338-348.

Nielen MM, van Schaardenburg D, Reesink HW, van de Stadt RJ, van der Horst-Bruinsma IE, de Koning MH, Habibuw MR, Vandenbroucke JP and Dijkmans BA. (2004). Specific autoantibodies precede the symptoms of rheumatoid arthritis: a study of serial measurements in blood donors. Arthritis Rheum 50:380-386.

Nie L, Wu G, Zhang W. (2006). Correlation of mRNA expression and protein abundance affected by multiple sequence features related to translational efficiency in Desulfovibrio vulgaris: a quantitative analysis. Genetics. 174(4):2229-43.

Oates, E. L., G. P. Allaway, G. R. Armstrong, R. A. Boyajian, J. H. Kehrl and B. S. Prabhakar (1988). Human lymphocytes produce pro-opiomelanocortin gene-related transcripts. Effects of lymphotropic viruses. J Biol Chem 263(21): 10041-10044.

Ohta K, Shichiri M, Kameya T, Matsubara O, Imai T, Marumo F and Hirata Y.(2000). Thymic hyperplasia as a source of ectopic ACTH production. Endocr J 47(4): 487-492.

Orntoft TF, Thykjaer T, Waldman FM, Wolf H, Celis JE. (2002). Genomewide study of gene copy numbers, transcripts, and protein levels in pairs of non-invasive and invasive human transitional cell carcinomas. Mol Cell Proteomics.1:37-45.

Paquet L, Bergeron F, Boudreault A, Seidah NG, Chretien M, Mbikay M and Lazure C. (1994). The neuroendocrine precursor 7B2 is a sulfated protein proteolytically processed by a ubiquitous furin-like convertase. J Biol Chem 269(30): 19279-19285.

Perrot S, Dieudé P, Pérocheau D, Allanore Y. (2013).Comparison of pain, pain burden, coping strategies, and attitudes between patients with systemic sclerosis and patients with rheumatoid arthritis: a cross-sectional study. Pain Med ;14(11):1776-85.

Pratt JM, Petty J, Riba-Garcia I, Robertson DH, Gaskell SJ, Oliver SG, Beynon RJ.(2002). Dynamics of protein turnover, a missing dimension in proteomics. Mol Cell Proteomics. 1(8):579-91.

Pritchard LEand White A. (2007). Neuropeptide processing and its impact on melanocortin pathways. Endocrinology 148(9): 4201-7.

Przewlocki R, Hassan AH, Lason W, Epplen C, Herz A and Stein C. (1992). Gene expression and localization of opioid peptides in immune cells of inflamed tissue: functional role in antinociception. Neuroscience 48(2): 491-500.

Qian Y, Devi LA, Mzhavia N, Munzer S, Seidah NG and Fricker LD.(2000). The C-terminal region of proSAAS is a potent inhibitor of prohormone convertase 1. J Biol Chem 275(31): 23596-23601.

Qiao-Ling Li, Erik Jansen ,Theodore C. (1999). Friedman Regulation of prohormone convertase 1 (PC1) by gp130-related cytokines Molecular and Cellular Endocrinology 158:143–152

Rantapaa-Dahlqvist S, de Jong BA, Berglin E., Hallmans G, Wadell G, Stenlund H, Sundin U and van Venrooij WJ. (2003). Antibodies against cyclic citrullinated peptide and IgA rheumatoid factor predict the development of rheumatoid arthritis. Arthritis Rheum 48:2741-2749.

Ray DW, Ren SG, Melmed S. (1996). Leukemia inhibitory factor (LIF) stimulates proopiomelanocortin (POMC) expression in a corticotroph cell line. Role of STAT pathway. J Clin Invest. 97(8):1852-9.

Rees DA, Hepburn PJ, McNicol AM, Francis K, Jasani B, Lewis MD, Farrell WE, Lewis BM, Scanlon MF, Ham J. (2002). Loss of ACTH expression in cultured human corticotroph macroadenoma cells is consistent with loss of the POMC gene signal sequence. Mol Cell Endocrinol. 189(1-2):51-7.

Rees LH, Burke CW, Chard T, Evans SW, Letchworth AT.(1975).Possible placental origin of ACTH in normal human pregnancy. Nature. 254(5501):620-2.

Renthal W, Nestler EJ. (2008). Epigenetic mechanisms in drug addiction. Trends Mol Med.14(8):341-50.

Righi A, Jin L, Zhang S, Stilling G, Scheithauer BW, Kovacs K and Lloyd RV. (2010).Identification and consequences of galectin-3 expression in pituitary tumors. Mol Cell Endocrinol 326(1-2): 8-14.

Ringholm A, Klovins J, Rudzish R, Phillips S, Rees JL, Schiöth HB.(2004). Pharmacological characterization of loss of function mutations of the human melanocortin 1 receptor that are associated with red hair. J Invest Dermatol. 123(5):917-23.

Rittner HL, Brack A, Machelska H, Mousa SA, Bauer M, Schäfer M, Stein C. (2001). Opioid peptide-expressing leukocytes: identification, recruitment, and simultaneously increasing inhibition of inflammatory pain. Anesthesiology. 95(2):500-8.

Rittner HL., Labuz D, Schaefer M, Mousa SA, Schulz S, Schäfer M, Stein C and Brack A. (2006). Pain control by CXCR2 ligands through Ca2+-regulated release of opioid peptides from polymorphonuclear cells. Faseb J 20(14): 2627-2629.

Rittner, H.L., Machelska, H., and Stein, C. (2005). Leukocytes in the regulation of pain and analgesia. J Leukoc Biol. 78:1215-1222.

Rolling C, Treton D, Pellegrini S, Galanaud P, Richard Y. (1996). IL4 and IL13 receptors share the gamma c chain and activate STAT6, STAT3 and STAT5 proteins in normal human B cells. FEBS Lett. 393(1):53-6

Rogers, J. and R. Wall (1980). A mechanism for RNA splicing. Proc Natl Acad Sci U S A 77(4): 1877-1879.

Rubinstein M, Mogil JS, Japón M, Chan EC, Allen RG, Low MJ.(1996). Absence of opioid stress-induced analgesia in mice lacking beta-endorphin by site-directed mutagenesis. Proc Natl Acad Sci U S A.;93(9):3995-4000.

Sanchez VC, Goldstein J, Stuart RC, Hovanesian V, Huo L, Munzberg H, Friedman TC, Bjorbaek C, Nillni EA. (2004). Regulation of hypothalamic prohormone convertases 1 and 2 and effects on processing of prothyrotropin-releasing hormone. J Clin Invest. 114(3):357-69.

Sato Y, Sugie R, Tsuchiya B, Kameya T, Natori M, Mukai K. (2001).Comparison of the DNA extraction methods for polymerase chain reaction amplification from formalin-fixed and paraffin-embedded tissues. Diagn Mol Pathol. 10(4):265-71.

Schauer E, Trautinger F, Köck A, Schwarz A, Bhardwaj R, Simon M, Ansel JC, Schwarz T, Luger TA. (1994). Proopiomelanocortin-derived peptides are synthesized and released by human keratinocytes. J Clin Invest. 93(5):2258-62.

Schäfer M, Carter L and Stein C. (1994). Interleukin 1 beta and corticotropin-releasing factor inhibit pain by releasing opioids from immune cells in inflamed tissue. Proc Natl Acad Sci U S A 91(10): 4219-4223.

Schellekens GA, Visser H, de Jong BA, van den Hoogen FH, Hazes JM, Breedveld FC, and van Venrooij WJ. (2000). The diagnostic properties of rheumatoid arthritis antibodies recognizing a cyclic citrullinated peptide. Arthritis Rheum 43:155-163.

Schiöth HB, Phillips SR, Rudzish R, Birch-Machin MA, Wikberg JE & Rees JL. (1999).Loss of function mutations of the human melanocortin 1 receptor are common and are associated with red hair. *Biochem Biophys Res Commun* **260**: 488–491.

Schnabel E, Mains RE, Farquhar MG. (1989). Proteolytic processing of pro-ACTH/endorphin begins in the Golgi complex of pituitary corticotropes and AtT-20 cells. Mol Endocrinol. 3(8):1223-35.

Scholzen TE, Kalden DH, Brzoska T, Fisbeck T, Fastrich M, Schiller M, Böhm M, Schwarz T, Armstrong CA, Ansel JC, Luger TA. (2000). Expression of proopiomelanocortin peptides in human dermal microvascular endothelial cells: evidence for a regulation by ultraviolet light and interleukin-1. J Invest Dermatol. 115(6):1021-8.

Scott DL, Kingsley GH (2006). Tumor necrosis factor inhibitors for rheumatoid arthritis. N Engl J Med 355: 704–712.

Seidah NG, Gaspar L, Mion P, Marcinkiewicz M, Mbikay M, Chretien M. (1990). cDNA sequence of two distinct pituitary proteins homologous to Kex2 and furin gene products: tissue-specific mRNAs encoding candidates for pro-hormone processing proteinases. DNA 9:415–424.

Seidah NG, Chrétien M. (1992). Proprotein and prohormone convertases of the subtilisin family Recent developments and future perspectives. Trends Endocrinol Metab. 3(4):133-40.

Seidah NG, Benjannet S, Hamelin J, Mamarbachi AM, Basak A, Marcinkiewicz J, Mbikay M, Chretien M and Marcinkiewicz M.(1999). The subtilisin/kexin family of precursor convertases. Emphasis on PC1, PC2/7B2, POMC and the novel enzyme SKI-1. Ann N Y Acad Sci. 885: 57-74.

Seidah NG, Day R, Marcinkiewicz M and Chretien M.(1993). Mammalian paired basic amino acid convertases of prohormones and proproteins. Ann N Y Acad Sci 680: 135-146.

Seidah NG, Marcinkiewicz M, Benjannet S, Gaspar L, Beaubien G, Mattei MG, Lazure C, Mbikay M and Chretien M. (1991). Cloning and primary sequence of a mouse candidate prohormone convertase PC1 homologous to PC2, Furin, and Kex2: distinct chromosomal localization and messenger RNA distribution in brain and pituitary compared to PC2. Mol Endocrinol 5(1): 111-122.

Seidah NG and Prat A. (2002). Precursor convertases in the secretory pathway, cytosol andextracellular milieu, Essays Biochem. (38)79–94.

Sharma A, Kumar M, Aich J, Hariharan M, Brahmachari SK, Agrawal A, Ghosh B. (2009). Posttranscriptional regulation of interleukin-10 expression by hsa-miR-106a. Proc Natl Acad Sci U S A.106(14):5761-6.

Shi SR, Cote RJ, Taylor CR (1997) Antigen retrieval immunohistochemistry: past, present, and future. J Histochem Cytochem 45:327–343.

Shi SR, Liu C, Taylor CR. (2007). Standardization of immunohistochemistry for formalin-fixed, paraffin-embedded tissue sections based on the antigen-retrieval technique: from experiments to hypothesis. J Histochem Cytochem. 55(2):105-9.

Shi SR, Taylor CR, Fowler CB, Mason JT. (2013). Complete solubilization of formalin-fixed, paraffin-embedded tissue may improve proteomic studies. Proteomics Clin Appl.7(3-4):264-72.

Simmons RM, Webster AA, Kalra AB, Iyengar S. (2002). Group II mGluR receptor agonists are effective in persistent and neuropathic pain models in rats. Pharmacol Biochem Behav. 73(2):419-27.

Simamura E, Shimada H, Higashi N, Uchishiba M, Otani H, Hatta T. (2010). Maternal leukemia inhibitory factor (LIF) promotes fetal neurogenesis via a LIF-ACTH-LIF signaling relay pathway. Endocrinology. 151(4):1853-62.

Sioud M. (2005). Induction of inflammatory cytokines and interferon responses by double-stranded and single-stranded siRNAs is sequence-dependent and requires endosomal localization. J Mol Biol.;348(5):1079-90.

Sitte N, Busch M, Mousa SA, Labuz D, Rittner H, Gore C, Krause H, Stein C and Schäfer M. (2007). Lymphocytes upregulate signal sequence-encoding proopiomelanocortin mRNA and beta-endorphin during painful inflammation in vivo. J Neuroimmunol 183(1-2): 133-145.

Smeekens SP and Steiner DF. (1990). Identification of a human insulinoma cDNA encoding a novel mammalian protein structurally related to the yeast dibasic processing protease Kex2. J Biol Chem 265(6): 2997-3000.

Smeekens SP, Steiner DF. (1991). Processing of peptide precursors. Identification of a new family of mammalian proteases. Cell Biophys. 19(1-3):45-55.

Smith AI, Funder JW. (1989). Proopiomelanocortin processing in the pituitary, central nervous system, and peripheral tissues. Endocr Rev.9:159–79.

Smith EM. (2003). Opioid peptides in immune cells. Adv Exp Med Biol 521: 51-68.

Smith EM and Blalock JE. (1981). Human lymphocyte production of corticotropin and endorphin-like substances: association with leukocyte interferon. Proc Natl Acad Sci U S A 78(12): 7530-7534.

Smith EM, Morrill AC, Meyer WJ and Blalock JE. (1986). Corticotropin releasing factor induction of leukocyte-derived immunoreactive ACTH and endorphins. Nature 321(6073): 881-882.

Spange S, Wagner T, Heinzel T, Krämer OH. (2009). Acetylation of non-histone proteins modulates cellular signalling at multiple levels. Int J Biochem Cell Biol. 41(1):185-98.

Stein C, Gramsch C and Herz A. (1990). Intrinsic mechanisms of antinociception in inflammation: local opioid receptors and beta-endorphin. J Neurosci 10(4): 1292-8.

Stein C, Hassan AH, Lehrberger K, Giefing J and Yassouridis A. (1993). Local analgesic effect of endogenous opioid peptides. Lancet 342(8867): 321-4.

Stein C, Pflüger M, Yassouridis A, Hoelzl J, Lehrberger K, Welte C, Hassan AH. (1996). No tolerance to peripheral morphine analgesia in presence of opioid expression in inflamed synovia. J Clin Invest. 98(3):793-9.

Stein C, Millan MJ, Yassouridis A, Herz A. (1998). Antinociceptive effects of mu- and kappa-agonists in inflammation are enhanced by a peripheral opioid receptor-specific mechanism. Eur J Pharmacol.155(3):255-64.

Stein C, Schafer M and Machelska H. (2003). Attacking pain at its source: new perspectives on opioids. Nat Med 9(8): 1003-1008.

Stein C, and Machelska H. (2011). Modulation of peripheral sensory neurons by the immune system: implications for pain therapy. Pharmacol Rev 63:860-881.

Stein C, and Küchler S. (2013). Targeting inflammation and wound healing by opioids. Trends Pharmacol Sci 34:303-312.

Steiner DF. (1998).The proprotein convertases. Curr Opin Chem Biol. 2(1):31-9.

Stephanou A, Fitzharris P, Knight RA and Lightman SL. (1991). Characteristics and kinetics of proopiomelanocortin mRNA expression by human leucocytes. Brain Behav Immun 5(4): 319-327.

Stevens CW.(2011). The evolution of opioid receptors. *Front Biosci* 14:1247–69.

Swaminathan S, Suzuki K, Seddiki N, Kaplan W, Cowley MJ, Hood CL, Clancy JL, Murray DD, Méndez C, Gelgor L, Anderson B, Roth N, Cooper DA, Kelleher AD.(2012). Differential regulation of the Let-7 family of microRNAs in CD4+ T cells alters IL-10 expression. J Immunol. 188(12):6238-46.

Szallasi Z. (1999). Genetic network analysis in light of massively parallel biological data acquisition. Pac Symp Biocomput. 5-16.

Tabas I, and Glass CK. (2013). Anti-inflammatory therapy in chronic disease: challenges and opportunities. Science 339:166-172.

Tadros H, Schmidt G, Sirois F, Mbikay M. (2011). Regulation of 7B2 mRNA translation: dissecting the role of its 5'-untranslated region. Methods Mol Biol. 768:217-30.

Takahashi A, Amemiya Y, Sarashi M, Sower SA, Kawauchi H. (1995). Melanotropin and corticotropin are encoded on two distinct genes in the lamprey, the earliest evolved extant vertebrate. Biochem Biophys Res Commun 213:490–8.

Takahashi A, Kawauchi H. (2006). Evolution of melanocortin systems in fish. *Gen Comp* Endocrinol148:85–94.

Takahashi A, Mizusawa K. (2013). Posttranslational modifications of proopiomelanocortin in vertebrates and their biological significance. Front Endocrinol (Lausanne). 4:143.

Tajerian M, Alvarado S, Millecamps M, Dashwood T, Anderson KM, Haglund L, Ouellet J, Szyf M, Stone LS.(2011). DNA methylation of SPARC and chronic low back pain. Mol Pain.7-65.

Tanaka M, Tanaka H, Ishikawa E. (1984). Immunohistochemical demonstration of surface antigen of human lymphocytes with monoclonal antibody in acetone-fixed paraffinembedded sections. J Histochem Cytochem. 32:452-454.

Tanaka, S. (2003). Comparative aspects of intracellular proteolytic processing of peptide hormone precursors: studies of proopiomelanocortin processing. Zoolog Sci. 20(10): 1183-1198.

Tanaka S. and Kurosumi K. (1992). A certain step of proteolytic processing of proopiomelanocortin occurs during the transition between two distinct stages of secretory granule maturation in rat anterior pituitary corticotrophs. Endocrinology 131(2): 779-786.

Tanaka S, Nomizu M and Kurosumi K. (1991). Intracellular sites of proteolytic processing of pro-opiomelanocortin in melanotrophs and corticotrophs in rat pituitary. J Histochem Cytochem 39(6): 809-821.

Tanaka Y, Imai T, Baba M, Ishikawa I, Uehira M, Nomiyama H, Yoshie O.(1999). Selective expression of liver and activation-regulated chemokine (LARC) in intestinal epithelium in mice and humans. Eur J Immunol. 29(2):633-42.

Tateno T, Izumiyama H, Doi M, Yoshimoto T, Shichiri M, Inoshita N, Oyama K, Yamada S, Hirata Y.(2007). Differential gene expression in ACTH -secreting and non-functioning pituitary tumors. Eur J Endocrinol. 157(6):717-24.

Taylor CR.(1994). An exaltation of experts: concerted efforts in the standardization of immunohistochemistry. Hum Pathol 25: 2–11.

Taylor CR. (2006).Standardization in immunohistochemistry: the role of antigen retrieval in molecular morphology. Biotech Histochem.81(1):3-12.

Thomas L, Leduc R, Thorne BA, Smeekens SP, Steiner DF, Thomas G. (1991). Kex2-like endoproteases PC2 and PC3 accurately cleave a model prohormone in mammalian cells: evidence for a common core of neuroendocrine processing enzymes. Proc Natl Acad Sci U S A. 88(12):5297-301.

Tooze J and Burke B. (1987). Accumulation of adrenocorticotropin secretory granules in the midbody of telophase AtT20 cells: evidence that secretory granules move anterogradely along microtubules. J Cell Biol. 104(4):1047-57.

Trelle S, Reichenbach S, Wandel S, Hildebrand P, Tschannen B, Villiger PM, Egger M, and Juni P. (2011). Cardiovascular safety of non-steroidal anti-inflammatory drugs: network meta-analysis. BMJ 342:c7086.

Tsong TY.(1991) Electroporation of cell membranes. Biophys J.60(2):297-306.

Ugleholdt R, Poulsen ML, Holst PJ, Irminger JC, Orskov C, Pedersen J, Rosenkilde MM, Zhu X, Steiner DF, Holst JJ. (2006).Prohormone convertase 1/3 is essential for processing of the glucose-dependent insulinotropic polypeptide precursor. J Biol Chem;281(16):11050-7.

Vanesa C. Sanchez, Jorge Goldstein, Ronald C. Stuart, irginia Hovanesian, Lihong Huo, Heike Munzberg, Theodore C. Friedman, Christian Bjorbaek, and Eduardo A. Nillni. (2004). Regulation of hypothalamic prohormone convertases 1 and 2 and

effects on processing of prothyrotropin releasing hormone J. Clin. Invest.114:357–369.

Van Epps DE, Saland L. (1984). Beta-endorphin and met-enkephalin stimulate human peripheral blood mononuclear cell chemotaxis. J Immunol;132(6):3046-53.

van Gaalen FA, Linn-Rasker SP, van Venrooij WJ, de Jong BA, Breedveld FC, Verweij CL, Toes RE, and Huizinga TW. (2004). Autoantibodies to cyclic citrullinated peptides predict progression to rheumatoid arthritis in patients with undifferentiated arthritis: a prospective cohort study. Arthritis Rheum 50:709-715.

van Gaalen FA, van Aken J, Huizinga TW, Schreuder GM, Breedveld FC, Zanelli E, van Venrooij WJ, Verweij CL, Toes RE and de Vries RR. (2004). Association between HLA class II genes and autoantibodies to cyclic citrullinated peptides (CCPs) influences the severity of rheumatoid arthritis. Arthritis Rheum 50:2113-2121.

Van Woudenberg AD, Metzelaar MJ, van der Kleij AA, de Wied D, Burbach JP and Wiegant VM. (1993). Analysis of proopiomelanocortin (POMC) messenger ribonucleic acid and POMC-derived peptides in human peripheral blood mononuclear cells: no evidence for a lymphocyte-derived POMC system. Endocrinology 133(5): 1922-1933.

Verma-Gandhu M, Bercik P, Motomura Y, Verdu EF, Khan WI, Blennerhassett PA, Wang L, El-Sharkawy RT, and Collins SM. (2006). CD4(+) T-Cell Modulation of Visceral Nociception in Mice. Gastroenterology 130:1721-1728.

Verri JWA, Cunha TM, Parada CA, Poole S, Cunha FQ, Ferreira SH (2006). Hypernociceptive role of cytokines and chemokines: targets for analgesic drug development? Pharmacol Ther 112: 116–138.

Vindrola O, Mayer AM, Citera G, Spitzer JA, Espinoza LR.(1994). Prohormone convertases PC2 and PC3 in rat neutrophils and macrophages. Parallel changes with proenkephalin-derived peptides induced by LPS in vivo. Neuropeptides. 27(4):235-44.

Vivian Hook Funkelstein L, Lu WD, Bark S, Wegrzyn J, Hwang SR. (2008). Proteases for processing proneuropeptides into peptide neurotransmitters and hormones, Annu. Rev. Pharmacol. Toxicol. 48:393–423.

Vivian Hook, Lydiane Funkelstein, Jill Wegrzyn, Steven Bark, Mark Kindy, Gregory Hook. (2012). Cysteine Cathepsins in the secretory vesicle produce active peptides: Cathepsin L generates peptide neurotransmitters and cathepsin B produces beta-amyloid of Alzheimer's disease. Biochimica et Biophysica Acta 1824:89–104.

Weigent DA, Blalock JE. (1987). Interactions between the neuroendocrine and immune systems: common hormones and receptors. Immunol Rev;100:79-108.

Westly HJ, Kleiss AJ, Kelley KW, Wong PK and Yuen PH. (1986). Newcastle disease virus-infected splenocytes express the proopiomelanocortin gene. J Exp Med. 163(6): 1589-1594.

Wiese M, Castiglione K, Hensel M, Schleicher U, Bogdan C, Jantsch J. (2010). Small interfering RNA (siRNA) delivery into murine bone marrow-derived macrophages by electroporation. J Immunol Methods. 353(1-2):102-10.

Wojdacz TK, Dobrovic A.(2007).Methylation-sensitive high resolution melting (MS-HRM): a new approach for sensitive and high-throughput assessment of methylation. Nucleic Acids Res. ;35(6):e41

Wintzen M, Yaar M, Burbach JP, Gilchrest BA. (1996). Proopiomelanocortin gene product regulation in keratinocytes. J Invest Dermatol.106(4):673-8.

Wipke BT, Allen PM (2001). Essential role of neutrophils in the initiation and progression of a murine model of rheumatoid arthritis. J Immunol 167: 1601–1608.

Wittert G, Hope P, Pyle D (1996). Tissue distribution of opioid receptor gene expression in the rat. Biochem Biophys Res Commun 218(3):877-81.

Wolkowitz OM, Epel ES, Mellon S. (2008). When blue turns to grey: do stress and depression accelerate cell aging? World J Biol Psychiatry.9(1):2-5.

Wollemann M, Benyhe S.(2004) Non-opioid actions of opioid peptides. Life Sci;75(3):257-70.

Yang CC, Ogawa H, Dwinell MB, McCole DF, Eckmann L, Kagnoff MF.(2005). Chemokine receptor CCR6 transduces signals that activate p130Cas and alter cAMP-stimulated ion transport in human intestinal epithelial cells. Am J Physiol Cell Physiol. 288(2):C321-8.

Yang D, Gereau RW 4th. (2002). Peripheral group II metabotropic glutamate receptors (mGluR2/3) regulate prostaglandin E2-mediated sensitization of capsaicin responses and thermal nociception. J Neurosci. 22(15):6388-93.

Yang D, Gereau RW 4th. (2003).Peripheral group II metabotropic glutamate receptors mediate endogenous anti-allodynia in inflammation. Pain. 106(3):411-7.

Yasothornsrikul S, Greenbaum KF, Medzihradszky T, Toneff R, Bundey R, Miller B, Schilling I, Petermann J, Dehnert A, Logvinova P, Goldsmith JM, Neveu WS, Lane B, Gibson T, Reinheckel C, Peters M. Bogyo V.Y.H Hook. (2003). Cathepsin L in secretory vesicles functions as a prohormone-processing enzyme for production of the enkephalin peptide neurotransmitter, Proc. Natl.Acad. Sci. U. S. A. 100; 9590–9595.

Yasothornsrikul. S. Toneff, S.R. Hwang, V.Y.H. Hook. (1998). Arginine and lysine aminopeptidase ctivities in chromaffin granules of bovine adrenal medulla: relevance to prohormone processing, J. Neurochem. 70;153–163.

Zhang CF, Dhanvantari S, Lou H, Loh YP. (2003). Sorting of carboxypeptidase E to the regulated secretory pathway requires interaction of its transmembrane domain with lipid rafts. Biochem J. 369(Pt 3):453-60.

Zhou A, Bloomquist BT and Mains RE. (1993). The prohormone convertases PC1 and PC2 mediate distinct endoproteolytic cleavages in a strict temporal order during proopiomelanocortin biosynthetic processing. J Biol Chem 268(3): 1763-1769.

Zhou A, Webb G, Zhu X and Steiner DF. (1999) Proteolytic processing in the secretory pathway. J. Biol. Chem. 274, 20 745– 20 748.

Zhu X, Rouille Y, Lamango NS, Steiner DF and Lindberg I. (1996). Internal cleavage of the inhibitory 7B2 carboxyl-terminal peptide by PC2: a potential mechanism for its inactivation. Proc Natl Acad Sci U S A 93(10): 4919-4924.

Zhou Y and Lindberg I. (1993). Purification and characterization of the prohormone convertase PC1(PC3). J Biol Chem 268(8): 5615-5623.

Zimmermann M.(1983). Ethical guidelines for investigations of experimental pain in conscious animals. Pain. (2):109-10.